

SIMULATION OF VAWT AND HYDROKINETIC TURBINES WITH VARIABLE
PITCH FOILS

by

Lindsay Damon Woods

A thesis

submitted in partial fulfillment

of the requirements for the degree of

Master of Science in Mechanical Engineering

Boise State University

May 2013

© 2013

Lindsay Damon Woods

ALL RIGHTS RESERVED

BOISE STATE UNIVERSITY GRADUATE COLLEGE

DEFENSE COMMITTEE AND FINAL READING APPROVALS

of the thesis submitted by

Lindsay Damon Woods

Thesis Title: Predicting Turbine Performance with a Dynamic Computer Model

Date of Final Oral Examination: 12 March 2013

The following individuals read and discussed the thesis submitted by student Lindsay Damon Woods, and they evaluated his presentation and response to questions during the final oral examination. They found that the student passed the final oral examination.

John F. Gardner, Ph.D. Chair, Supervisory Committee

James R. Ferguson, Ph.D. Member, Supervisory Committee

Jairo E. Hernandez, Ph.D. Member, Supervisory Committee

The final reading approval of the thesis was granted by John F. Gardner, Ph.D., Chair of the Supervisory Committee. The thesis was approved for the Graduate College by John R. Pelton, Ph.D., Dean of the Graduate College.

ACKNOWLEDGEMENTS

This thesis was funded through the generous support of Idaho National Laboratory through the Center for Advanced Energy Studies. Without the support of Kurt Myers, Dr. Gardner, and the LDRD team, this thesis would not have been possible. I would like to thank Max Badesheim and Kate Huebschmann at the writing center for your patience in helping me find a way through all the words and figures to a coherent thesis and for making this report ten times better than it would have been otherwise. Thank you Dr. Hernandez for your work on the committee and providing me with your insight and comments. Thank you Dr. Ferguson for asking the hard questions that helped me refine this thesis and for informing me of more turbine research to be done in Switzerland. It was a wonderful opportunity that I would not have had were it not for you. For all the other grad students in room ME 314: Mike, Paul, Derek, Dan, and Hope, thank you for answering dozens of questions and turning a dreary lab at BSU into a friendly place where I could laugh and learn while I worked. Thank you to my parents for their unwavering support and overwhelming love and encouragement. Lastly, thank you Dr. Gardner for the amazing gift of this opportunity. Thank you for your abiding commitment to always do the right and sensible thing, even if it doesn't win you praise and recognition. When we first met, I could have gone in any number of different directions in engineering. Thank you for your inspiration to pursue energy efficiency and to look at every solution with a fair but critical eye. You've changed my life.

ABSTRACT

A dynamic computer model of a turbine was developed in MATLAB in order to study the behavior of vertical axis wind and hydrokinetic turbines with articulating foils. The simulation results corroborated the findings of several empirical studies on various turbines in both wind and water currents. The model was used to analyze theories of pitch articulation and to inform the discussion on turbine design. Several new patents and proposed configurations were tested. Simulation results showed that pitch articulation allowed Darrieus-style vertical axis wind turbines to start from rest. The tip speed ratio was found to increase rapidly, carrying the turbine into very fast rotational velocities. The simulations revealed a region of high efficiency for wind turbines at high rates of rotation and demonstrated the advantages of using a dynamic generator load. The model was also used to study the behavior of hydrokinetic turbines in restricted environments like irrigation canals – a situation where the Betz analysis is not suitable. Further study showed that when a turbine is inserted in a channel, the resulting blockage causes the development of potential energy in the form of hydraulic head upstream of the turbine. The model was used to predict the efficiency of hydrokinetic turbines in this situation and the water level rise that would occur upstream.

TABLE OF CONTENTS

ACKNOWLEDGEMENTS	iv
ABSTRACT.....	v
LIST OF TABLES	ix
LIST OF FIGURES	x
LIST OF ABBREVIATIONS.....	xiii
CHAPTER ONE: INTRODUCTION.....	1
The Scope of the Study	1
CHAPTER TWO: BACKGROUND.....	6
Early Examination of the Topic	6
The Betz Theory of Efficiency	16
Articulating Foils	19
Turbine Modeling	25
CHAPTER THREE: METHODOLOGY	27
The Structure of the Model.....	27
Defining the Geometry and the Initial Conditions.....	30
Calculating the Lift and Drag at Each Foil	33
Calculating Torque.....	36
CHAPTER FOUR: MATLAB MODEL	43

Developing the Model for a VAWT	43
Model Verification.....	52
CHAPTER FIVE: RESULTS	62
Using the Model to Inform Design Decisions	62
Ideal Blade Articulation.....	63
Ideal Generator Loading	66
CHAPTER SIX: HYDROKINETIC TURBINES	70
Differences between Wind and Water Turbine Behavior.....	70
Feedback Loops: Power Production, Position Changes, and Induction	76
Determining Water level Rise.....	77
Adapting the Model for Hydrokinetic Turbines	78
CHAPTER SEVEN: CONCLUSION	85
Rotational Behavior	85
Articulation	86
Generator Loading	87
Hydroturbines	88
Future Work	89
Summary.....	89
REFERENCES	91
APPENDIX A.....	96
Geometric Transformation by Matrices.....	96
APPENDIX B	100
MATLAB Code and Simulink Figures.....	100

APPENDIX C	104
Additional Tables and Figures	104

LIST OF TABLES

Table 1	Outputs of MATLAB model simulations for sinusoidal pitch articulation and low resistance.....	109
Table 2	Outputs of MATLAB model simulations for sinusoidal pitch articulation and high resistance.....	110
Table 3	Outputs of MATLAB model simulations for a fixed pitch turbine	111
Table 4	Outputs of MATLAB model simulations for THAWT with fixed pitch	111

LIST OF FIGURES

Figure 1	Sketch of a Darrieus-style Water Turbine [8].....	6
Figure 2	Sketch of a Savonius (Drag-Based) vertical axis water turbine [8].....	7
Figure 3	Streamlines around an airfoil. Figure reproduced from [9]	9
Figure 4	Lift and drag on an airfoil. Figure taken from [10].....	10
Figure 5	Graph of Turbine Power Output versus TSR [12]	15
Figure 6	Using the Betz Theory to Predict Maximum Efficiency Based on the Ratio of Exiting Flow to Incoming Flow Velocity	18
Figure 7	Installation of a BlackHawk TR-10 VAWT developed by Bruce Boatner [22]	22
Figure 8	Side-view of BlackHawk foil tilting.....	23
Figure 9	An example of articulated foil pitch in rotation.....	25
Figure 10	Simplified Model of the Program Showing Inputs and Feedback Loops.....	28
Figure 11	The motion and three geometric frames of a model for a vertical axis turbine	32
Figure 12	Diagram of the Lift and Drag forces for a VAWT at rest ($\omega = 0$) as viewed from above.....	34
Figure 13	The angle of attack and Induced velocity on the wing of a vertical axis turbine. Figure taken from [17]	35
Figure 14	Diagram of the Lift and Drag Forces and Local Velocity for a VAWT in motion (TSR =1).....	36
Figure 15	Vector components of the free-stream velocity and the tangential velocity at a foil	38

Figure 16	Lift and drag on a foil with ψ and α displayed.....	41
Figure 17	Overall view of the MATLAB Simulink model and its functions.....	43
Figure 18	The Coefficient of Power of a Turbine as a Function of the Induction Factor	45
Figure 19	MATLAB model inputs and feedback loops accounting for induction	47
Figure 20	MATLAB model: flow conditions and calculating torque.....	48
Figure 21	MATLAB Model Rigid Body Dynamics	49
Figure 22	MATLAB Model Feedback Loops and Power Calculation	51
Figure 23	Three-bladed Darrieus VAWT used for tests by Dominy et al [19].....	53
Figure 24	MATLAB simulation output of a fixed-pitch turbine at 22 mph.....	54
Figure 25	Results of a wind-tunnel test of a fixed-pitch 3-Bladed VAWT at wind-speed of 6m/s. Words and figure from [18].....	57
Figure 26	MATLAB simulation results for turbine with sinusoidally varying pitch at wind-speed of 7m/s	57
Figure 27	Power and TSR output of model based on BlackHawk TR10 at a wind-speed of 13 mph.....	59
Figure 28	MATLAB model outputs graphed over BlackHawk field data from Emmett.....	60
Figure 29	SCADA Data Provided by BlackHawk Showing Measurements of Efficiency vs TSR.....	62
Figure 30	MATLAB simulation results in a study attempting to optimize the magnitude of the sinusoidal pitch at a simulated wind-speed of 18 mph.	64
Figure 31	Contrast of available torque between fixed-pitch and articulating-pitch VAWTs based on MATLAB Model simulations	65
Figure 32	Increasing the generator load in a MATLAB simulation	67
Figure 33	How the TSR of the MATLAB Simulation responded to increasing generator load.....	67

Figure 34	How the Power of the MATLAB Simulation responded to increasing generator load.....	68
Figure 35	Streamlines and pressure distribution from a Betz analysis applied to a hydroturbine. Figure and description from [13].....	72
Figure 36	Curvilinear streamlines and new estimate of pressure distribution on a hydroturbine. Figure and description from [13].....	72
Figure 37	Analysis Using Two Streamtubes for in the Analysis of a Turbine in Open Chanel Flow [15].....	75
Figure 38	MATLAB calculation of the change in stream depth.....	79
Figure 39	CAD image of THAWT and flume set up for experimental testing at Oxford [20]	80
Figure 40	Side View of the Hydrovolts Turbine with Hinged Wings [25].....	83
Figure 41	Schematic of full MATLAB model for wind turbines.....	103
Figure 42	Close-up of a BlackHawk TR-10 VAWT developed by Bruce Boatner [20] showing tilt and articulation	104
Figure 43	SCADA Data Provided by BlackHawk Showing Measurements of RPM vs Wind-Speed	105
Figure 44	SCADA Data Provided by BlackHawk Showing Measurements of TSR versus Wind-Speed.....	106
Figure 45	SCADA Data Provided by BlackHawk Showing Measurements of Efficiency vs Wind-speed.....	107
Figure 46	SCADA Data Provided by BlackHawk Showing Measurements of Power vs. Wind-speed	108
Figure 47	Hydrovolts Class II Turbine 1 - 10 kW capacity depending on flow. Photo courtesy of Hydrovolts Inc	112
Figure 48	The Lift Coefficient of a NACA 0014 airfoil at Two Different Reynold's numbers from Sandia Wind-Tunnel tests [9].....	112
Figure 49	The Drag Coefficient of a NACA 0014 airfoil at Two Different Reynold's numbers from Sandia Wind-Tunnel tests [9].....	113

LIST OF ABBREVIATIONS

BEM	Blade Element Momentum Theory
BSU	Boise State University
CAES	Center for Advanced Energy Studies
DOE	U.S. Department of Energy
EIA	Energy Information Administration
FEM	Finite Element Method
HAWT	Horizontal Axis Wind/Water Turbine
LEED	Leadership in Energy Efficient Design
MATLAB	Matrix Laboratory Software
NACA	National Advisory Committee for Aeronautics
NREL	National Renewable Energy Laboratory
SCADA	Supervisory Control and Data Acquisition
THAWT	Transverse Horizontal Axis Water Turbine
TSR	Tip Speed Ratio
VAWT	Vertical Axis Wind/Water Turbine

CHAPTER ONE: INTRODUCTION

The Scope of the Study

Harnessing the elements to do useful work is nothing new. There are records of windmills installed in Persia dating back to 200 BC [1]. Even before the industrial revolution thousands of wind and water mills were installed in the English countryside in order to pump water for irrigation and mill grain into flour (hence the terms watermill and windmill). What has changed over the centuries is how effectively people are able to make use of these vast energy resources. People now understand how these systems operate and have the ability to design sophisticated control systems to moderate exactly how much energy is to be pulled from a resource at any one time.

Wind and water turbines are no longer widely used as a means of milling grain, but thousands are now employed in the production of electricity. Although most of society uses energy from coal, gas, and nuclear energy resources, wind and water turbines share a number of advantages over traditional power facilities. Some of these advantages include: the ability to operate without producing or emitting any noxious gases, carbon dioxide or other greenhouse gases, and the ability to run on free and renewable fuel sources.

In 2010, alone over 37,000 Megawatts of new wind power-generating capacity were installed worldwide [2], and many experts predict that wind could make up to 20% of the U.S. electricity needs by the year 2030 [3]. The current U.S. electricity market share of wind and water energy stands at 3% and 8% respectively as of 2011 [4].

However, some major hurdles stand between the energy in the flow of wind and water and its delivery as a steady electric current in people's homes. For example: when the velocity of air or water varies, the turbine must compensate for the variance in its power output either by changing the angle of the rotor blades or by adjusting the generator load, which alters its rotational speed. A dynamic model of the system is an invaluable diagnostic tool, and can greatly aid in the design of new and more efficient systems. The goal of this research was to develop just such a tool.

The conventional method of converting wind energy into electricity is by building large, three-bladed Horizontal Axis Wind Turbines (HAWT's for short). These turbines are designed to operate with three blades that generate a lift force when the wind passes over them. This lift causes the blades to spin like a propeller with the axis of rotation parallel to the ground. The resulting torque from the spinning blades turns the shaft of a generator, which converts the kinetic energy into electricity. Vertical Axis Wind Turbines (VAWT's) operate in much the same way, but as opposed to spinning like a propeller they rotate with the axis rotating perpendicular to the ground like a helicopter blade. Both turbines operate on the same principles of lift and drag. While horizontal turbines are in widespread use today, vertical axis turbines are only beginning to emerge in the market.

A current niche market has emerged around small and distributed power generation [5]. Some developers seek to install small wind turbines on their buildings in order to gain Leadership in Energy Efficient Design (LEED) credits. LEED credits are generally used as a metric for how sustainable and environmentally friendly a structure is by offsetting some of a building's energy usage by generating the power onsite [6].

Traditionally, these credits have been earned by using solar power, but now several small wind developers are also seeking to have their turbines installed on building roofs as a way of capturing energy in windy urban areas [7].

While hydroelectric power is certainly not as easy to install in urban environments as wind turbines might be, hydro power offers one major advantage over wind: it provides steady, reliable, predictable power, making it an excellent base-load power source although the power available does vary on a slow time-scale (month to month and year to year) depending on water levels and snow-packs. Here in the United States, many hydroelectric resources have been developed already, and increasing their number have the potential to cause serious environmental strain on landscapes, communities, and fish populations [6]. However, one new resource that is currently being considered for development by the Department of Energy is the installation of hydrokinetic turbines in irrigation canals and small dams that do not currently have any electric generating capacity. Hydrokinetic turbines are hydroelectric generators that do not require significant hydraulic head. Conventional hydroelectric dams use a structure such as a concrete wall to develop a significant water level rise upstream of the turbine, which increases the pressure and the energy in the jet of water running through the bottom of the dam across the turbine. Hydrokinetic turbines, on the other hand, harvest energy from the flow of water in a stream as it is, with no structure or significant pressure increase or water level drop from a large reservoir behind a dam. Several companies are now seeking to deploy hydrokinetic turbines in irrigation canals. Irrigation canals are man-made structures. And so, installing turbines in canals has a very light environmental

impact. Few irrigation canals have significant fish populations or floating debris both of which often discourage hydrokinetic turbine development in rivers.

Another possible source of hydro power comes from tapping the potential energy in dams that are currently not producing electricity. According to a report prepared by Oak Ridge National Laboratory [8], of the 80,000 dams currently built in America, only 3% are producing electricity. The report estimates that 54,000 non-powered dams could produce up to twelve Gigawatts of power, enough to power about nine million homes. Unfortunately, since each location and situation is different, it is not easy to apply a universal power generating system for all of them. However, small hydrokinetic turbines can be adapted to applications in a wide range of settings. This is where a computer model of a potential turbine could be of great use. Being able to predict the power generated at each site allows for the calculation of the payback period of installing a turbine.

Computer models can focus on various physics and different scales estimating the performance of a wind or hydrokinetic turbine. These models can be used to inform design decisions and demonstrate the risks and advantages of installing a turbine in a particular flow resource. Estimation of an area's wind resources are done by many large wind developer firms. These firms use proprietary software in order to estimate the wind resources available at a particular site by collecting wind speed and direction at a particular location for long periods of time. The data is compiled into wind maps and wind roses, which show the average annual wind speed and direction in a given setting. These inputs are then used to predict how much power could be harvested given various

layouts for turbine installation and to estimate the ideal location and spread of individual wind turbines in a 'wind farm.'

Other software models used to estimate the performance of turbines operate on a much more detailed level. As opposed to the resource mapping of large areas as mentioned earlier, Computational Fluid Dynamic (CFD) models are often based on fluid mechanics equations of many small sections of a fluid in a control volume. The results from these equations can be used to examine the behavior of fluid packets (of air or water) passing over an individual foil of a turbine. Other CFD or Finite Element Method (FEM) models are used to describe the interworking of the turbines themselves.

The level of detail for the model developed in the following research is on a scale between FEM and wind resource maps. This particular computer model was constructed in the program MATLAB¹. MATLAB is a computer program that supports some code scripts in addition to a block-diagram interface. It includes solid body mechanics, bulk flow analysis, and fast dynamics. In addition, it has the ability incorporate a range of data conditions by including such things as variable wind speeds as part of the input. However, this model's greatest value lies in predicting the performance and power output of a single turbine when it is given a set of conditions to compare and contrast the performance of various design iterations for an installation. It can do this without necessarily delving into the extreme detail of how each moving part works in terms of geometry and kinetics and not necessarily delving into the detailed design specifications on material properties such as strength and stiffness.

¹ MATLAB is a product of MathWorks Inc.

CHAPTER TWO: BACKGROUND

Early Examination of the Topic

Today, America's wind and hydro resources remain plentiful. Up to 12,000 megawatts of power capacity are available in currently untapped small-head resources [7]. "[This is] the potential equivalent to increasing the size of the existing conventional hydropower fleet by 15%" [7]. These resources are now becoming economically feasible to develop thanks to new turbine technology.

Many turbine designs have been proposed over the years to maximize the power production from flows of water and wind. One of the early designs that is uniquely American is the Darrieus vertical axis turbine. This turbine was extensively researched by the US government, and many were built and tested in the 1980s as a result of federal funding. The Darrieus turbine is a lift machine that uses foils rotating around a fixed vertical mast with a generator that can be located at either end of the machine axis.

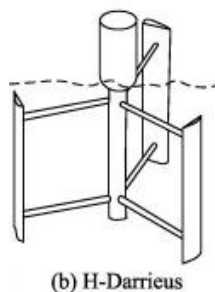


Figure 1: Sketch of a Darrieus-style Water Turbine [8]

Darrieus turbines are one of two main species of VAWT. The second kind of VAWT is known as a Savonius rotor. The Savonius rotor is similar in design to a Darrieus turbine. They both rotate along a vertical axis, and have a generator located at one end of the rotor shaft.

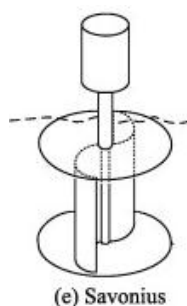


Figure 2: Sketch of a Savonius (Drag-Based) vertical axis water turbine [8]

Unlike a Darrieus turbine, the Savonius operates on the principle of drag as opposed to aerodynamic lift “catching” the flow of a fluid in wings shaped like halves of a bucket. The fluid glides more smoothly around the curved back of the wing, and catches and slows in the concave sides of the wings. When the Department of Energy launched a study of vertical axis wind turbines, Darrieus turbines were studied while Savonius turbines were not. The reasons for this are three-fold. First, Savonius machines are generally much heavier than Darrieus turbines. Secondly, Savonius wind machines are not able to handle high winds and are subject to catastrophic failure when they experience high velocity gusts. Lastly, the Savonius vertical axis turbines operate on the principle of drag forces, and drag machines are inherently less efficient than lift machines in most applications [8].

All turbine blades operate on the principles of lift and/or drag. The goal of any turbine design is to capture the maximum amount of energy from the flow of a fluid. The conversion of flow energy into work is done by converting the linear velocity of the fluid flow into rotational velocity of a rotor. The more the blades resist the flow, the more torque is developed on the generator shaft. The torque on the shaft is related to the energy that can be captured from the flow. Torque, a unit of force times distance, is measured in Newton-meters. Knowing the rotational speed of the shaft (radians per second) and the torque on the shaft (Newton-meters) allows one to calculate the energy captured from the flow by the turbine. Prior to the nineteenth century, most turbines were designed to maximize the drag force on each blade to increase the torque. Traditional wind and water wheels used either large flat paddle-like shapes or buckets to “catch” the wind or water flow as they drift with the current. For these machines, their maximum tip speed of the rotor can never be greater than the free-stream velocity. In the last century, most turbine designs have attempted to maximize lift instead of drag as the primary aerodynamic force that drives rotation.

The drag force on an object is a combination of the object’s shape, and the roughness of its surface. Similarly, the lift force also depends on an object’s shape. For a non-symmetrical object in a moving fluid, the streamlines move around the two different sides of the object differently before meeting at the trailing edge; see Figure 3.

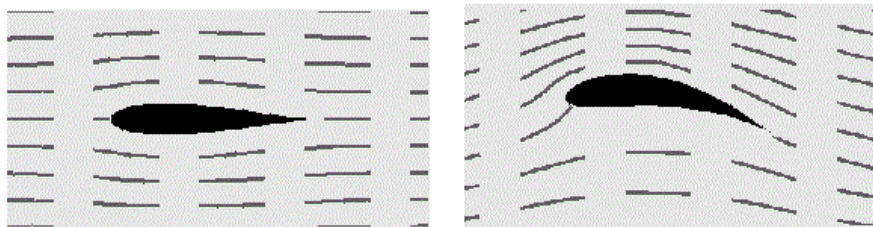


Figure 3: Streamlines around an airfoil. Figure reproduced from [9]

This deflection in the flow as seen in Figure 3 result either from the shape of the object or its angle to the flow causing a lower pressure on the side of the object with the higher velocity (the side of the object with the narrower stream-tubes; e.g., the curved side of a semicircle). This pressure differential results in lift — the aerodynamic force perpendicular to the flow. Modern turbines operate by using airfoils or hydrofoils for wings that are shaped to maximize the lift force. The lift force and drag forces on the wings produce a torque on the rotor. The rotor is connected to a generator that uses the torque and rotation of the rotor shaft to excite an electric current.

While drag is an aerodynamic force on an object that is parallel to the flow — e.g. the current of a river or what most people call “wind resistance”— lift is the aerodynamic force that is perpendicular to the flow. Thus, by definition, the lift and drag forces on an object are always perpendicular to each other regardless of its orientation as in Figure 4.

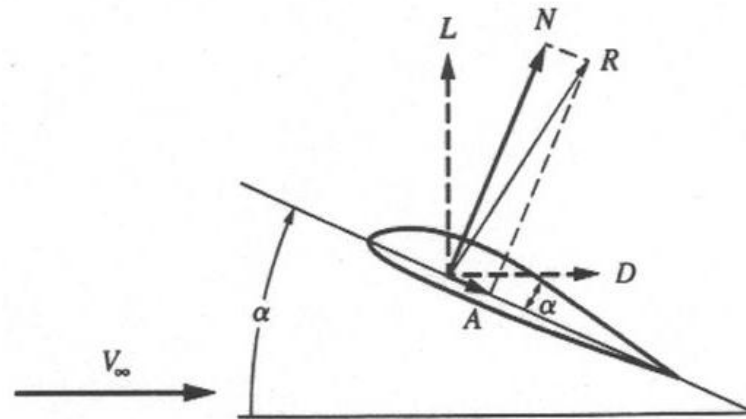


Figure 4: Lift and drag on an airfoil. Figure taken from [10]

V_{∞} = Free-stream fluid velocity

α = Angle of attack

L = Lift force

D = Drag force

R = Resultant force

The lift and drag forces displayed in Figure 4 can be combined through vector addition into a resultant force, R. Although the direction of the lift and drag force vectors depend only on the direction of fluid flow, the orientation of an object (such as a foil) determines its angle of attack. The angle of attack, α , is the difference in angles between the relative fluid velocity and the chord of the foil. The magnitudes of the lift and drag forces on an object are dependent on the value of α .

The three foils of a horizontal axis turbine experience a smaller range of α as compared to their VAWT counterparts. Most horizontal axis turbines today can minimize their ranges of α by adjusting the pitch of the foils in order to maximize the lift force while minimizing the drag on the foils. The goal of pitch adjustment is to maintain the foil at an optimal value of α , which is usually between $5^{\circ} - 12^{\circ}$, depending on the

shape of the foil and the fluid velocity. These smaller the angles of α generally maximize the lift force without greatly increasing the drag force. Once α exceeds a “critical” value of about 15° - 20° , then the flow separates from the foil reducing the lift force so that the drag force dominates. This is a condition known as stall. Stall is a flow condition that affects both horizontal and vertical axis turbines. It is sometimes used for speed-control, but often is blamed for limiting power performance. If stall occurs, the turbine will lose all of its torque and will rapidly decelerate. Figure 52 and Figure 53 in APPENDIX C show the lift and drag profiles of a foil profile that was used in the model.

Most modern turbines have ways of changing the angle of the foils in order to influence the lift force and consequently change the torque on the generator shaft. Often this is done to prevent over-loading the bearings on turbines that could result in severe mechanical or structural failure should the forces grow too large. At other times, this is done to reduce the power output of the turbines to better match the needs of the grid. If the need for power is suddenly reduced, the operators of wind farms are sometimes required to stop the turbine’s power output or to at least reduce it to prevent over-loading the grid curtailing the power output of the wind farm. This is done by a process of “furling” the turbines. They do this by feathering the blades: changing the α bit by bit until the magnitude of the lift forces and consequently the torque on the generator is sufficiently reduced.

Lift-based turbines have the ability to rotate at much higher speeds than drag-based turbines. This is because blades at the end of a drag-based rotor can never travel faster than the linear velocity of the fluid flow. The buckets of an old water wheel are pushed along by the flow of the river, and have no ability to move faster than the flow

unless acted on by an outside force. However, the foils of a lift rotor can and often do exceed a tip-velocity faster than the ambient stream velocity. Both lift and drag coefficients have similar maximum values, but the lift machines are able to harness much more power because their rotors can reach much higher rotational velocities than the rotors of drag machines. Since Darrieus turbines are more efficient and lighter than Savonius machines [8] [1], these were the VAWTs that received special attention by researchers at the U.S. Department of Energy.

The rotational speed of the turbine is based on the on the rotor diameter and the speed of the foils. For lift-based turbines, the tangential velocity of the foils often exceeds the fluid velocity. The ratio between the blade speed and the free-stream fluid velocity is the Tip Speed Ratio. The tip speed ratio (TSR or λ) is equal to the rotational velocity times the radius divided by the free stream velocity. In mathematical terms, it appears thus: $\lambda = \omega \times \frac{R}{V}$

In order to develop functioning turbines, the lift and drag profiles of the airfoils to be used must be well understood. The lift and drag of these foils is what provides the torque necessary to turn the generator and produce power. Extensive research has been conducted. Governments as well as private enterprises, such as Boeing, determine the lift and drag profiles of various airfoils. And much design effort has been devoted to optimizing turbine performance under steady-state conditions. However, great insight can be gained from looking at a dynamic model that combines these two fields. During the space race between USA and the USSR, many researchers were dedicated to calculating the lift and drag of a number of different shapes of airfoils over a range of flow speeds, as they sought to find the right shape of foil for taking a heavy object into

space. These studies concentrated on maximizing lift and minimizing drag for peak performance. However, the lift and drag data for airfoils past their stall angle is rare. Few designs for aircraft wings were considered through 180° of angles of attack (few planes remain airborne after exceeding the stall angle of about 15°). Much data has been gathered for airfoils of all shapes and sizes with very narrow angles of attack. Very little lift and drag data for different airfoil shapes, however, is published for angles of attack that go past the stall angle (usually about 15°). The analysis of flow over the wing of a vertical axis turbine requires the lift and drag profiles through an angle of attack of 360° (or at least 180°). Research papers that included full 360° analysis were not developed and published until the 1970s.

Following the 1973 Oil Crisis (and consequently a renewed public interest in keeping energy sources domestic), several government labs received funding to do research into alternative energy. One of these labs, Sandia National Laboratory in Albuquerque, New Mexico spent much time and effort developing designs for vertical axis wind turbines (VAWTs). Their research included analysis of several NACA (National Advisory Committee for Aeronautics) airfoil profiles in a range of flow conditions, testing the lift and drag of each at a range of angles of attack from 0° to 180° . This data was tabulated according the Reynolds number of the flow. The Reynolds number is a ratio of inertial forces to viscous forces in a fluid.

$$Re = \frac{V\rho L}{\mu}$$

V = Fluid velocity
 L = Chord length of the foil
 ρ = Fluid density
 μ = Fluid viscosity

This dimensionless number, developed in 1883 by Osborne Reynolds [11] can be calculated for any fluid flow. This allows the lift and drag data of many airfoils to be compared against the same dimensionless parameter. The lift and drag data for this computer model came from a report published by Sandia National Laboratory written by Robert E. Sheldahl, and Paul C. Klimas [12].

The set of data gathered in the above report forms the base of the dynamic computer model that was developed in this thesis. Information from this study allows for the calculation of the physical forces exerted on the blades of the model turbine at any moment by interpolating from the lift and drag data presented in these tables. A dynamic model requires lift and drag data through 360° range of foil rotation. The wind-tunnel data allows for the development of a fully dynamic model that would accommodate a range of speeds, flow conditions, and blade articulations. The data tabulated consisted merely of lift and drag coefficients for several differently shaped airfoils. These coefficients can be applied to both wind and water flows for calculating foil lift and drag forces to determine the overall torque on the machine developed from the flow conditions.

Knowing this, and being equipped with a solid set of aerodynamic/hydrodynamic data available for airfoils, focus turned towards the dynamics of power production. Many turbines are currently equipped with generators that operate given a constant or nearly constant rotational input. The pitch, yaw, and brake systems on large horizontal axis wind turbines are employed to keep the blades rotating at as close to constant a rate as possible.

For turbines, the Tip Speed Ratio (TSR) provides an important metric for comparing turbine performance because the TSR is always related in some way to achieving the goal of power production. Research done at Sandia National Lab demonstrates the importance of the Tip Speed Ratio on the power coefficient of the turbine. As the TSR increases, the power production follows a quadratic curve.

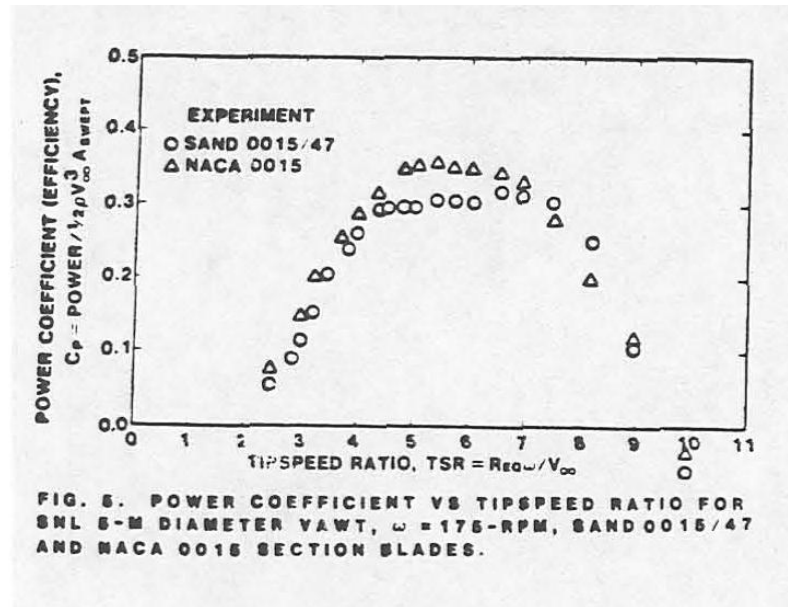


Figure 5: Graph of Turbine Power Output versus TSR [12]

In the figure above, data is plotted from tests at Sandia National Lab showing that as the TSR increases, the efficiency of the turbine (in this case the coefficient of power) rises and falls in a quadratic fashion. In other words, changing the TSR of the turbine affects the generator performance and the loads required of it. Often the TSR is controlled by the loading of the generator; other times the generator load is fixed and the TSR is influenced solely by the flow velocity. When the flow velocity is kept constant (as in a laboratory experiment), the more resistance that is supplied by the generator - the

more torque is required of the turbine (from the lift and drag of the foils) and the slower the turbine rotates.

The report [13] from which Figure 5 was taken focused on the optimization of blade shapes in order to achieve the ideal tip speed ratios for power production. It was assumed that the foil angles would stay fixed throughout their rotation around the central axis of the VAWT's. As such, the Sandia lab focused on sharp stall, and wide drag bucket designs for the airfoils studied. However, a second route exists for optimizing efficiency of the turbine: having the blades pitch while they are rotating. Some work has been done on the theory of dynamic pitch, but little empirical work has been done on the matter. In a recent study [14], Staelens et al. presented a compelling argument for the ideal amplitude of a theta varying pitch: "The maximum amplitude of the sinusoidal correction function is set equal to the maximum difference between the local geometric angle of attack α , and the blade static stall angle α -stall." The above theories have the potential to dramatically change the operation of standard VAWTs and greatly increase their efficiency. They are explored in the model that was developed.

The Betz Theory of Efficiency

Typical analysis of wind and water turbines is done by applying the Betz analysis in order to determine the efficiency of the turbine and the energy available in the fluid flow. The Betz theorem was developed by the engineer Albert Betz in 1919 [11]. The analysis began with a basic hypothesis of how much energy is available in the fluid flow. If the water flowing through a turbine is considered to be a control volume, then the kinetic energy (KE) of its body is one half of the mass times the velocity squared. The

energy extracted by the turbine was found by taking the difference between the upstream and downstream velocities, V_1 and V_2 .

$$\text{Kinetic Energy} = \frac{1}{2}mV^2$$

$$\text{Turbine Energy} = \frac{1}{2}m(V_1^2 - V_2^2)$$

m = Mass of the fluid (in a control volume around the turbine)

V_1 = the upstream velocity

V_2 = the downstream velocity

Betz then applied the continuity equation, which states that the mass flow rate must remain constant; that is, the mass flow rate upstream of the turbine is the same as the flow rate downstream of the turbine. The flow rate through the turbine itself is then equal to the average flow rate just upstream and just downstream of the turbine:

$$\dot{m}_1 = \rho A_1 V_1 = \rho A_2 V_2 = \dot{m}_2$$

$$\dot{m} = \rho A \frac{1}{2}(V_1 + V_2)$$

\dot{m}_1 = Mass flow rate upstream of the turbine

\dot{m}_2 = Mass flow rate downstream of the turbine

A_1 = Area of the flow upstream of the turbine

A_2 = Area of the flow downstream of the turbine

ρ = Density of the fluid

V_1 = Area of the flow upstream of the turbine

V_2 = Area of the flow downstream of the turbine

Differentiating the turbine energy equation above, and then substituting the flow rate with the flow rate of the turbine given above yields the power available in terms of the density of the fluid, the area of the turbine, and the difference between the upstream and downstream velocities.

$$P = \frac{1}{2} \dot{m} (V_1^2 - V_2^2)$$

$$P = \frac{1}{2} \rho A \frac{1}{2} (V_1 + V_2) (V_1^2 - V_2^2)$$

P = Power

Graphing this equation against a ratio of $\frac{V_2}{V_1}$ with ρ and A held constant yields the

following:

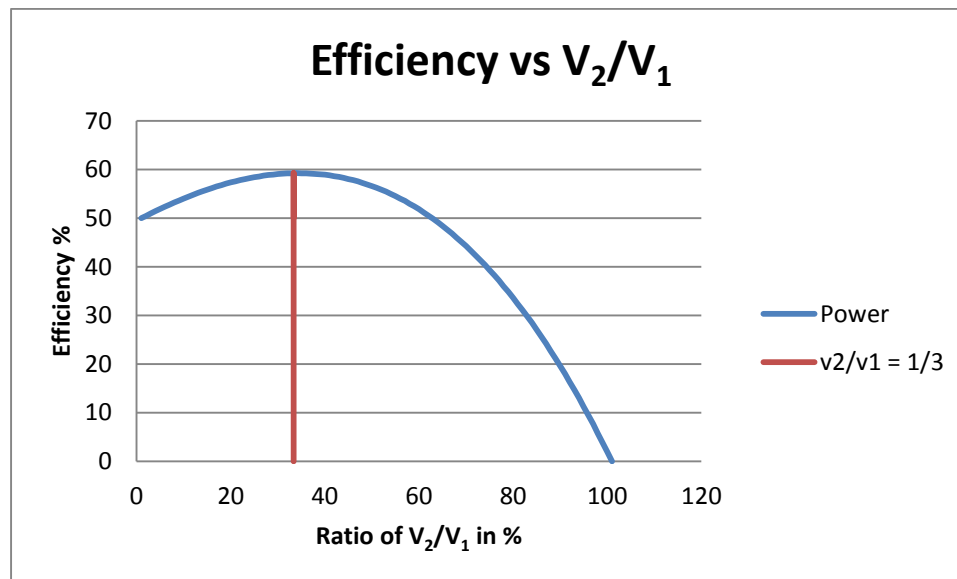


Figure 6: Using the Betz Theory to Predict Maximum Efficiency Based on the Ratio of Exiting Flow to Incoming Flow Velocity

As can be seen, according to this theory, the maximum efficiency that can be achieved by a turbine harvesting kinetic energy from a fluid flow is 59.3% when the ratio of $\frac{V_2}{V_1}$ is at exactly one third [11].

Articulating Foils

The articulation of airfoils (also referred to as ‘wings’ or ‘blades’) is a term used to describe the alteration of the pitch of foils as they rotate about the turbine axis. This is one particular control feature of wind and water turbines that models can be used to explore. In order to understand the ways that foils can be articulated, it is important to understand the three major turbine designs that are prevalent today. These turbine rotor types include horizontal axis turbines, vertical axis turbines (usually of the Darrieus design), and Savonius rotors.

Most commercial wind turbines today are large horizontal axis turbines [15]. Although large horizontal turbines can effectively harvest energy from wind, they have several drawbacks. They are significantly less efficient when subjected to low, unsteady, or turbulent flow conditions. Horizontal turbines are also designed to capture wind approaching from one particular direction. If the wind’s direction changes, the turbine performance quickly drops. Then, the entire nacelle and blades must be rotated by some mechanism at the top of the tower to turn and face the new direction. Large horizontal turbines are also equipped with pitch mechanisms that allow for furling the turbine to reduce mechanical damage during high wind velocities and to shed power to serve the needs of the grid.

Vertical machines, in contrast, can handle low, unsteady, and turbulent flow conditions far better than horizontal machines [16]. And, they can capture wind blowing from any direction, without requiring any external adjustment. Depending on the design, some VAWTS (and HAWTs) are even able to take advantage of stall at high velocity

conditions — using a self-limiting device to avoid mechanical and structural damage during very high winds.

Unfortunately, VAWTs are not without their own set of drawbacks. The Darrieus wind turbine is not able to start rotating from zero velocity. Once the turbine is rotating, the lift and drag forces on the wings are self-sustaining so that the turbine will continue to rotate and generate torque without outside help. This is due to the induced velocity developed by the wings, which provides the blades with a more beneficial angle of attack. However, sufficient induced velocities (and corresponding α values) only develop when the tip-speed-ratio reaches a value of 1 or more. In fact, in the Department of Energy project in Albuquerque, scientists had to find creative ways to get the turbines to start generating power. This is evident in an anecdote from a Sandia report: “Putting the test turbine in motion was no easy feat – researchers patiently waited for the wind to begin to blow, strapped themselves onto the roof of the building and spun the blades by hand. Whenever a thunderstorm would blow into Albuquerque the engineers rushed to the laboratory, climbed the roof, and began turning the blades” [1]. Obviously full installations do not rely on scientists physically turning them, but they do require some mechanical device to begin the rotation. Thus, these turbines act as a power *draw* before they can act as a power *source*, putting additional strain on the grid. Conventional gas turbines face the same problem.

Due to the difficulty of self-starting, designs have been proposed for combining Darrieus turbines with a central Savonius rotor so that the turbine would begin rotating of its own accord without the need of a power draw. Several of these combinations are in operation in Taipei [17]. However, the engineers at Sandia decided that incorporating the

components required for the Savonius machine would be too large, and would add too much stress to the overall turbine.

Other scientists have challenged the notion that no VAWTs can self-start. Some studies have been done on Darrieus style VAWTs that show them beginning to rotate from a complete standstill. One of the most recent of these studies [18] was conducted by developing a numerical model of a small VAWT (an empirical test was conducted in a wind-tunnel). This study has provided some of the most useful data against which the computer model may be tested. Experiments were performed on a horizontal axis water turbine in a flume at the University of Oxford [19]. The measurements from the study provided empirical data that were used as a metric against which the performance of the MATLAB model could be judged.

While some have concluded that starting a two-bladed Darrieus turbine is impractical because it would only happen under certain wind conditions, new studies have shown promise for three-bladed turbines [18]. Novel elements are also being incorporated into the traditional Darrieus patent, including mechanisms to change the pitch of the blades. Changing the pitch of the blades can change the angle of attack of the resultant wind for each blade. Even a fixed-pitch VAWT allows for better lift, contributing to the self-starting of a three-bladed turbine. Some machines have even been outfitted with pitch-control components operated electronically. While this may sound expensive (and it is), some of the data suggests that implementation of pitch-control devices could dramatically increase the annual energy output of the turbine. A report by Hansen et al. [20] states: “The optimized pitch enhanced the turbine performance at the design point and in a relatively narrow wind speed domain around it. In off-design

conditions the optimized pitch was detrimental to the turbine performance, thus imposing optimizations at other wind speeds. For a pitch variation optimized throughout the low wind domain, an increase of almost 30% in the annual energy production of the turbine could be obtained.”

One of the most innovative features that can be incorporated into the design of new turbines is accomplished by controlling the pitch using simple mechanical arrangements and cables in the machine that allow the blades to change their angle of attack dynamically. It negates the need to install any electronic controls of pitch whatsoever. This feature may also alleviate some of the dynamic stall losses, which reduce efficiency. In addition, the entire rotor can also be allowed to freely tilt into the flow, allowing a unique response to wind and water flow in any direction.

A recent design capitalizing on this idea was the BlackHawk Project developed by Bruce Boatner [21].



Figure 7: Installation of a BlackHawk TR-10 VAWT [21]

This turbine features a global journal bearing at the center of the rotor allowing the rotor arms to tilt from side to side.

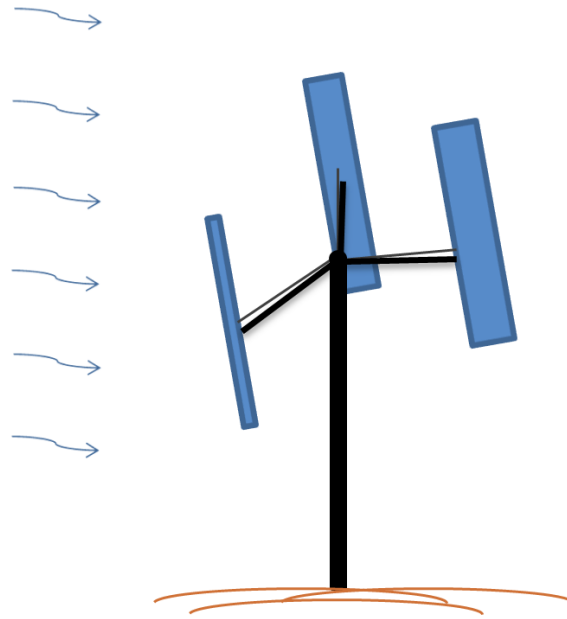


Figure 8: Illustration of BlackHawk turbine with tilting foils

It is small in scale (a rotor diameter of 7ft and a weight of only 120 lbs), and provides a rated power output of 1.5 kW. Because of its small size and light weight, when the wind hits the structure, the drag from the foils causes the whole rotor to tilt against the flow. As this happens, rods between the foils and the rotor hub alternately push or pull the foils into a different angle based on the rotor tilt. They are designed in such a way that as the rotor tilts against the wind, the wings are pitched into a favorable angle of attack, α , developing lift and allowing the rotor to begin rotating at the relatively low speed of 7 mph. As the foils rotate along the tilted plane, their angles change, based on whether they are on the low or high side of the rotor corresponding to the upwind and downwind sides of the turbine. The design intent was to obtain the best α for the foils as

they rotate by adjusting them in a periodic motion. This design was studied extensively using the computer model developed in this thesis.

Ideally, turbines would be able to articulate their foils to catch the best angle at every point in their rotation around the axis in order to maximize their torque. This is the theory that Staelens et al. explores in his paper [14]. He posits three ideal examples of turbine articulation. The first concept is to keep α at slightly less than the local stall angle, ensuring maximum lift. Unfortunately, this concept cannot be realized in a physical turbine because in order to maintain this constant angle, two discontinuities are required during the rotation — one at 90° and one at 270° . A second concept proposed a slightly more gradual adjustment at these points, but still requires sudden changes in blade angles that could prove disastrous to a mechanical system at high speeds. The third concept Staelens proposed to increase efficiency was to vary the pitch sinusoidally through the full rotation — allowing for smooth transitions of blade angles, while still capturing some of the advantages of keeping α close to the stall angle and maintaining high lift coefficients and maximizing drag on the forward sweep. One example of articulation can be seen in Figure 9.

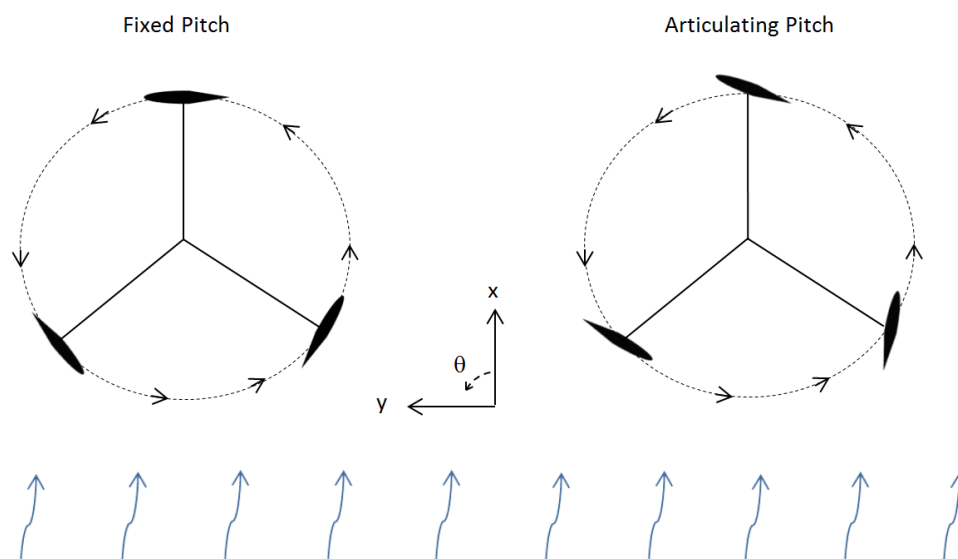


Figure 9: An example of articulated foil pitch in rotation

The first two of these ideas on pitch articulation prove thus far to be physically unattainable because of the difficulty of abruptly changing the angles of the foils mid-rotation; it would break any motor or system attempting to do so. Yet the theory remains intriguing. And since computer models have no physical restrictions, these theories can be applied to dynamic models of wind and water turbines to verify their predictions of maximum efficiency and confirm the mathematic estimations that were established. From here, developers may choose a path forward that approximates this ideal variable pitch behavior with physical models that capitalize on these theories. Variable pitch is of economic interest to VAWT developers because many VAWTs lack the ability to start from rest. Dynamic pitching of the blades throughout the rotation if done properly can solve this problem.

Turbine Modeling

Physical experimentation of new turbine designs often proves to be both costly and time consuming. Each new design iteration may require many hours of research and

manufacturing time. Once the machine is built, instruments must be installed and extensive tests administered to verify the performance. A computer model that predicts performance of new design iterations can radically streamline the process. It allows manufacturers to focus on those new designs that have the most potential for innovation and improvement over past designs. Some of the new design features include generator loading and foil articulation. The details of the model are described in the following chapter.

CHAPTER THREE: METHODOLOGY

The Structure of the Model

The turbine model is set up as a system with a series of inputs, outputs, and a natural feedback loop. It was used to simulate the behavior of various VAWT and hydrokinetic turbine arrangements to see how the designs reacted to different situations and how they could be improved. The state variables included the turbine's angle, rotational velocity, and the induced flow velocity (all physical quantities changing with time). The inputs included those variables outside the system such as wind-speed and air temperature. The state variables were the variables required to define the system dynamics and included the outputs of the integrals. The parameters of the system were constants of the model like inertia, length, mass, diameter, airfoil profile, etc. The information from each iterative step of the system (some of which comes through feedback loops) is used to compute the lift and the drag on the foils. The lift and drag information on each foil is then used to calculate the torque on the rotor due to aerodynamic forces. A feedback loop subtracts the torque due to the generator from the aerodynamic torque to give the net torque. The information from the net torque allows for the calculation of the resulting rotational velocity (ω) and the position (θ). The velocity and the position are then used as inputs to a simplified model of a generator, which then calculates the theoretical power output. A full schematic model with feedback loops appears in APPENDIX B (Figure 45), while a simplified model is shown in Figure 10.

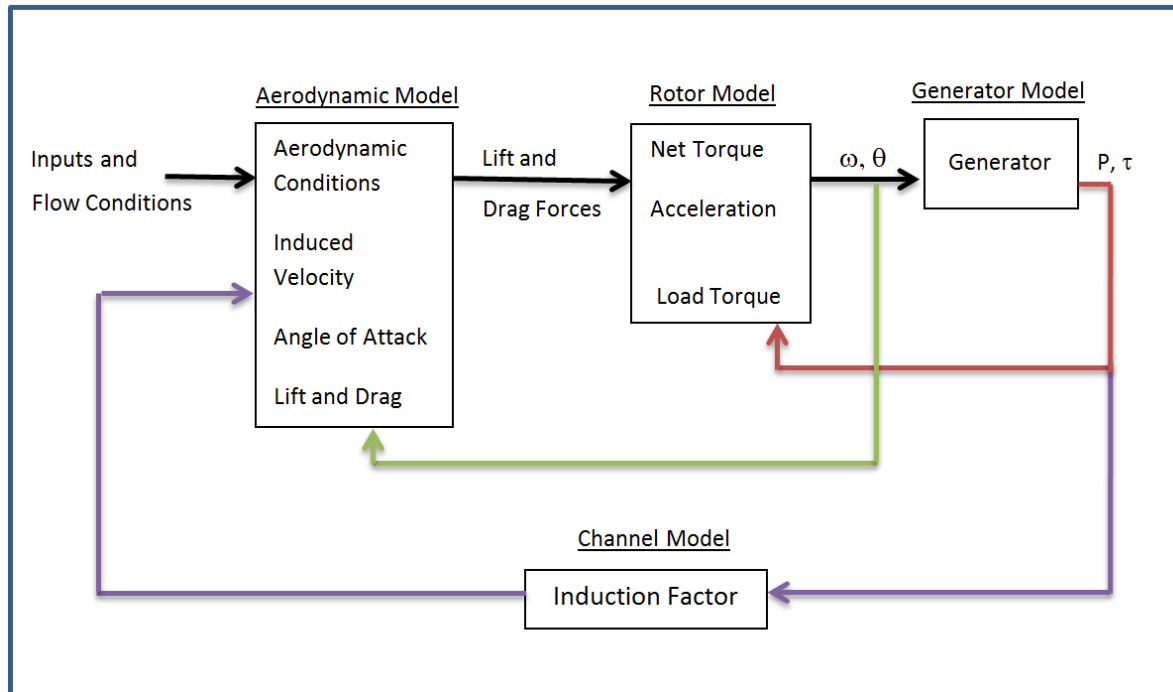


Figure 10: Simplified Model of the Program Showing Inputs and Feedback Loops

- θ = Rotor position
- ω = Rotational velocity
- P = Power
- τ = Torque

The overall system consists of four models all working together. Feedback loops connect the outputs of some models so they can be used as inputs for others. The aerodynamic model calculates the lift and drag forces on a foil given the incoming fluid velocity and rotor speed and position. The rotor model inputs include the lift and drag forces on each foil as well as resistive torque from the generator load. The rotor model then uses that information to compute the rotor's resultant position and rotational speed. The rotor model outputs are then given to the generator model, which provides a resistive torque on the rotor and estimates the power output. The power output is used by the

channel model to estimate how much the fluid slows through the turbine and when applicable estimates the resulting water level rise in a channel.

There are three feedback loops between the models that allow the system to function. The first feedback loop (in red) is from the generator model to the rotor model. This loop accounts for the reduction in the available torque to account for energy passing out of the system through the generator. The second feedback loop (in green) is from the rotor model back into the aerodynamic model to give its current configuration. This way, the model accounts for the change in position of the turbine after each time step. The third feedback loop (in purple) from the generator model back to the aerodynamic model uses the power output of the generator model to compute the relative wind, the resulting induction factor, relative wind, and the angle of attack. The induction factor accounts for how much the flow velocity entering the turbine is reduced because of the energy extracted by the generator.

This simplified modeling scheme is used by many mathematicians and engineers as a model for turbines of all kinds. It is a mathematical expression of how energy is gathered from a stream. The features that are unique to this particular model include a complex induction factor calculation and a reference to empirically verified lift and drag data. The equations for calculating instantaneous torque are some of the most complex in the model because they include both the lift and drag coefficient determination and a set of complex geometrical transformations. The most important feature of the model however, is not simply its organization, but how it is used to answer fundamental questions of dynamic response to changes in flow conditions, and the exploration of peak efficiency as a function of foil articulation throughout the turbine's rotation.

Defining the Geometry and the Initial Conditions

The first section in the model is the input information of the aerodynamic conditions and rigid body dynamics. Initial geometric (rigid body) conditions include the position and rotational speed of the foils. The aerodynamic conditions consist of the fluid properties, the airfoil lift and drag properties, and the inertia of the system. The fluid properties are the velocity and density of the flow, as well as the fluid viscosity. The two fluids used in this analysis were water and air at standard ambient temperature and atmospheric pressure (25 °C and 100 kPa).

One of the main differences between the models for wind turbines and the models for turbines was the blockage feedback loop. The fluid properties of air allow it to be very compressible. Thus, in an open space, there are no significant upstream air-flow changes due to the installation of a wind turbine. Water on the other hand acts as an incompressible fluid. The incompressibility of water leads to an upstream depth change when the installation of a turbine in a channel restricts the path of the flow.

The lift and drag properties were those defined by Sheldahl and Klimas [11] for two different symmetrical airfoils labeled NACA 0015 and NACA 0018. These two airfoil profiles were chosen because the data of their lift and drag properties were readily available and closely matched the foil installed on the BlackHawk TR-10 (NACA 0014). The lift and drag coefficients were listed for 11 different Reynolds numbers between 10,000 and 10,000,000. The lift and drag coefficients were provided for 119 different angles of attack between 0° and 180°. The values are mirrored from 180° to 360° as is shown in APPENDIX C (Figure 52 and Figure 53). Double linear interpolation was used

to compute specific lift and drag properties for any angle and any Reynolds number within that range.

For all velocity conditions below a Reynold's number of 10,000, the lift and drag conditions for the lowest recorded Reynolds values were used (those at $RE=10,000$). A Reynold's number of 10,000 with a chord length of 0.25m is associated with a flow velocity of less than 0.062 m/s (0.015 mph) for wind and a velocity of less than 0.011 m/s (0.025 mph) for water. These flow velocities were a full order of magnitude lower than the lowest setting of velocities used in the simulations (0.5 m/s). The only exception to this was for the few simulations that were run with a ramping flow velocity starting from zero. Even so, the step of values between 0 m/s and 0.06 m/s was reasonable for a fluid velocity ramp from 0 m/s to 15 m/s over a period of several minutes.

The inertia of the system was a result of the the rotor's mass. The inertia of the turbines was calculated by using a thin-shell approximation; this assumed the mass of the turbine wings to be evenly distributed around the rotor like a hollow cylinder. As the inertia is increased, the turbine resists sudden changes in velocity. In some instances, this can be a good thing. A high value of inertia will add stability to the turbine and will allow the turbine to keep rotating when the fluid velocity decreases momentarily. However, a high inertia will also result in a delayed start-up of the system. It can be difficult to propel this system into motion from rest.

In order to properly calculate the lift and drag on the foils at any one moment, the model needed a clearly defined geometry. The equations of motion that the model was built upon consisted of a series of coordinate transformations represented as matrices. There were three transformations from the global position of the rotor to the individual

angle of each foil. The first set of axes (called Frame Z) is a fixed, global frame that defines rotation of the foil about the z axis in terms of an angle θ (Theta). The second frame (A) rotates with the rotor. It shares the same z axis as frame Z, but its x and y move with θ at a rotational velocity of ω (Omega). Frame B is translated out to the foil itself where its y axis is tangent to the circle of rotation. Frame B shares the same direction for x as frame A, but its z axis is offset from frames 1 and 2 by a distance of R, the turbine's radius. The foil coordinate frame (C) shares the z axis of frame B, but is rotated so that its x axis is in line with the chord of the foil. The pitch of the blade is described by ψ .

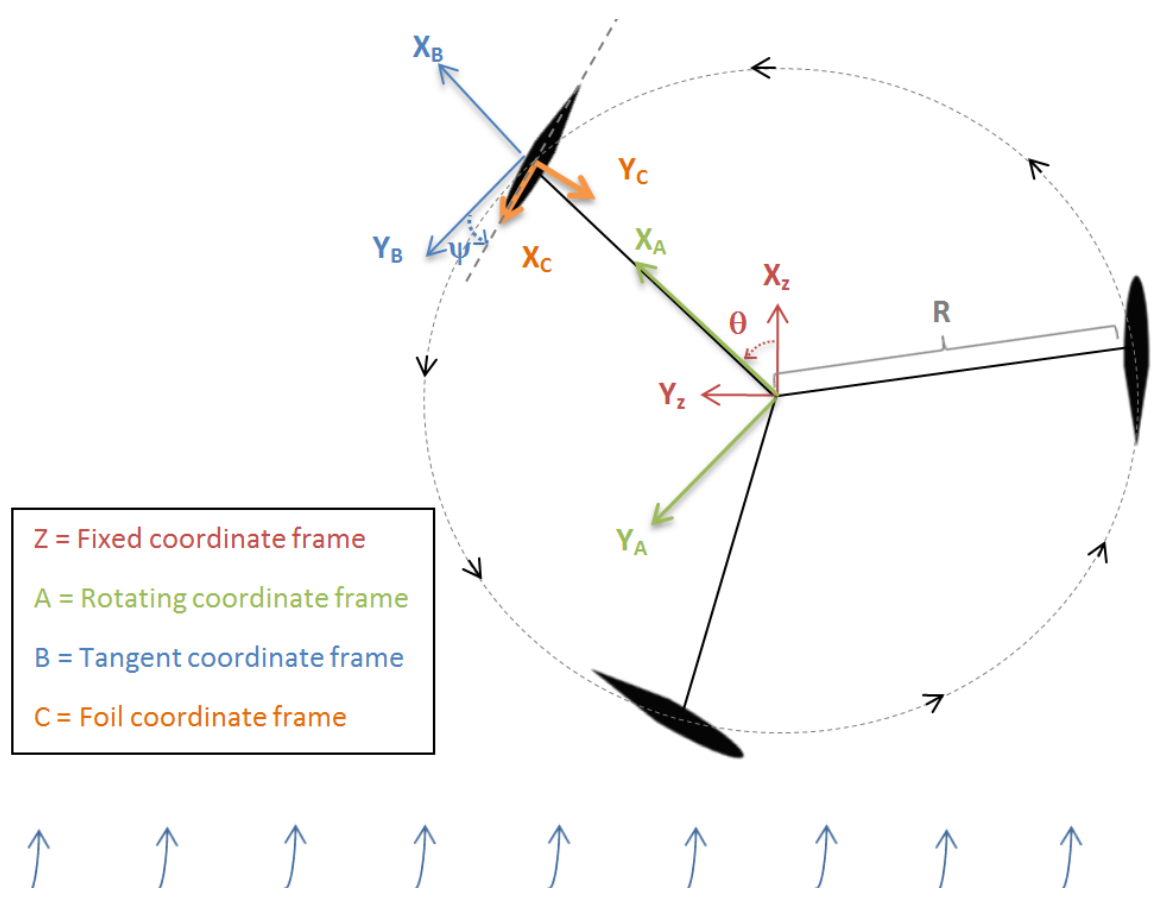


Figure 11: The motion and three geometric frames of a model for a vertical axis turbine

The reason there are four frames as shown in Figure 11 is to provide a coordinate frame that could describe the angle of attack on the foil so that the lift and drag could be calculated according to the relative velocity at each foil. The product of these three transformations allows for smooth communication between the global geometry of the model and the individual pitch of each blade at every point in the rotation. Frame A to Frame B translates between the rotor and the end of each arm. Frame B to Frame C translates between the rotor arm and the pitch of the foil. Frame Z provides the information on the position and rotational velocity of a foil at any time while Frame C provides the information on the pitch of the foil and the angle between the foil and the relative velocity. The complete matrices and equations can be seen in APPENDIX A.

Calculating the Lift and Drag at Each Foil

When a fluid passes through a turbine, the two aerodynamic forces of lift and drag develop on each foil. These two forces are at orthogonal angles to one another — with the drag being parallel to the relative velocity at each foil just as shown in Figure 4. If one were to take a snapshot of a vertical axis turbine at rest as viewed from above, one would find these two forces acting on every foil like the diagram shown in Figure 12.

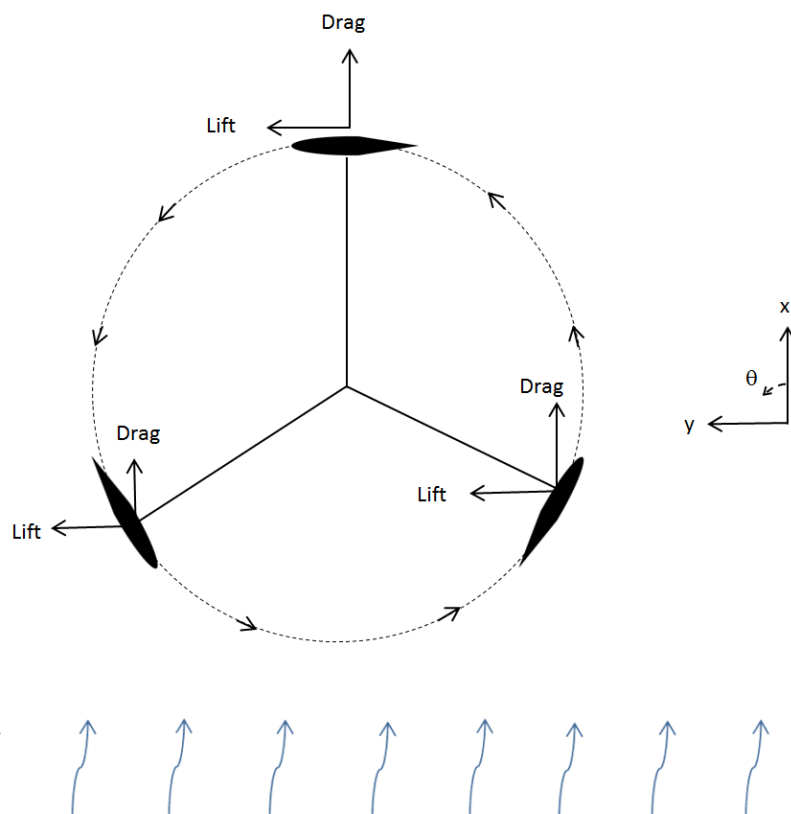


Figure 12: Diagram of the Lift and Drag forces for a VAWT at rest ($\omega = 0$) as viewed from above

For the purposes of this analysis, turbines with three foils were the primary focus of the study. By calculating the net force at each foil (the sum of the lift and drag forces) assessed, one can calculate the net effect of the six forces at work (three lift forces, and three drag forces). This net force, multiplied by the rotor radius, is equal to the torque of the machine at any given moment. This torque, then, is the energy per radian that can be used for the generator to provide an electric current.

Once the turbine in this example begins rotating, the relative velocity experienced at each foil becomes a combination of the free-stream velocity and the rotation of the foil. This changes the local fluid velocity and the resulting lift and drag forces both in terms of magnitude and direction. The local velocity at each foil can be determined using the

principles of vector addition to account for both the free-stream velocity and the velocity of the foil. This is shown in graphical form in Figure 13.

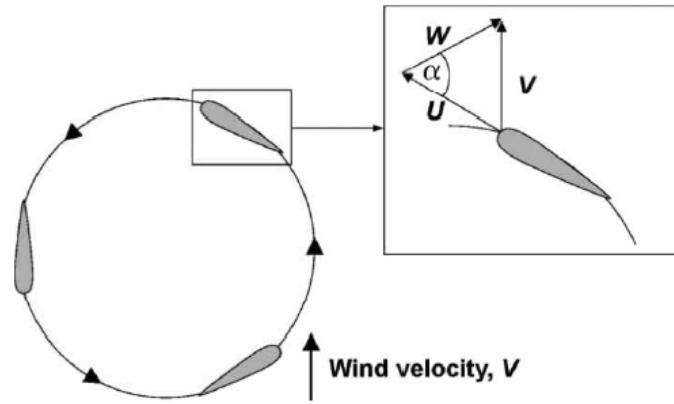


Figure 13: The angle of attack and Induced velocity on the wing of a vertical axis turbine. Figure taken from [18]

U = The velocity vector of the wing

V = The velocity vector of the fluid

W = The local velocity or relative velocity at the tip of the wing

The net velocity at each wingtip is referred to as the local velocity because it is different for each wing of the turbine (whereas the ambient fluid velocity is universal and independent of the wing's motion). In a way, this is like the wind on someone's face when they are standing on the prow of a moving ship. The wind that they feel is not only due to the ambient conditions (the same wind they'd feel standing still) — instead they feel a net wind that is a combination of both the ship's movement and the ambient wind. The rotation of the turbine alters the angle of net velocity to a direction that more closely resembles the circular arrangement of the foils as they fly around the rotor. This decreases α , increases the lift, and allows the turbine to spin up rapidly into a regime

where power production can begin. An illustration detailing the different velocities and aerodynamic forces on the wings for a rotating turbine is shown in Figure 14.

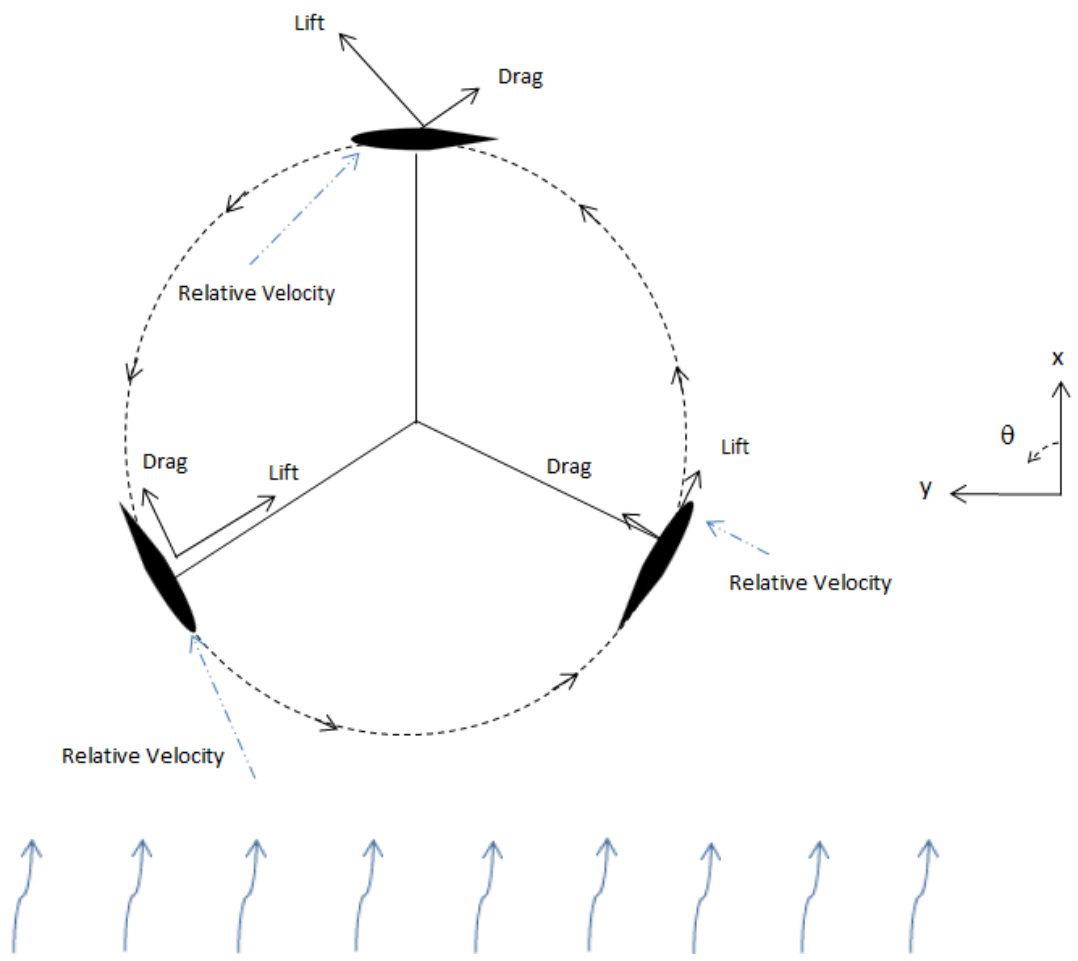


Figure 14: Diagram of the Lift and Drag Forces and Local Velocity for a VAWT in motion (TSR =1)

Calculating Torque

The geometric transformations allow the position of the foil to be calculated at any instant. The rotational speed and free-stream velocity define the local velocity at each foil. Knowing the direction of the local velocity and the position of the foil provides

one the means to calculate the angle of attack at each foil. With the information of the local velocity and angle of attack at each foil, the lift and drag forces are calculated by interpolating from tables of data [12]. The sum of the lift and drag forces leads to a net force or resultant force on each foil. The product of the resultant force vector on each foil and that force's perpendicular distance from the rotor gives the torque that the foil's arm exerts on the rotor. The sum of these three torques (one for each foil) is the total torque on the rotor that results in the rotation of the turbine.

This mathematical process was implemented as a script in MATLAB so that knowing the position and rotational velocity of the foils, the fluid properties, and the free-stream velocity, the torque on the rotor can be determined. The script was called `comp_torque` and can be seen in its script form in APPENDIX B.

The total flow velocity is broken into three components: X, Y, and Z. The three components of the flow velocity account for wind/water flow from the North (X), the East (Y), and vertically (Z). Vertical flows were not considered in this research, and could be a topic for future exploration. For the purposes of this study, the Z component was left at a value of 0. Assuming that the axis of the VAWT is the upward-pointing Z-axis, the flow experienced in the X-direction is the sum of the free-stream flow in the X-direction, and the X-aspect of rotational velocity. The flow experienced in the Y-direction is the difference of the free-stream flow in the Y-direction and the Y-aspect of rotational velocity. These components are shown in Figure 15.

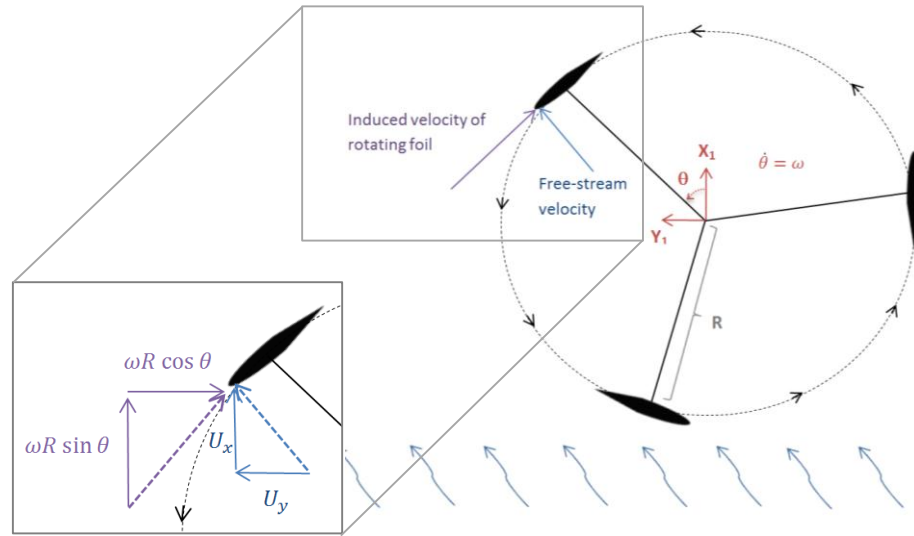


Figure 15: Vector components of the free-stream velocity and the tangential velocity at a foil

By adding each of the directional components together as shown in Figure 15, one can find the resultant, or relative velocity at each foil. The relative velocity vector, \mathbf{U}_T , is described by the following mathematical breakdown of the three dimensional vector in the global coordinate system (frame Z):

$$\mathbf{U}_{T_Z} = (U_x + \omega R \sin \theta)\hat{i} + (U_y - \omega R \cos \theta)\hat{j} + (U_z)\hat{k}$$

In order to transform this vector from the global coordinate frame system to the axes at the foil, the three elements of \mathbf{U}_{T_Z} are multiplied by the transformation matrix ${}^Z\Pi_C$ to account for the orientation and pitch of the foil. The pitch is given by the value of ψ , which is the angular difference between the chord of the foil and the line tangent to the perimeter of rotation at that position (see Figure 11). The alteration of ψ is the articulation function that was manipulated to change the pitch of the foil as it rotates.

APPENDIX B provides the full details of the development of ${}^Z\Pi_C$.

The transformation of the total relative velocity from the global frame to the foil frame is as follows:

$${}^z\Pi_C \times \mathbf{U}_{TZ} = \mathbf{U}_{TC}$$

$$\begin{bmatrix} -\sin \theta + \psi & \cos \theta + \psi & 0 & R \sin \psi \\ -\cos \theta + \psi & -\sin \theta + \psi & 0 & R \cos \psi \\ 0 & 0 & 1 & 0 \\ 0 & 0 & 0 & 1 \end{bmatrix} \times \begin{bmatrix} U_{TZx} \\ U_{TZy} \\ U_{TZz} \\ 0 \end{bmatrix} = \begin{bmatrix} U_{TCx} \\ U_{TCy} \\ U_{TCz} \\ 0 \end{bmatrix}$$

The resulting vector, \mathbf{U}_{TC} , describes the relative velocity in terms of the axes aligned with the foil that includes the pitch of the foil. The pitch can be treated like a function, or simply left as ψ , which indicates a turbine with a fixed pitch. For example, in Figure 15, the pitch is fixed with $\psi = 0^\circ$.

Once the direction of the relative velocity is understood in relation to the axes at the foil, the angle of attack is the arctangent of the y component of the relative velocity divided by the x component (in terms of the axes at the foil) of the relative velocity: $\alpha = \tan^{-1} \frac{U_{TCy}}{U_{TCx}}$. The value of α is iterated between 0 and 2π so data can be interpolated from tables. This is done by the following condition:

$$\text{if } \alpha < 0, \text{ then } \alpha = \alpha + 2\pi$$

While the direction of the relative velocity is known by \mathbf{U}_T , its magnitude is computed as the square root of the sum of the squares of each directional velocity.

$$U_{tot} = \sqrt{(U_{TZx})^2 + (U_{TZy})^2}$$

U_{tot} is the magnitude of the total flow velocity.

The total flow velocity in addition to the fluid properties allows one to compute the Reynolds number.

$$Re = \frac{\rho U_{tot} C}{\mu}$$

Knowing α and the Reynolds number, the coefficients of lift and drag (C_l and C_d) were interpolated from a table of values from previous experimental results [12]. Given the chord length and span length of foils (C and H respectively), the lift and drag forces could be computed using the following equations:

$$\text{The lift force: } L = \frac{1}{2} \cdot C_l \cdot \rho \cdot U_{tot}^2 \cdot C \cdot H$$

$$\text{The drag force: } D = \frac{1}{2} \cdot C_d \cdot \rho \cdot U_{tot}^2 \cdot C \cdot H$$

The only difference between the two aerodynamic force equations is that for the purposes of the MATLAB code, the sign (+ or -) of the lift force was based on the sign of alpha (this had to do with how the geometry in the model was defined). The lift and the drag forces on the foil produce a moment or torque on the origin of the rotational system (the hub where the generator is located for VAWTs). Recall that the direction of the lift and drag forces is always dependent on the direction of the relative velocity at the foil.

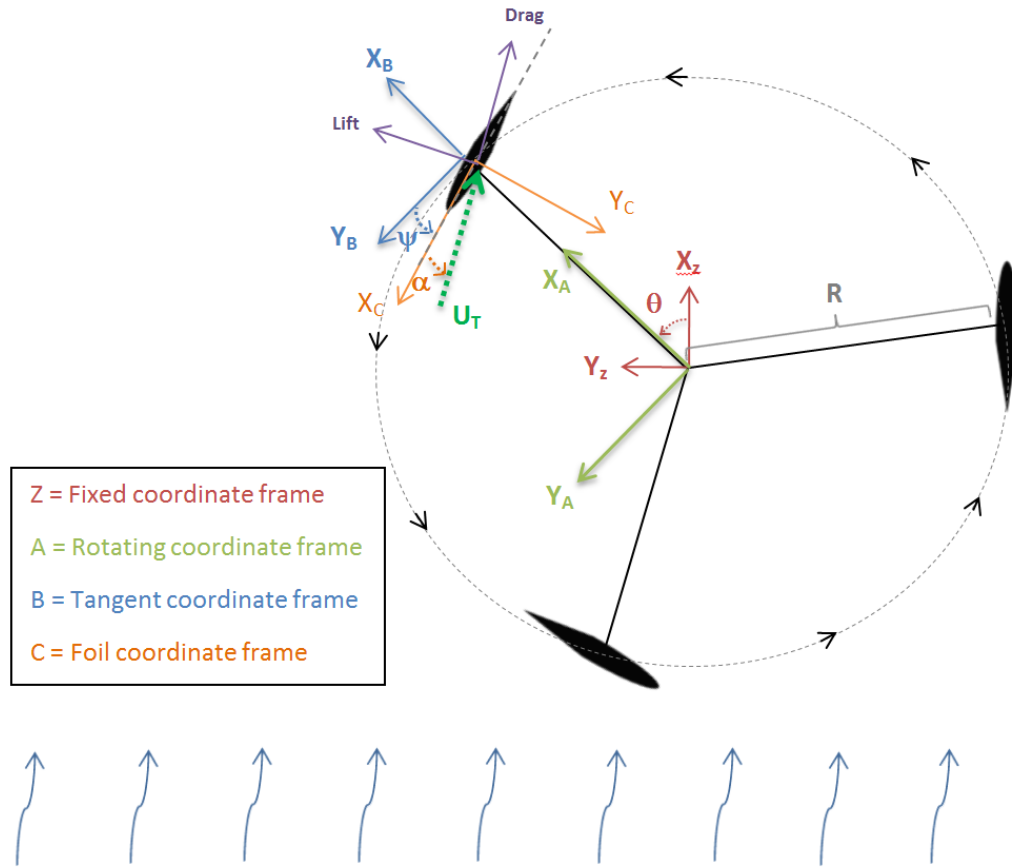


Figure 16: Lift and drag on a foil with ψ and α displayed

The resulting torque from the lift and drag displayed in Figure 16 is calculated using matrix transformations to transform the forces on the rotating foil to the fixed center of rotation. See Appendix A for complete details on the development of the transformation matrix, ${}^c\Pi_Z$, as shown.

$${}^c\Pi_Z = \begin{bmatrix} \cos \theta + 90 + \psi & -\sin \theta + 90 + \psi & 0 & -R \cos \theta \\ \sin \theta + 90 + \psi & \cos \theta + 90 + \psi & 0 & R \sin \theta \\ 0 & 0 & 1 & 0 \\ 0 & 0 & 0 & 1 \end{bmatrix}$$

The transformation matrix allows for the communication between the forces at the foil and the conditions at the fixed center of rotation. Torque is a product of the forces and their distance from the center. The drag force was defined as working in the positive x direction and the lift force working in the positive y direction. The distance from the center of rotation was the product of the radius and the corresponding trigonometric functions associated with each component:

$$\mathbf{R} = \begin{bmatrix} R \cos \theta \\ R \sin \theta \\ 0 \\ 1 \end{bmatrix} \quad \mathbf{F} = \begin{bmatrix} D \\ L \\ 0 \\ 0 \end{bmatrix}$$

The torque then becomes a product of these three matrices: $\tau = \mathbf{R} \times {}^c\Pi_z \times \mathbf{F}$.

This matrix multiplication simplifies down to a single equation as follows:

$$\tau = R \cdot L \cdot \sin(\psi + \alpha) - R \cdot D \cdot \cos(\psi + \alpha)$$

CHAPTER FOUR: MATLAB MODEL

Developing the Model for a VAWT

The computer model developed in this thesis is designed to mimic what would happen in a physical environment. The mathematical equations presented in the preceding chapter were translated into a system in MATLAB's program, Simulink. Simulink features a simple interface that allows one to see the calculations in block diagram form and clearly illustrates the model structure. The general structure of the model appears in Figure 10 while the specific blocks are shown below.

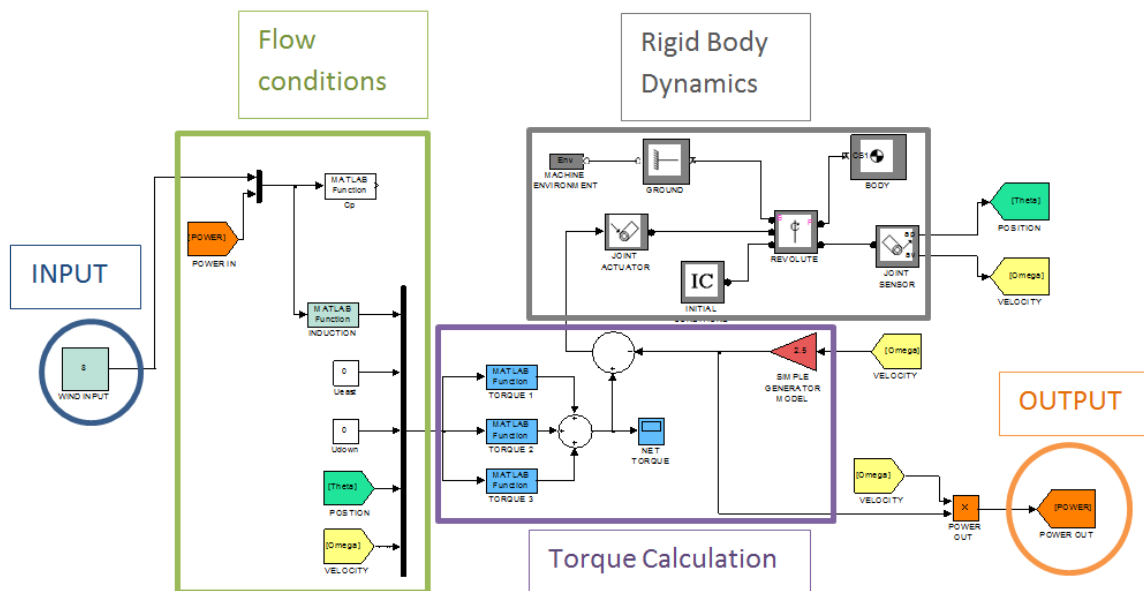


Figure 17: Overall view of the MATLAB Simulink model and its functions

The first section of the model was gathering initial conditions and calculating the torque at each foil. Three inputs for torque calculation include the fluid velocity, the rotor position, and the rotor velocity. The input fluid velocity is given in three different vector components: U_x , U_y , and U_z . For most simulations, U_y and U_z were left at zero. The input for U_x is not the free-stream velocity (which was usually a constant), but instead is an average of the upstream and downstream velocities. The free-stream velocity and the downstream velocities are different, because some of the kinetic energy is converted into another form of energy by the turbine through the generator.

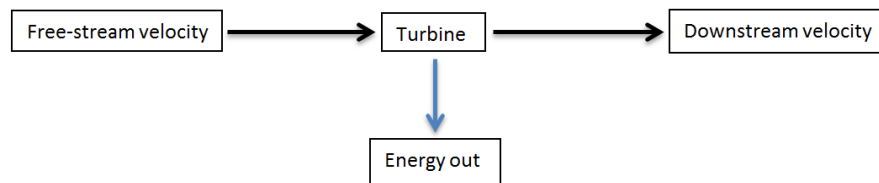


Figure 18: Energy flow diagram

The flow velocity experienced by the leading foil of the turbine is approximately equal to the free-stream velocity, while the flow velocity experienced at the downstream foil is approximately equal to the downstream velocity. Therefore, U_x enters the torque calculations through a feedback loop that accounts for the change in velocity as the wind passes through the turbine. This change in velocity is understood through the induction factor.

The induction factor is a ratio of the fluid velocity upstream of a turbine to the fluid velocity downstream of the turbine. The more energy is extracted from the flow by the turbine, the more the flow downstream of the turbine will slow. As such, the induction factor can also function as the ratio of the turbine power to the power in the

fluid flow [15]. This factor (symbolized by the letter a) is a function of the coefficient of power of the turbine:

$$C_p = 4a(1 - a)^2$$

C_p = Coefficient of Power

a = Induction Factor

When solving the equation for a (the axial induction factor), a cubic curve results as shown below.

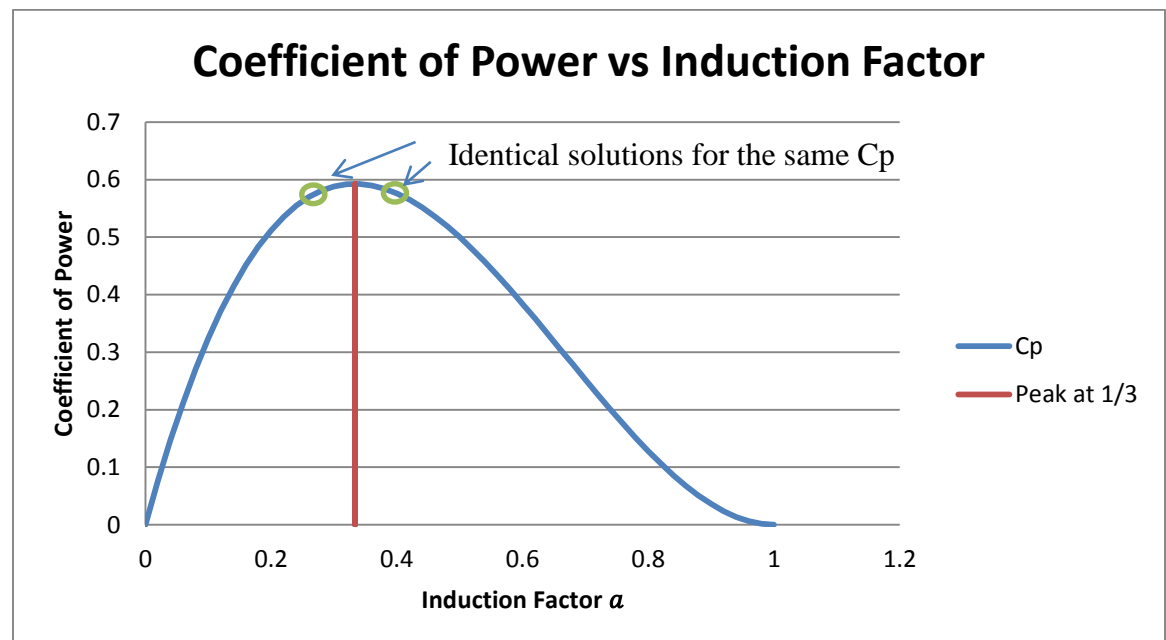


Figure 19: The Coefficient of Power of a Turbine as a Function of the Induction Factor

The dilemma that this curve presents is that for every coefficient of power, there are two possible values for the induction factor — one as the turbine is on its way towards peak efficiency and one value that represents the turbine's performance fall down from peak efficiency. In a physical setting, as the power draw increases, the torque on the generator shaft increases, slowing down the flow. Eventually, the generator load

may be increased so much that the turbine will reduce its rotational speed and its coefficient of power will decrease as the flow comes to a near stand-still around the foils. This is the second half of the curve. Beyond an induction factor of $\frac{1}{3}$, the coefficient of power will begin reducing down to zero even as induction increases. At an induction factor of 1, the coefficient of power is zero because $a = 1$ means that the fluid does not flow past the turbine — it stops as if hitting a wall. No flow past the turbine means that the turbine is not rotating and no power generation is occurring.

The induction factor becomes a part of the input because the flow input conditions must account for how the flow slowed past the turbine in the previous time step. Yet, the factor is a function of the output and so it is not possible to plug this straight into the program (because two solutions exist for every point). In order to resolve this issue, the data points on the curve were tabulated in a spreadsheet and an interpolation program was used. When the turbine reached peak efficiency, a slight increase was added to the coefficient of power to prevent the program from interpolating from the wrong half of the curve (showing increases in efficiency, when the turbine's efficiency was decreasing). The free-stream fluid velocity input was kept as a constant value for a majority of the simulations. However, some simulations were performed with a free-stream velocity input that was a ramping value (velocity increasing with time) or as a velocity that varied sinusoidally with time (to mimic unsteady wind conditions).

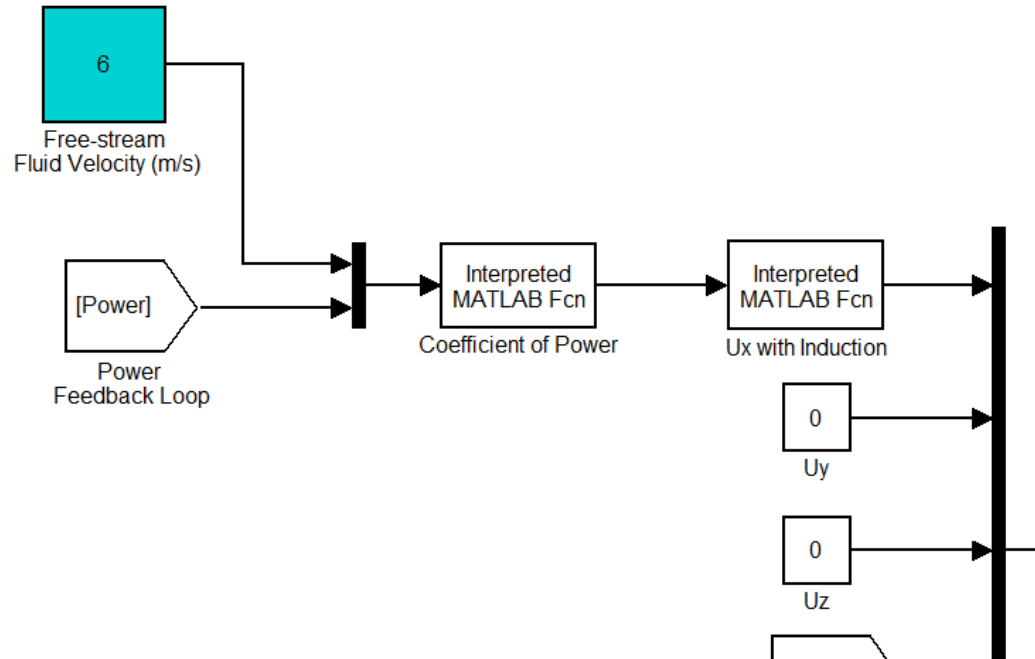


Figure 20: MATLAB model inputs and feedback loops accounting for induction

The information from the power output and the free-stream velocity were used to calculate the turbine's coefficient of power or C_p . This was done in a MATLAB function based on the following equation:

$$C_p = \frac{P}{\frac{1}{2}\rho AU^3}$$

U = Free-stream velocity of the fluid
 P = Power Extracted by the turbine
 A = Area of flow intercepted by the turbine
 ρ = density of the fluid

This was the value of the coefficient of power that was incorporated into the interpolation function that determined the induction factor, a . The induction factor allowed one to determine the downstream fluid velocity based on the upstream velocity:

$U_2 = a \cdot U_1$ and the input velocity was the average of the upstream and downstream velocities, $U_x = \frac{U_1 + U_2}{2}$, where U_1 is the upstream velocity and U_2 is the downstream

velocity. This then gave the value of U_x and the same process would be applied for any velocity in the y direction, but for the simulations performed in this study, the value of U_y was left at 0, otherwise induction would apply to U_y as well. The value of U_x was used to then compute the flow conditions that lead to the calculation of the torque as shown in Figure 21.

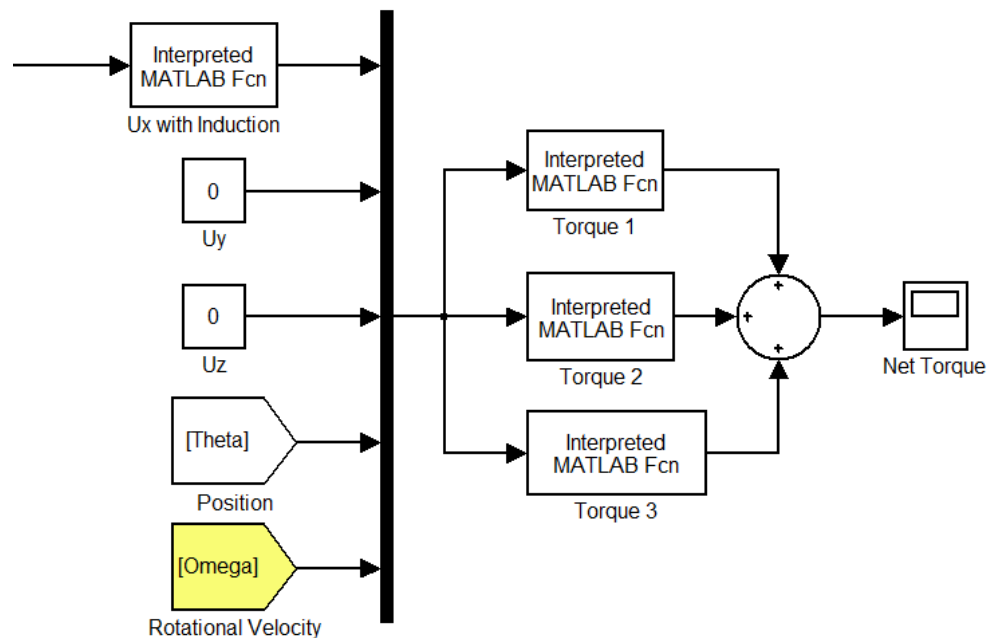


Figure 21: MATLAB model: flow conditions and calculating torque

The inputs are fed into MATLAB function blocks where the `comp_torque` script is used to calculate the lift and drag on the foils as well as the net torque on the system. There are three function blocks to calculate the torque: one for each foil. The equations inside each torque function block are the same, but an offset to the position, θ , is added in. Were there to be four foils equally spaced, there would be four torque function blocks with 90° added for each consecutive function. In this example, there are three foils

equally spaced around the rotor and so the position information for Torque 1 is simply θ , the position for Torque 2 is $\theta + 120^\circ$, and the position for Torque 3 is $\theta + 240^\circ$. The result of each torque function is added to each of the others to find the combined torque on the rotor from each of the aerodynamic forces on every foil.

The model includes a geometric environment developed in Simulink as shown in Figure 22. The features were a part of MATLAB's Simscape and SimMechanics toolboxes. The incoming arrow on the left indicates the net torque input from the lift and drag on the blades from Figure 21. The "machine environment" and "ground" blocks at the top of Figure 22 describe the geometry of the system. The "joint actuator" translates the torque into forces on the body of the turbine and the "revolute" block articulates these forces into movements in the structure itself.

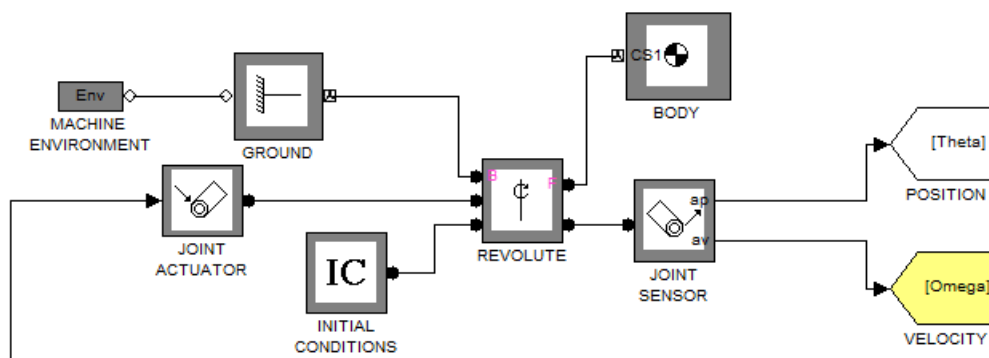


Figure 22: MATLAB Model Rigid Body Dynamics

The rigid body dynamics establish the mass and inertial properties. There are two outputs from the rigid body dynamics of the model. The first is the "body" block. It generates a 3D image that visualizes the movement of the system through another MATLAB feature that is part of the SimMechanics toolbox. This information could be used to connect the program with other 3D modeling software to show a fully developed

turbine prototype rotating in response to varying flow conditions. The second output of the rigid body dynamics section, the “joint sensor,” provides two important details: the rotational velocity and the position of the foils.

The power output of the turbine is modeled as a simple DC generator with voltage being proportional to the rotational velocity. The rotational velocity is passed through an amplifier called a gain, r . This gain functions as a simple generator model that is associated with a certain amount of torsional resistance on the rotation of the rotor.

$$\text{Torque on the shaft from the generator: } \tau_{Gen} = r \cdot \omega$$

Increasing or decreasing the gain has the same effect as increasing or decreasing the load (torsional resistance) of a generator. The output of the generator model (τ_{Gen}) is then multiplied with the rotational velocity, ω , and this value is equal to the power output.

$$P = \tau_{Gen} \cdot \omega$$

P = Power output of the turbine (Watts)

τ_{Gen} = Torque on the shaft from the Generator (Newton-meters)

ω = Rotational velocity of the turbine (radians per second)

The DC generator model and power output are shown schematically in Figure 23.

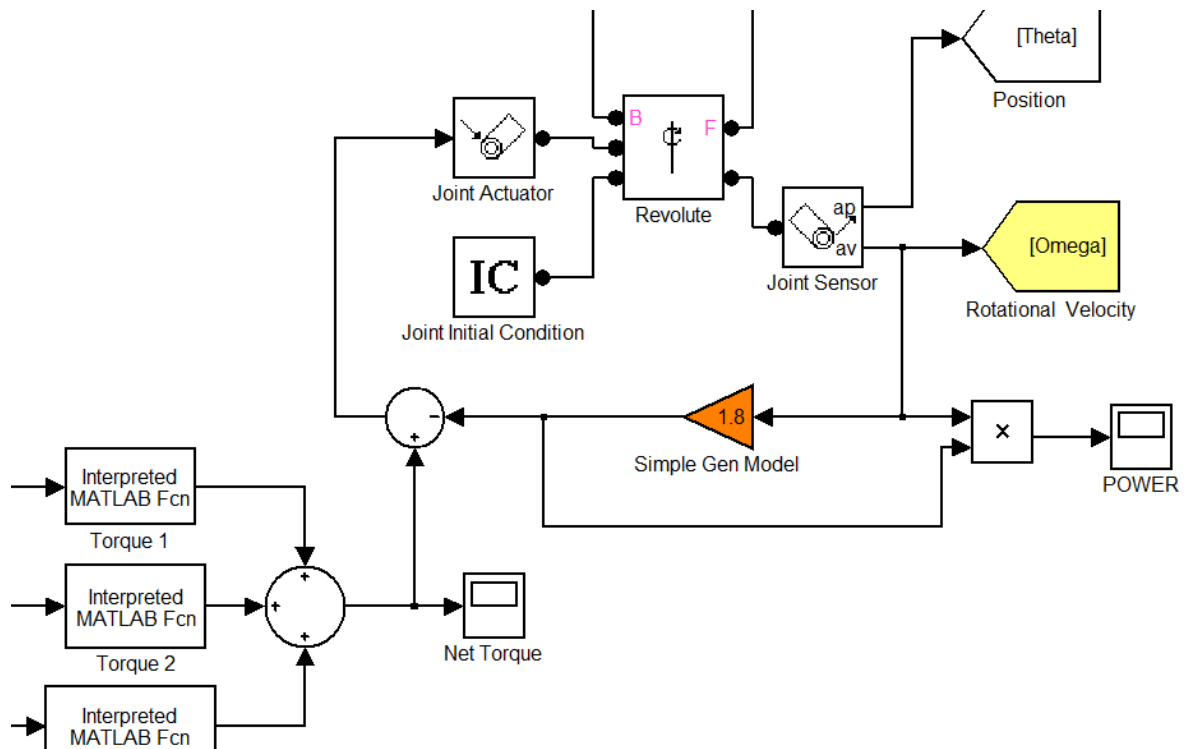


Figure 23: MATLAB Model Feedback Loops and Power Calculation

The torsional resistance of the generator (called “Simple Gen Model”) is then subtracted from the overall torque on the rotor that was developed by the aerodynamic forces on the foils.

$$\tau_{net} = \tau_{foil 1} + \tau_{foil 2} + \tau_{foil 3} - \tau_{Gen}$$

The resultant torque on the shaft, τ_{net} , is the difference between the aerodynamic torque from each foil and the generator torque. This is the input torque given to the “Joint Actuator” block that is part of the rigid body dynamics of the system.

Model Verification

The model developed in this thesis is a set of mathematical equations that represent the simplified versions of machines. A model can be useful in predicting the way that a physical machine may respond to a novel situation, but only if it matches the machine's performance when subjected to the same input conditions. The model was initially verified by a series of hand calculations and the outputs were compared against other empirical references. The first step of the process was to confirm the accuracy of the main script in the model that computed torque. Verifications were performed by recreating several static situations (snapshots) from the MATLAB model and working through the calculations by hand. This ensured that the coding and algebra of the model was correct and would work in simulations. These hand calculations of torque were compared against the output of the MATLAB model — specifically the comp_torque script.

Once the turbine model was developed, the simulation results of the running model were contrasted with the empirical data from other wind-tunnel tests. One such test was performed at Durham University in which a three-bladed Darrieus VAWT was set up in a wind-tunnel (as seen in Figure 24). The rotor was attached to a three-phase permanent magnet generator with a rating of 200W [18].

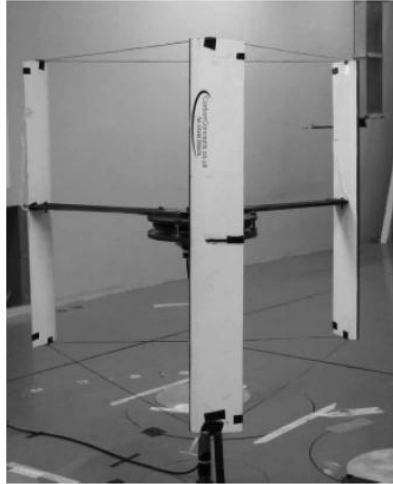


Figure 24: Three-bladed Darrieus VAWT used for tests by Hill et al [18]

Although no power measurements were reported in the wind-tunnel tests, the acceleration and rotational behavior of the turbine in the wind-tunnel proved to be of great use in measuring the MATLAB model against a physical machine. The turbine went through a period of slow rotation before there would be a sudden increase in rotational velocity that leveled out at a high TSR of about 13. This was the same behavior evidenced in the simulations of MATLAB model, although the model exaggerated these trends to some extent.

The first model tested was a fixed-pitch VAWT based on a simple H-Darrieus VAWT with fixed foils (no articulation). This was modeled after a machine built and tested in a wind-tunnel at Durham University. It was also a constrained version of the BlackHawk turbine. Upon the one of the first runs of the simulation, a curious pattern of rotational speed occurred. If the resistance of the generator was set too high in proportion to the free-stream velocity, the turbine would reach a steady rotational speed at about 0.8 – 0.9 TSR. When the generator load was reduced to a low enough value, the turbine would accelerate to a TSR of close to 1 for a while, and then suddenly transitions to a

very high rotational speed of up to 7 TSR and an efficiency of close to 50%. A sample simulation is shown in Figure 25.

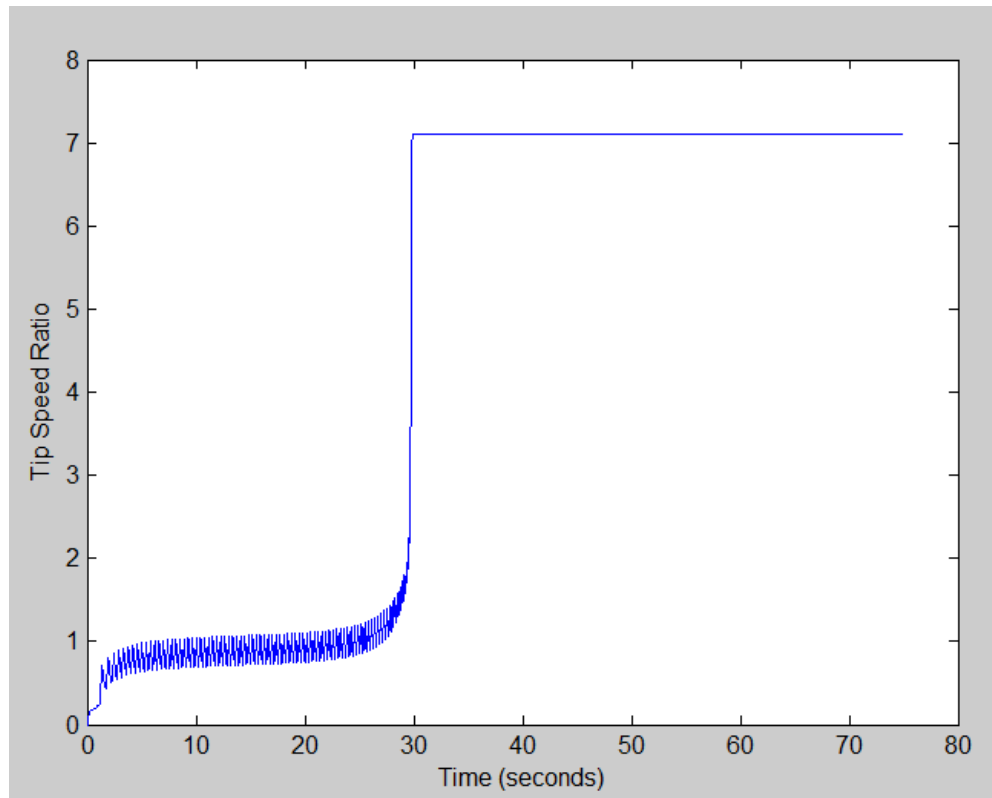


Figure 25: MATLAB simulation output of a fixed-pitch turbine at 22 mph

This pattern repeated itself for a variety of simulations. It shows the remarkable change in behavior that occurs for a turbine once $TSR > 1$. Until that point, the model predicts very low power yields, until little by little, the turbine accelerates to a $TSR = 1$ and the induced flow from the foil rotation becomes just as important as the incoming flow. At this point, the angle of attack is reduced and the lift coefficients significantly increase. Once the TSR reached a value of one, then the direct speed of the wind was equal to the tangential velocity of the blades as they rotated, ensuring that at least 50% of the flow velocity's direction was due to the rotation of the turbine itself. The higher the TSR, the more the local velocity at each blade was influenced by the induced velocity of

the blade that came before it, ensuring a smaller angle of attack and higher lift values as the flow assumed that of a circle more and more and less as a direct flow.

The behavior shown in Figure 25 is not mirrored perfectly in the physical world, and one might take this to be a sign of the model failing to work at all. However, this behavior was evident in a battery of tests through several different generations and rebuildings of the model. And, although no physical turbine would realistically reach a TSR of 7 with an incoming wind speed of 22 mph (this would mean a rotational speed of close to 950 RPM for a turbine with a 3ft radius), there are several reasons that indicate that the model is merely an exaggeration of real behavior. Manufacturers never let their engines reach such velocities because of catastrophic failures to their hardware. Even the BlackHawk turbine failed at the INL installation during a heavy wind-storm when the brakes failed to hold the turbine back.

The behavior is also likely exaggerated in the MATLAB model by the use of data from a table. The data were taken in increments of degrees, and is not continuous. Therefore, there may be a more subtle behavior at low angles of attack that the linear interpolation of the table does not pick up. In addition, the generator developed in the model makes no distinction between the loads on the turbine due to friction vs. the load on the turbine due to the resistance of the generator. All turbines will have some level of friction regardless of the load that will limit their runaway speed. In the model though, significantly reducing the load makes the turbine behave as if there is no friction from the rotor bearings allowing it to spin freely when no load is applied.

However, the prediction of the model though it may not ever come to fruition in a physical environment offers insight into a key aspect of VAWTs — that there exists a

region of stable behavior with high power outputs that is only accessible once the TSR reaches a value greater than one. A group of professors at West Virginia University developed a numerical model that predicted similarly high values of TSR [22].

The pattern of a slow rotation until a relatively sudden acceleration and an eventual plateau at a very high rotational speed is not unique to the MATLAB model. In the wind-tunnel tests of a fixed-pitch VAWT [18], a similar (but less extreme) pattern emerges. In a test performed by a group at Durham University, a 3-bladed VAWT machine was set up in a wind-tunnel originally built for automotive testing. The turbine was equipped with a permanent magnet axial flux generator that had zero-cogging torque when there was no electric load. During the tests, the rotor was held stationary until the flow in the tunnel had stabilized. Data capture began at the moment of release. The team found three regimes of behavior: linear at the start, a plateau between a TSR of 1 and 1.5, and then a rapid rise to equilibrium at a TSR of 3.

For simulations of a fixed-pitch turbine, the rotor would never reach a TSR larger than about 1.3. This was seen by the Durham research team as well when they stated that there was “a very small torque margin available in the ‘plateau’ region.” When a pitch variation is added into the computer model, the rotor’s behavior mimics the behavior recorded in the wind-tunnel test [18] but on a different time scale. The wind-tunnel model from Durham has a much longer time-scale that could be due to friction in the bearings, the fixed-pitch of its foils or turbulence and wake effects. The MATLAB model was created using the same dimensions as the turbine tested at Durham.

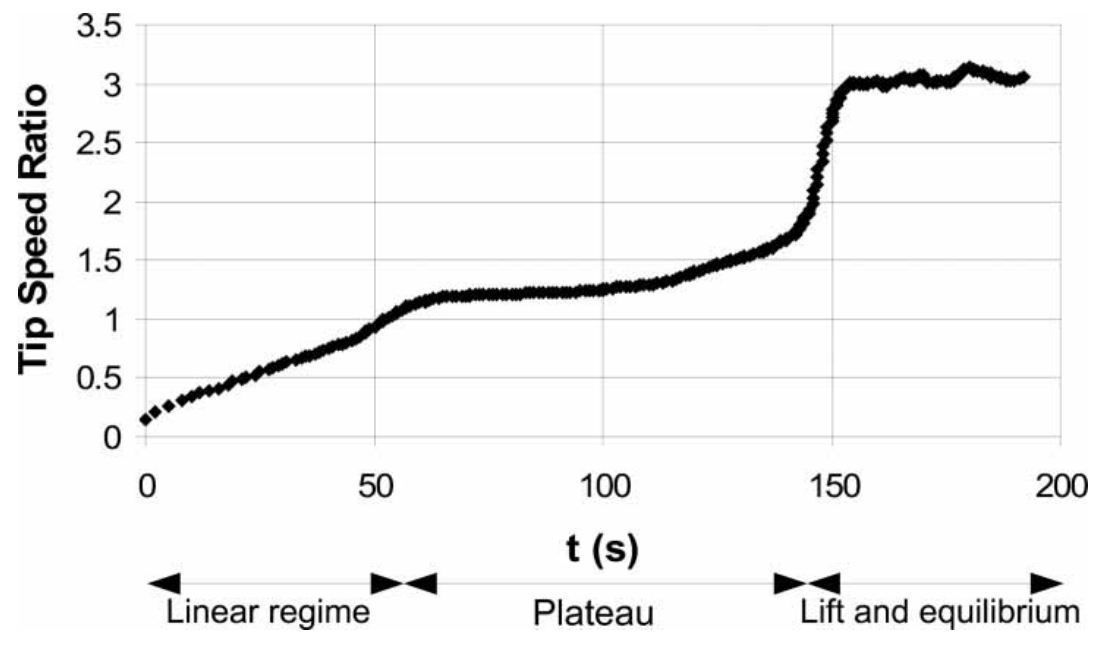


Figure 26: Results of a wind-tunnel test of a fixed-pitch 3-Bladed VAWT at wind-speed of 6m/s. Words and figure from [18]

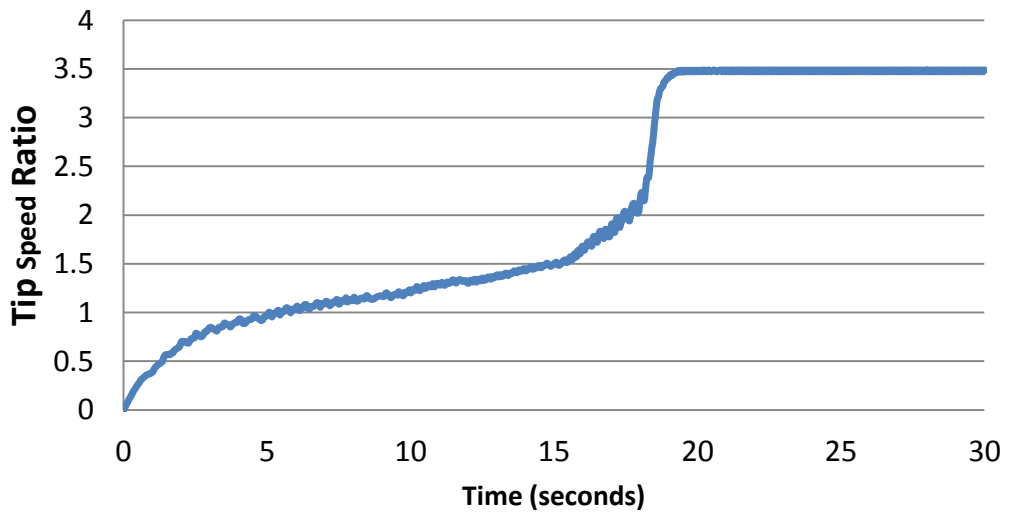


Figure 27: MATLAB simulation results for turbine with sinusoidally varying pitch at wind-speed of 7m/s

Once it was confirmed that the simulation behavior consistently matched patterns of behavior in other machines, the model was tuned to the specific dimensions of the BlackHawk TR10 VAWT developed by Boatner [21]. The BlackHawk turbine was analyzed in great detail in the model. Of particular interest was the nature of the pitch articulation and if it could be optimized any further. The BlackHawk pitches in a periodic pattern with an amplitude of a few degrees.

Data were collected by the BlackHawk team at one of their turbine installations in Emmett, ID. These data measurements were used to check the correspondence between the physical model and the simulation results, verifying the MATLAB model. The BlackHawk TR10 was able to start from rest at a wind-speed of 7 mph (3.1 m/s). The MATLAB model showed similar start-ups occurring between 5 and 9 mph [Figure 29]. The model matched neatly with the physical machine in this regard; however, the rate of acceleration was much higher than expected in the model. In the model, the turbine would rock back and forth but it would only make one or two rotations before within 20 seconds, it would suddenly begin to rotate quickly enough to develop a high enough rotational velocity, ensuring that the angle of attack on the foils was much more favorable than that of a direct wind. This was clearly seen in the effect that the TSR had on power production.

The turbine model would begin to rotate, the TSR would increase, as the TSR increased, the range of α decreased, and the lift and torque increased as well. The combined effect of increasing rotational momentum and an increase in the lift on the blades showed how quickly a turbine could go from producing very little power to harvesting its full potential.

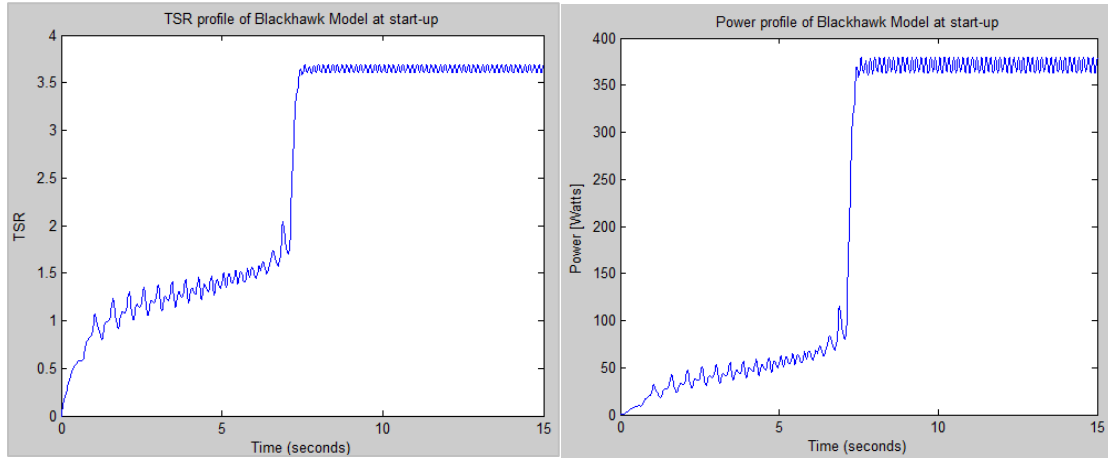


Figure 28: Power and TSR output of model based on BlackHawk TR10 at a wind-speed of 13 mph

The performance of a BlackHawk TR-10 VAWT was collected on May 15th 2011 in Emmett ,Idaho by the developers using a Supervisory Control and Data Acquisition (SCADA) device. The SCADA device recorded the rotational speed of the turbine, the resistive load provided by the generator, and the power output. An anemometer recorded the wind-speed at the location. Using these measurements, the turbine efficiency and its TSR could be calculated. The data from the BlackHawk turbine is displayed in Figure 29 along with the simulation outputs for a turbine model of the same dimensions and at the same wind speed. The load for the generator in the model was set so that the turbine rotated near the lower end of rotational speeds for the BlackHawk turbine to account for friction in the bearings.

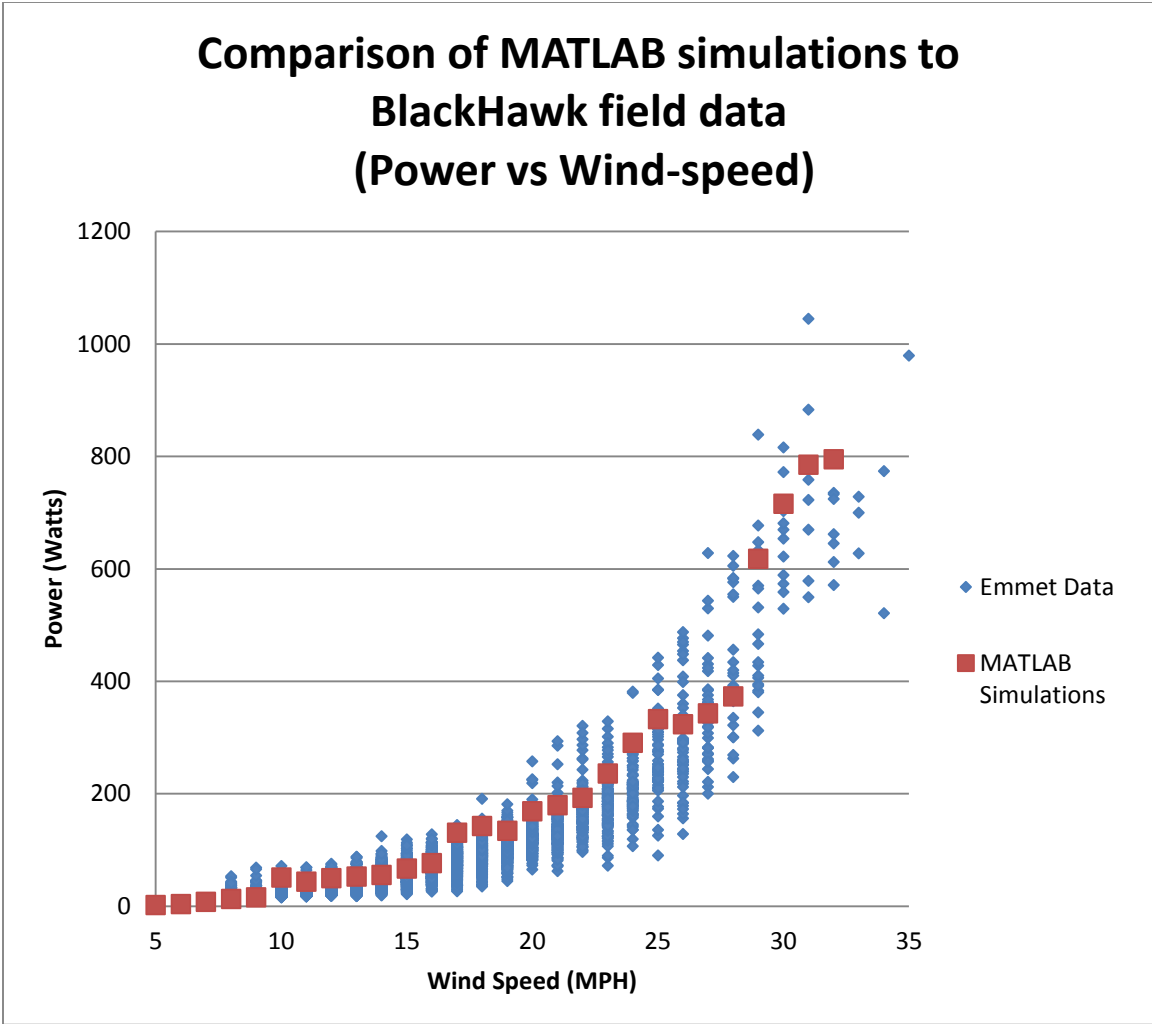


Figure 29: Comparing the power output of MATLAB simulations to BlackHawk field data from Emmett

As one can see from Figure 29, the MATLAB model was able to simulate the behavior of the TR10 fitting within the range of data available. The main difference between the simulations and the physical turbine was that the model predicted the same power outputs, but for lower rotational velocities than the TR 10. These rotational velocities are shown in Figure 30.

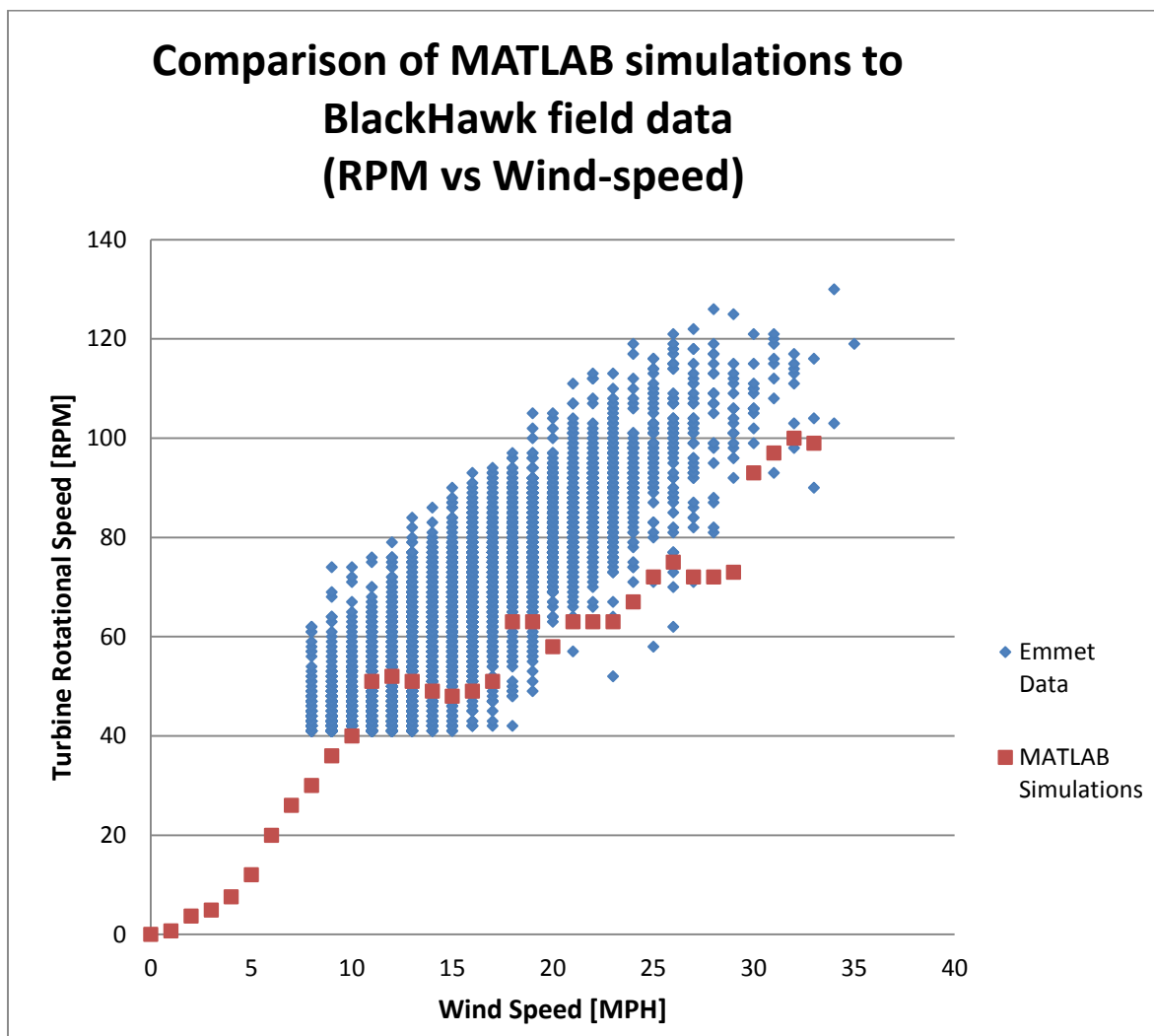


Figure 30: Comparing the rotational speeds of MATLAB simulations to BlackHawk field data from Emmett

The rotational speeds for the simulation were generally lower than those of the BlackHawk turbine for the same power outputs. This is possibly due to turbulence and friction in the bearings of the physical model. For example at a wind-speed of 17 MPH, the TR 10 in Emmett had an average power output of 72 Watts at 83 RPM whereas the MATLAB model simulated power production of 77 Watts at 55 RPM. The MATLAB model also predicted much greater power production was possible at higher TSRs.

CHAPTER FIVE: RESULTS

Using the Model to Inform Design Decisions

Even the SCADA data, if extrapolated, shows the potential for much higher efficiencies. Figure 31 shows the data collected from the BlackHawk TR 10 charting the turbine efficiency against the TSR. As the TSR is increased, the turbine becomes much more efficient. In fact, one of the main concerns of the research team at INL studying the BlackHawk TR10 was that it rotated far too slowly in low winds. Their second concern was that it rotated too quickly in high winds (but this was due to worries about material failure not low power production).

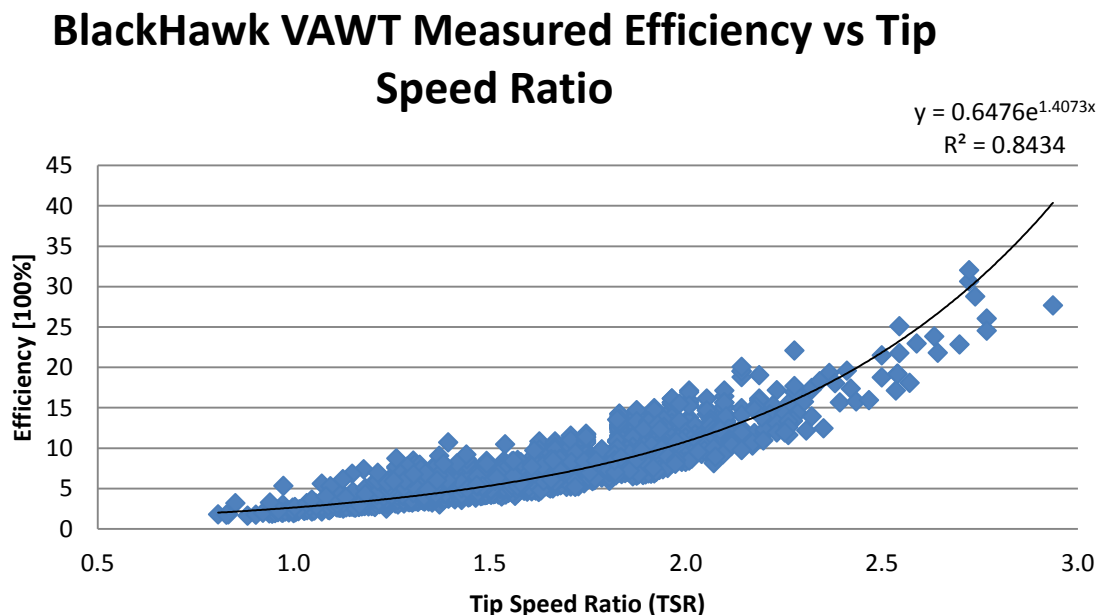


Figure 31: SCADA Data Provided by BlackHawk Showing Measurements of Efficiency vs TSR

Ideal Blade Articulation

One feature that the model highlighted was the importance of pitch articulation to start-up. A MATLAB simulation of a model with no pitch articulation (foils tangent to the circle of rotation) predicted no more than 25 Watts being produced even at 27 mph of wind, whereas the model with articulated pitch (at high load, and low RPM) predicted a power output of over 400 Watts (APPENDIX C, Figure 50).

Experimentation with the MATLAB model confirmed Staelens et al.'s predictions [14] that a sinusoidal pitch variation was optimal as a realistic compromise for achieving ideal angles of attack without discontinuous changes in the pitch of the foil. Subsequent simulations of the MATLAB model revealed an optimized realistic articulation magnitude of between 8 and 9 degrees. This was the magnitude at which the tip speed ratio peaked, providing the most power. The graph of one of the tests performed is shown in Figure 32 where the pitch, ψ , varies sinusoidally with θ , where θ is in line with the radial arm of the turbine, and the flow is defined as positive in line with the direction of the fixed X-axis at $\theta = 0$. In other words, at $\theta = 0$, the radius is pointing downwind. The pitch was varied according to the equation:

$$\psi = M \cdot \cos \theta$$

Cp vs Magnitude of Sinusoidal Pitch Articulation

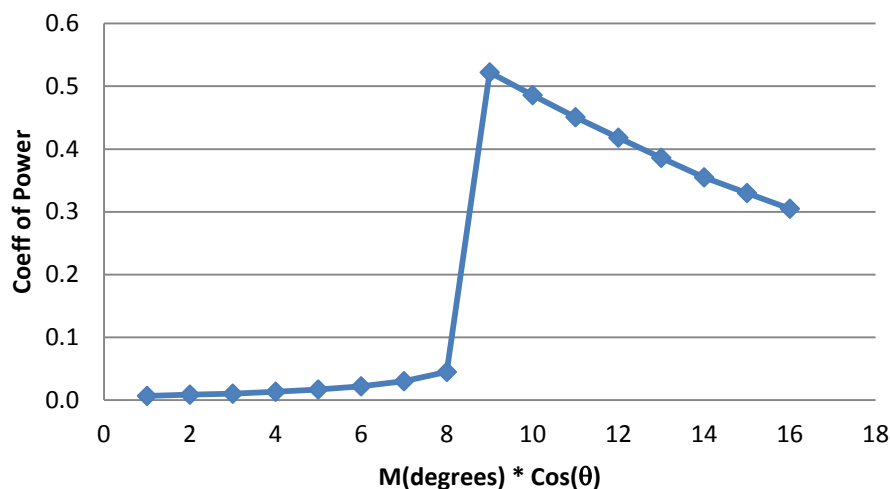


Figure 32: MATLAB simulation results in a study attempting to optimize the magnitude of the sinusoidal pitch at a simulated wind-speed of 18 mph.

Figure 33 shows the results of various simulations of a VAWT model with varying magnitudes of sinusoidal pitch variation in line with the direction of the wind. A large spike occurs between a magnitude of eight and nine degrees. The reason for this discontinuity is because once the pitch amplitude reached a value greater than eight degrees, the turbine was able to reach high TSRs changing the range in α . Further investigation at more detail showed the ideal magnitude to be a value of 8.6° .

The dramatic difference in performance between an articulating and a fixed-pitch VAWT is shown in Figure 33.

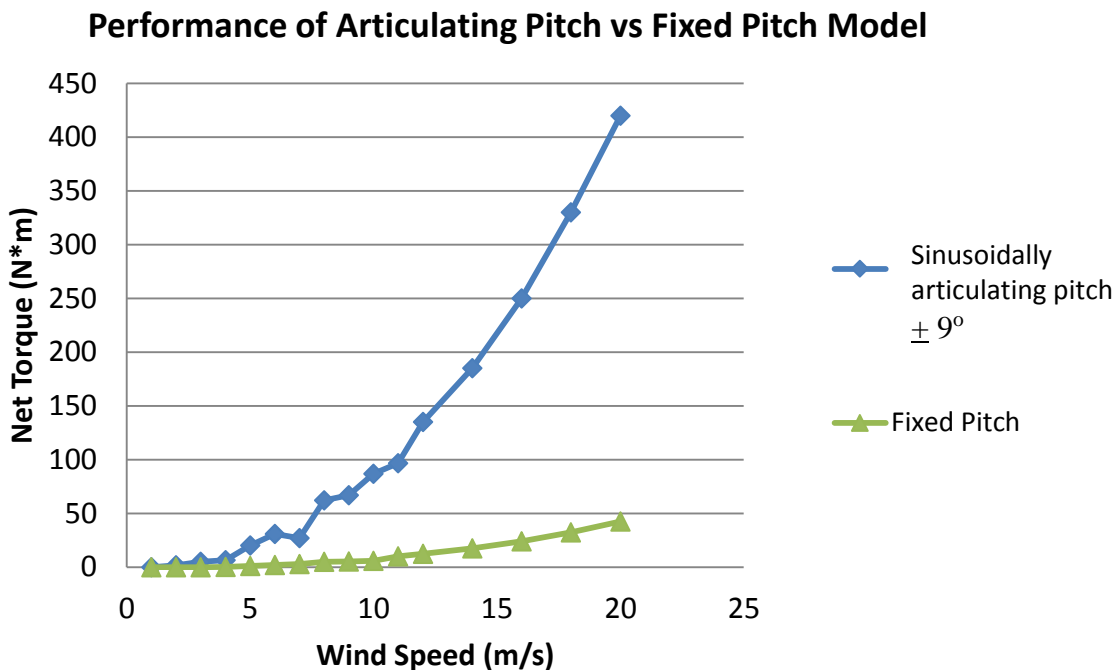


Figure 33: Contrast of available torque between fixed-pitch and articulating-pitch VAWTs based on MATLAB Model simulations

As Figure 33 illustrates, the articulation of the foils provides significantly more torque to the rotor because of higher lift coefficients. This allows for greatly increased power production over fixed-pitch H-Darrieus VAWTs. The data shown in Figure 32 indicates that the ideal pitch articulation was a sinusoidal variation of the pitch by 8.6° . This function had a maximum positive pitch deflection (outward from the circle of rotation) occurring on the windward point of rotation and negative deflection (inwards toward the center of rotation) on the leeward point. This is similar to the conclusion reached by an experimental study that found “the best performance is achieved at pitch angle about 8° ” [23]. Another study came to a more general conclusion that “the amplitude of the sinusoidal correction function is set equal to the maximum difference between the local geometric angle of attack and the blade static stall angle” [6]. This is a sinusoidal function varying in amplitude by approximately 11° .

Ideal Generator Loading

The MATLAB model demonstrated the effectiveness of having a dynamic generator load that could change according to differences in the flow conditions. Having a low generator load at start-up or slow rotational velocity conditions allowed the turbine model to begin rotating from rest. Minimizing the generator load for low-wind velocities allowed the turbine to reach high values of TSR, reducing the angle of attack and increasing lift (in low wind-velocity conditions), a high TSR did not necessarily mean dangerously high rotational speeds. Once the turbine reached a TSR greater than one, slowly adding to the generator load increased the power output and reduced the rotational speed. Overloading the generator caused the model turbine to go into a stall condition and it would rapidly decelerate. Too great of a generator load in the initial stages of the simulation would prevent the turbine from spinning at all. However, the danger does remain of having a turbine under-loaded at high velocity conditions. Rotational speeds greater than 200 RPM had the possibility of compromising the materials and structure of the BlackHawk TR10 — a problem that can be solved either with a more conservative loading scheme (as was done with BlackHawk) or constructing a machine out of higher strength materials that could manage the tensile and bending stresses of high rotation. Three graphs are shown below of MATLAB simulations at a wind-speed of 20 mph that demonstrate the effects of increasing the load on a turbine until stall is reached.

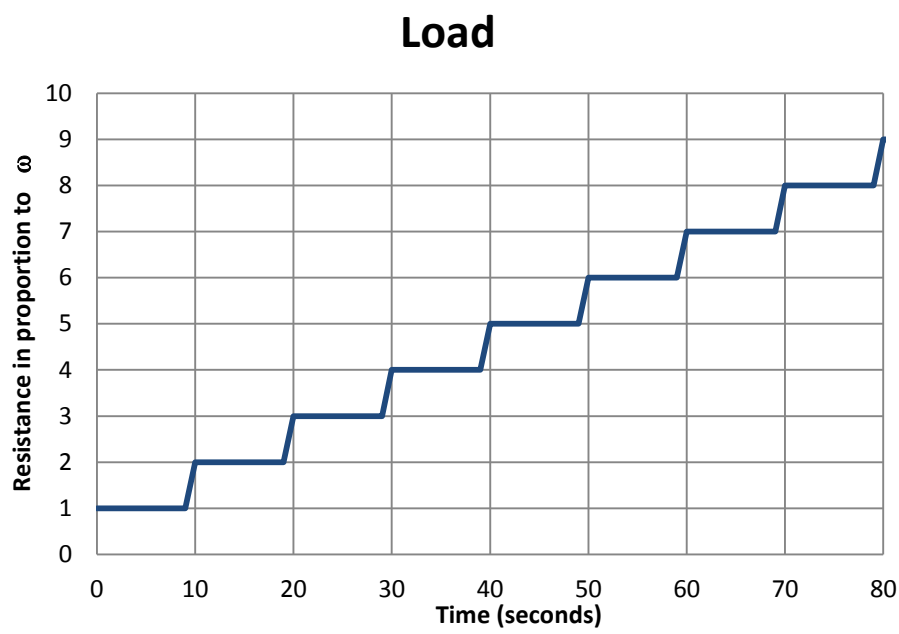


Figure 34: Increasing the generator load in a MATLAB simulation

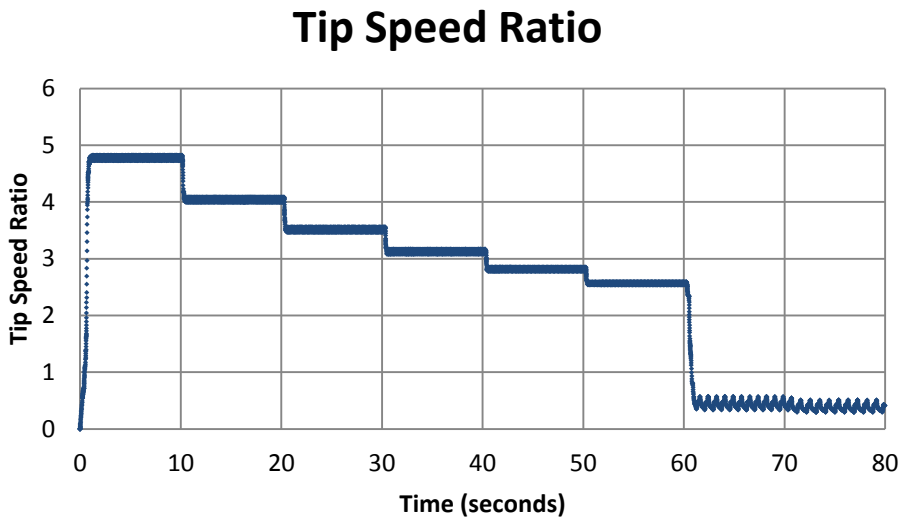


Figure 35: How the TSR of the MATLAB Simulation responded to increasing generator load

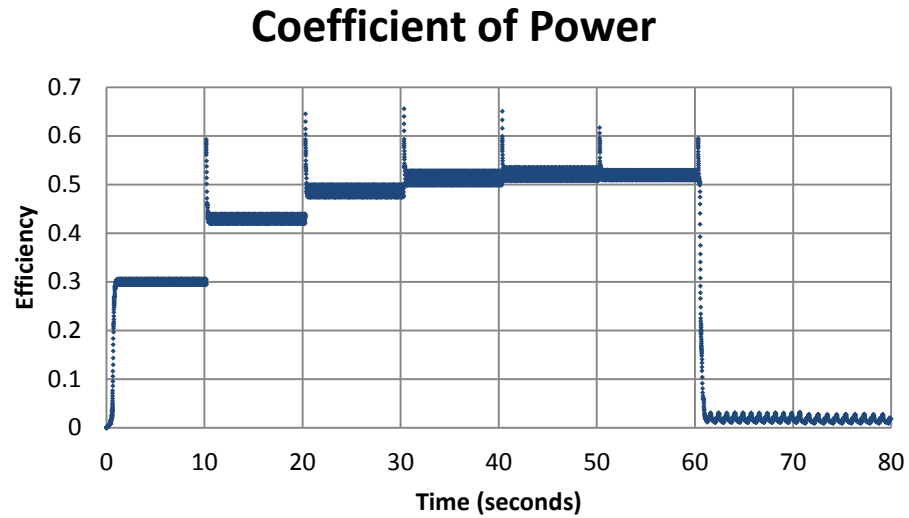


Figure 36: How the efficiency of the simulated turbine responded to increasing generator load

As one can see from Figure 36, increasing the generator load has a significantly beneficial impact on the power production for the first several steps. The increased torque on the generator reduces the rotational speed but still increases the power output to a certain point. However, with each subsequent load increase, there is a smaller effect on the power and the turbine becomes less rotationally stable. Eventually, the lift forces acting on the turbine are not great enough to continue turning, and the turbine loses speed, and in doing so, the induced velocity of each rotation is very small with high angles of attack — essentially the turbine reaches a stall condition. While this is better

than a turbine self-destructing from high rotational speeds, it has a devastating effect on the power production of the turbine.

CHAPTER SIX: HYDROKINETIC TURBINES

Differences between Wind and Water Turbine Behavior

After the development of the wind-turbine model, the focus of the research turned towards adapting the model for hydrokinetic turbines. One of the first issues to be dealt with was the effect the installation of a hydrokinetic turbine had on the upstream flow. The effect a wind turbine might have on the up-stream airflow is often of little interest. Wind turbines are installed in open areas with no significant blockage. As a result, the upstream effects of a VAWT are generally not considered in the fluid-flow analysis unless the turbines are installed in an array where the turbulence of the lead turbine can have a negative effect on the performance of the downwind turbines. However, a turbine placed in an open channel of water has a major impact on upstream flow conditions. Although much research has been devoted to increasing the efficiency of hydroelectric power from conventional dams, very little has been written on the characteristics of water turbine efficiencies in open channels with free flow and low-head resources. One cannot assume that these turbines behave according to the Betz limit the way that wind turbines do.

The Betz limit states that the maximum efficiency of a turbine in free fluid flow is 59.3% [11]. It is a simple physical analysis that has helped to form our modern understanding of turbine efficiencies, and will be covered in more detail later. However, the hydrodynamics of a turbine in a restricted channel with only one free surface requires a different approach in order to properly estimate potential power production.

Installing a turbine in an open channel of water has a peculiar effect on the flow. The turbine slows the flow of the water over a certain cross-sectional area and blocks part of the stream. Assuming incompressible flow, the mass flow rate upstream and downstream must be the same if no water is being diverted, based on the continuity equation. In mathematical terms, the continuity equation is stated as $A_1V_1 = A_2V_2$, where A refers to the cross-sectional area of the channel, and V refers to the average velocity of the flow through the channel. When a turbine is added to the channel, it effectively reduces the cross-sectional area of the channel. Since the cross-sectional area of the stream is reduced, one might expect the flow velocity to increase at this point.

Yet, when a turbine is installed in a channel, “blockage” occurs. Blockage is the fluid mechanics term for saying that placing an obstruction in an open channel will cause the water level to rise upstream of that obstruction. In other words, the water level will be deeper upstream of the turbine. Following traditional fluid mechanics equations, there are a few different possible outcomes. The energy built up in this water level rise can be dissipated thermodynamically through turbulent wake and cavitation. A hydraulic jump may also occur downstream depending on the Froude number (the ratio of inertial forces to gravitational forces). This means that depending on the velocity of the flow, the water level may actually rise up again *downstream* of the obstruction in the channel.

Bounded fluid flows and the possibility of phenomena like hydraulic jumps cannot be properly analyzed with a simplified Betz analysis of efficiency. The equation is better suited for different situations, namely free fluid flows with no blockage. The Betz method assumes a slipstream with optimal conditions, incompressible flow, and a fixed control volume with axial flow. In a simplified Betz analysis, the streamlines

expand to three times their initial area after they pass through the turbine forming a trapezoidal shape and assumes an even pressure distribution on the blades Figure 37.

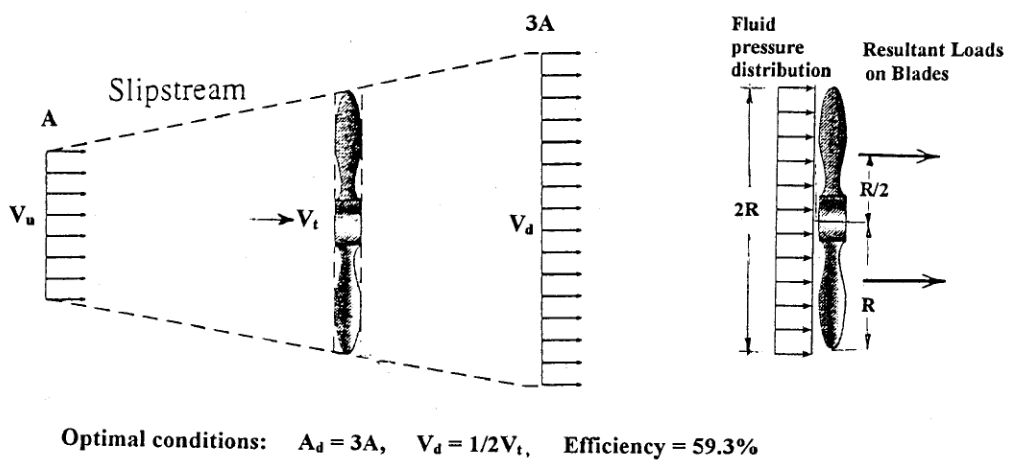


Figure 37: Streamlines and pressure distribution from a Betz analysis applied to a hydroturbine. Figure and description from [24]

However, recent studies [24] have estimated that the fluid behaves in a much more curvilinear fashion where the streamlines bend around the blades in tight curves rather than in straight lines as seen in Figure 38.

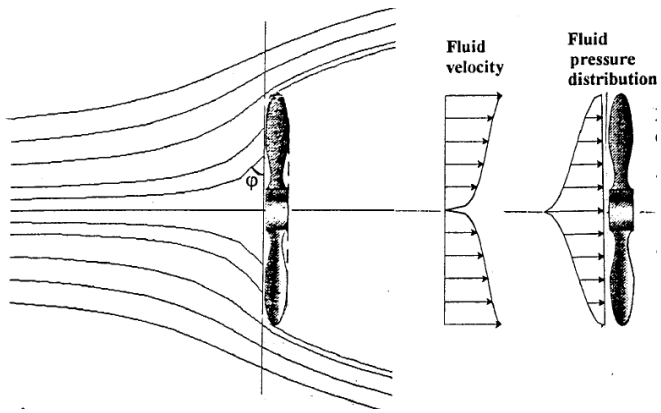


Figure 38: Curvilinear streamlines and new estimate of pressure distribution on a hydroturbine. Figure and description from [24]

Figure 37 assumes incompressible flow on a turbine. What the authors of the study contend is that the curvilinear analysis provides a much better model for the

behavior of a turbine in a low-head resource (2m or less). The lower pressure can result in uneven distributions of force on the turbine blades when kinetic (not potential) energy is dominant in the resource. When there is low head and kinetic energy is the main resource, turbines have been shown to experience much lower efficiencies.

A further difference from the Betz assumptions of even pressure distribution arises when a turbine is placed near a channel's surface. Rather than the streamlines expanding evenly (as shown in Figure 37), the water's surface acts as a boundary that is different than the walls of the channel. Although calculating the flow around an object in a constricted pipe (with uniform boundaries on all sides) is a common problem in fluid mechanics textbooks, the nature of an open channel — where the open surface allows water to be displaced upstream and around the object—adds a new dimension to the analysis.

Experimental results [25] have shown that it is possible for water turbines installed in channel flow to far exceed the Betz limit of efficiency. The reason for this is due to the blockage that is developed. The value of the blockage is the ratio of the cross-sectional area of the obstruction (in this case the turbine) to the cross-sectional area of the channel. $B = \frac{\text{Turbine cross-sectional area}}{\text{Stream cross-sectional area}}$ The cross-sectional area of the turbine is the area intercepted by the device in the flow — what one would see if looking at the turbine in a plane taken from a vertical cross-section of the channel — or the area of the silhouette the turbine would make if a large light were placed at one end of the channel.

The blockage ratio influences how much water will actually be pushed upstream, functioning as a sort of low-head hydraulic dam. This low-head dam provides an extra source of energy for which the Betz equation does not account. This is because the Betz

theorem is designed to analyze systems in which a turbine is located far away from any boundaries to fluid flow. Generally, this is a very safe assumption for wind turbines and for tidal turbines that are located in open waters deep beneath the water's surface. However, for tidal turbines located close to the surface of the water (or turbines in an irrigation channel), the surface effects of the blockage must be taken into consideration. Furthermore, installing a turbine in a stream can have a significant impact on the upstream water level. For wind turbines, the air passing around the turbine is not restricted in any way other than the atmospheric pressure of the surrounding air and so it has free boundary conditions. However, for water flowing around a turbine in small rivers, there are four restrictive boundary conditions that must be considered: the three walls of the channel and the free surface of the water.

Whelan et al. [25] analyzed the flow of a turbine in a channel by starting with the same methodology as Betz: with the continuity equation and the analysis of a stream-tube. In the Betz analysis, stream-tubes start at the cross-sectional area of the turbine, and then expand in a bell shape at the turbine. Stream-tubes passing around the turbine are generally not analyzed in the Betz analysis. However, in the Whelan et al. analysis, two different stream-tubes are considered in the model: one that passes through the turbine and one that passes around it. The velocities of these two stream-tubes both change, but by different amounts, and so one must average the two to find the actual downstream velocity. The difference between the downstream velocities factor is key in programming a simulation of a turbine.

The Blade Element Momentum Method (BEM) was also used in the study of hydrokinetic turbines placed in a flume [25]. The BEM focuses on the analysis of stream lines as they pass from free-stream conditions through the turbine.

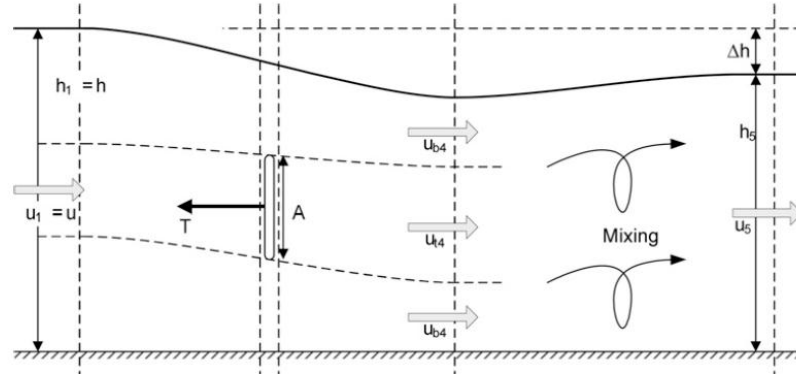


Figure 39: Analysis Using Two Stream-tubes for in the Analysis of a Turbine in Open Chanel Flow [25]

By studying multiple stream-tubes with the BEM, it was concluded that potential energy does in fact develop in the flow upstream of the turbine. The team looked at multiple stream-tubes at different stages of the flow in what others have termed a “Double Multiple Stream-tube Analysis” [26] that accounted for some of the wake effects in the flow. A research team at Oxford [27] applied the continuity and energy equations at selected stages in the flow to arrive at the following quartic equation relating the change in velocity for stream-tubes both passing through and around the turbine:

$$\frac{Fr^2}{2}\beta_4^4 + 2\alpha_4 Fr^2 \beta_4^3 - (2 - 2B + Fr^2) \times \beta_4^2 - (4\alpha_4 + 2\alpha_4 Fr^2 - 4)\beta_4 + \left(\frac{Fr^2}{2} + 4\alpha_4 - 2B\alpha_4^2 - 2\right) = 0$$

Fr = Froude Number

B = Blockage ratio

β_4 = Downstream bypass flow velocity coefficient

α_4 = Downstream turbine flow velocity coefficient

Although this is a remarkably powerful mathematical tool, it is merely a part of the overall software program used to estimate power from a turbine in a range of dynamic conditions. Applying the BEM to each condition by hand would take an excessive amount of time. This is why a computer program that can process thousands of these calculations in a minute would be helpful. Therefore, BEM calculations form an important part of a dynamic computer model as well.

Feedback Loops: Power Production, Position Changes, and Induction

The end goal of implanting a turbine into a fluid flow is to gather energy from the flow and convert it into electricity. The greater the load of the generator, the more the turbine blades will resist the fluid flow, and the more torque is siphoned off from the turbine reducing the acceleration of the rotor. The torque used for power generation is subtracted from the incoming torque, so the model geometry experiences net torque. As the generator load increases, the fluid velocity field downstream of the turbine will decrease. This means that on a smaller scale the downstream blade of the machine will see a significantly slower flow than the upstream blade. This is how energy is harvested from the flow. The kinetic energy of the flow is transferred to rotational energy of the turbine through lift and drag forces. In the Betz analysis of turbines, this ratio of change between the upstream and downstream velocities is known as the induction factor. This factor allows the program to run iterations of the flow simulation. The more energy recovered from the flow, the more the downstream fluid velocity will decrease. If the induction is not incorporated into the program, then increasing the generator load has no effect on the incoming fluid velocity and the model will show greater power outputs than are physically possible.

Determining Water level Rise

The models for hydrokinetic turbines in a channel required an additional set of equations in order to calculate the rise of the fluid level due to the turbine. The water level rises when a turbine is inserted into a channel that is restricted on three sides but has an open surface, such as an irrigation canal. Two different theorems can be used to study the behavior the first is the Bernoulli energy equation, which assumes viscous forces are negative and that the fluid is incompressible.

The Bernoulli energy equation has the form: $\delta = (y_1 - y_2) + \frac{1}{2g} (V_1^2 - V_2^2)$

And, the continuity equation is as follows: $V_1 H_1 = V_2 H_2$.

δ = Hydraulic head (m)

y_1 = upstream elevation (m)

V_1 = upstream fluid velocity (m/s)

H_1 = upstream fluid depth (m)

g = gravitational constant (m/s²)

y_2 = downstream elevation (m)

V_2 = downstream fluid velocity(m/s)

H_2 = downstream fluid depth (m)

What emerges from the analysis of the Bernoulli and continuity equations is the fact that the water level change (δ) depends upon the relationship between the velocity of the upstream flow, the gravitational constant, and the grade of the flow. These properties have been conveniently combined into the Froude number as mentioned earlier.

It is the value of the Froude number that allows one to predict how much the water level will rise both downstream and upstream of the turbine.

The Froude number is defined as: $\frac{U}{\sqrt{g \cdot h}}$

U = Flow velocity (m/s)

g = Gravitational constant (m/s²)

h = Depth of the fluid (m)

Capitalizing on the work from the research team at Oxford University [27], which had performed an elaborate and detailed study of the behavior of water flow past a turbine in a channel, the following equation was used to estimate the water level rise upstream of the turbine:

$$\frac{1}{2} \rho g b (h^2 - (h - \Delta h)^2) - T = \rho b h u \left(\frac{u h}{h - \Delta h} - u \right) \quad [27]$$

T = Thrust (Power/Velocity)

b = Width of the channel

u = Flow velocity at the blades

h = Water level depth upstream of the turbine

Δh = Change in water level depth between the depths upstream and downstream of the turbine

The solution for Δh was achieved via MATLAB and can be seen in APPENDIX B. This solution was included in the MATLAB model to track water level rise. This is one of a set of monitors of the turbine performance in the model. These monitors consisted of data outputs in both numerical and graphical form. The properties monitored in the system included the power output, the upstream water level rise, the induction, the coefficient of power, and the torque generated by each wing.

Adapting the Model for Hydrokinetic Turbines

Although the structure of the model remained consistent between wind turbines and hydroturbines, several new features were added to account for the differences

between these two. One such feature incorporated into the hydro-models was an estimation of the upstream water level rise.

The features added to the hydroturbine model included new parameters for the channel dimensions of the stream, and the initial stream depth. The hydro-models also included the calculation of the Froude number. The most significant difference was the addition of a calculation to estimate the rise of water level upstream of the turbine. This calculation (shown in Figure 40 and APPENDIX B) consisted of four different pieces of information: the stream depth, the power draw of the generator, the velocity of the fluid flow through the turbine, and the diameter of the stream or channel. The fluid velocity at the turbine depends on the free-stream velocity, the blockage ratio, the stream depth, and an estimate of how much the stream depth will change.

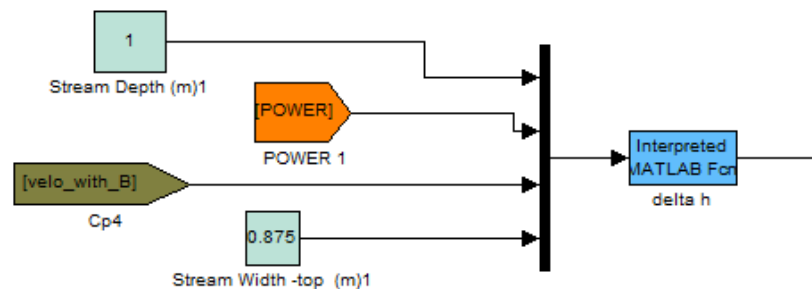


Figure 40: MATLAB calculation of the change in stream depth

For the water-based turbine, the model was re-designed to have the same physical properties as that of a HAWT that was developed by a team at Oxford [28].

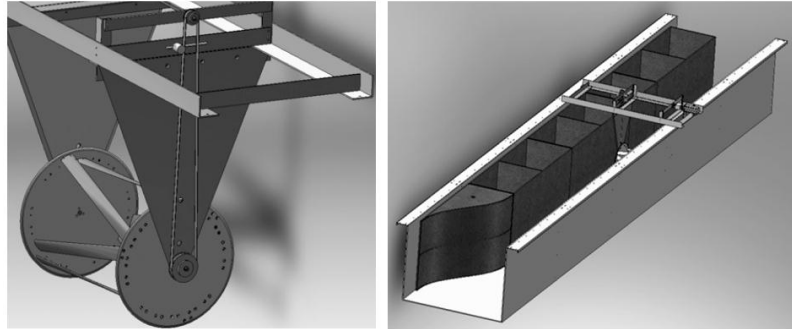


Figure 41: CAD image of THAWT and flume set up for experimental testing at Oxford [28]

The group researching the Transverse Horizontal Axis Water Turbine (THAWT) at Oxford used a large flume to test the machine's efficiency. The data from these tests were used as a metric for the MATLAB model that was developed. The switch of using the model from a vertical axis wind turbine to transverse horizontal axis water turbine involved only a few changes in the math and structure of the model. The rotational geometry remained the same. The fixed input conditions of channel dimensions and inertia were updated as were the state parameters of flow speed, fluid density, and viscosity to reflect the new aspects of the problem.

According to the tests performed at Oxford, the THAWT produced close to 55 Watts at a TSR of 3 and a Froude number of 0.22. The Froude number, a ratio of inertial forces to gravitational forces, indicates the fluid behavior around an object resisting the flow. Simulations performed on the computer model showed power production ranging between 47 and 64 Watts at a TSR of 3 and a Froude number of 0.24. While some points of comparison were similar, the model showed a very different trend from the physical tests. The two sets of data are compared in Figure 42 and Figure 43.

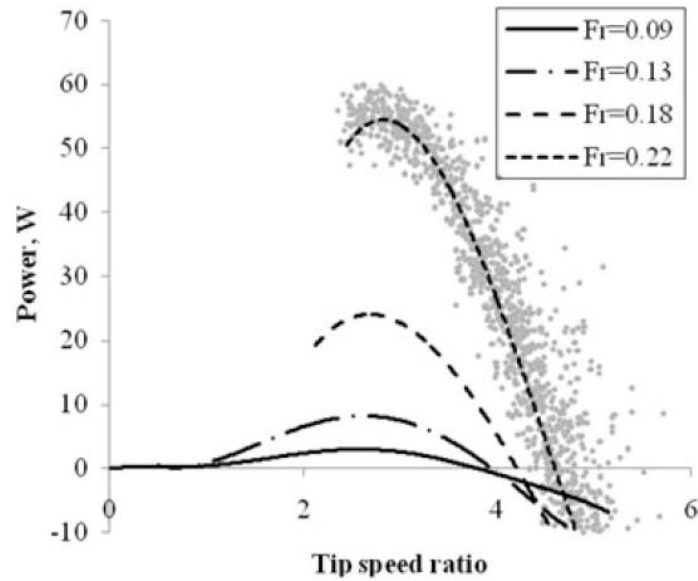


Figure 42: THAWT data from Oxford flume tests on turbine. Figure taken from [28]

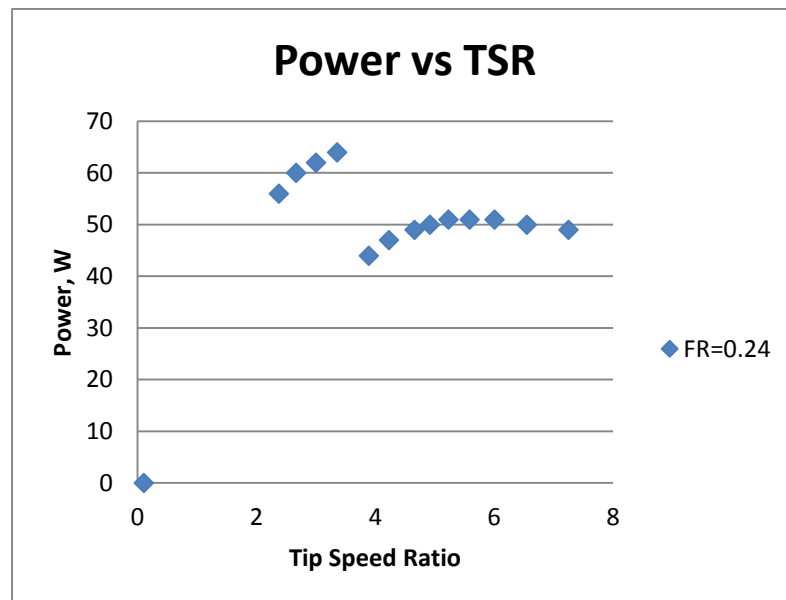


Figure 43: THAWT data of MATLAB simulations based on Oxford turbine dimensions

Both the empirical tests and the simulation results showed a peak of power production occurring near a TSR of 3, with decreasing power production at higher TSRs (see APPENDIX C, Table 4). However, the MATLAB simulations show a very different

curve after a TSR of 4. Rather than continuing to decline, there is a second local maxima occurring at a TSR of 6. The simulation tests were performed using the same flow, but with varying generator load. The information on the generator load was not available from the report [28]. The variance in generator loading could be one reason for the difference in the findings. The model for the hydrokinetic turbine remains an area open to further research and refinement.

The latter half of the research was focused on the performance of run of the river hydroturbines, one of which was a drag-based turbine that operated like the Hydrovolts flip-wing turbine [29]. The flip-wing turbine functions much like a paddle-wheel. In a paddle-wheel, the blades enter the stream as they rotate and get pushed downstream by the current. There is now resistance as the wheel rotates because the blades returning to the upstream position are passing through air rather than water flow. The Hydrovolts turbine operates on the same principle. The blades encounter resistance on the downstream rotation, but very little when they are returning upstream. Instead of passing through air on their return upstream though, the wings are set on a hinge that keeps them flat. When rotating downstream, there is a pin that catches the blade and prevents it from spinning all the way around. This simple mechanical action allows minimal resistance for the blades going against the current, and maximizes the drag on those blades going with the current.

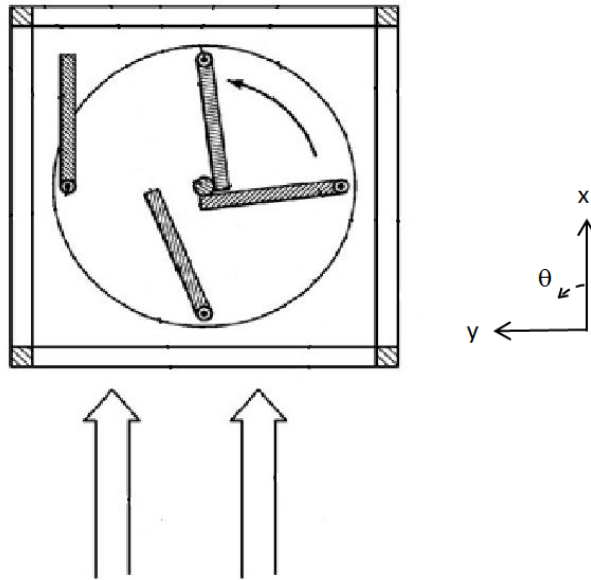


Figure 44: Side View of the Hydrovolts Turbine with Hinged Wings [29]

The angle of attack for the Hydrovolts turbine was calculated in a different manner. Rather than relying on the arctangent of rotational velocity vs. wind velocity, alpha was defined in two different stages: For the first half of the rotation ($0 \rightarrow \pi$), the angle of attack is 0 as the foil presents its leading edge to the current. For the second half of the rotation, ($\pi \rightarrow 2\pi$), as the foil pivots and its edge is pushed against the center shaft, the angle of attack is directly equal to current position (theta). Once the rotation is complete, the foil flips and presents its leading edge to the current once again. While this flip takes time in real-life, it was approximated as instantaneous in the model. When the foil flips, the angle for the next half of the rotation is 0° as the foil freely pivots to match the direction of the incoming flow.

The Hydrovolts design was intended to maximize drag on the foils going downstream, and minimize lift on the foils rotating into the current. The foils on the Hydrovolts machine are currently flat plates, rather than cambered foils. And so, a

different set of lift and drag data was used for the lift and drag value interpolation function. These values came from research into the ideal blade shape for rowing. A team of researchers at the University of Birmingham, UK [30] built several scale models of oar blades and compared their performance to that of a flat plate in a flume. Aside from having different foils, the Hydrovolts design differed significantly from the previous turbines studied in other ways as well. It was a drag machine as opposed to a lift-based turbine, and had very different geometric constraints on the foils throughout the rotation. Thus, a new model was constructed in MATLAB to reflect these differences, although much of it was built on the skeleton of the past models. The code for the new geometric constraints appears in APPENDIX B.

CHAPTER SEVEN: CONCLUSION

The purpose of the study was to analyze the behavior of different small-scale turbines for power generation. Mathematical models built in MATLAB and Simulink facilitated the analysis. What emerged from the model simulations was a deeper understanding of vertical axis wind turbine dynamics at start-up, and the differences associated with installing a hydroturbine in an open channel.

The models that were constructed for this analysis were validated in part by a number of empirical datasets from the literature. Power outputs of the VAWT at the Durham wind-tunnel, the THAWT at the Oxford flume, and the BlackHawk TR10 in Emmett were all matched to by the simulation results of each respective model. The behavioral patterns were consistent although the time-scales varied, and there was a slight difference in rotational speeds. Importantly, the model of the VAWT exhibited the same dynamic start-up as that of physical models being tested in other laboratories.

Rotational Behavior

Simulations indicated that for VAWTs starting-up from rest, the rotor velocity did not step up slowly with increasing flow velocity. Rather, the turbine's rotational velocity was shown to increase quite suddenly, going from a low rate of rotation to a high one in just a few short seconds. The high rotational velocities in simulations coincided with very high estimates of power production as well. A very promising region of power production appeared to exist for wind turbines that reached a TSR of 4 or more. Similar

conclusions were reached by another research team, [18], and it would seem that the concept would be worth exploring for future VAWT development.

Once a critical rotational velocity was attained (usually about 1.5 TSR), the simulations consistently predicted that a turbine would rapidly accelerate to a high rotational velocity with a TSR in the range of 6 to 9 where it would level out. This kept the local flow at each foil dominated by the induced velocity. The induced velocity maintained very low angles of attack (high lift, low drag) at each foil throughout the rotation. Unfortunately, the material constraints of the BlackHawk TR10 did not permit the turbine rotor to reach such high speeds. Yet, the research showed that a turbine with stronger wings has the potential to benefit from increased rotational speeds.

Articulation

The results of the MATLAB analysis showed a potential for significant improvements in efficiencies by using new turbine pitch configurations. Staelens et al. predicted that higher efficiencies could be achieved for vertical axis turbines that were built with the ability to articulate their blades' pitches throughout the rotation [14]. The computer model was used to test the effectiveness of several different theories of pitch articulation.

The first models were configured for turbines with blades that had foils with a fixed-pitch. Although fixed-pitch turbines did perform adequately when given a high initial velocity, they failed to do well in low-flow conditions and often failed to start from rest. The model was then used to test the pitch articulation methods of the BlackHawk

TR10 machine, and hydrovolts flip-wing style water turbine. Running many simulations with these models indicated that a sinusoidally varying pitch of $\pm 8.6^\circ$ with the maximum deflection occurring at the windward point was best for all-around turbine implementation. For turbines not starting from rest, but beginning from an initial rotational velocity higher than 1.5 TSR, fixed-pitch turbines did not perform significantly worse than their articulating counterparts.

The models of fixed-pitch turbines failed to start-up when provided with same initial conditions as those turbines with pitch articulation that rotated. The simulations of fixed-pitch VAWTs showed the turbines that would appear to rock back and forth, but could never complete full or consistent rotations in a simulated flow. The ideal pitch articulation is based on instantaneous alterations in the foil angle, which is not physically possible [14]. The best compromise was found to be the use of a sinusoidally varying pitch throughout the rotation in line with the wind direction. The amplitude of articulation had to be a balance between the two regions of performance ($TSR < 1$ and $TSR > 1$). In general, the greater the pitch amplitude, the easier it was for the turbine to begin rotating from rest, but the less efficient it was at high rotational speeds.

Generator Loading

The models of the VAWTs were able to diagnose some of the problems with turbine start-up and offered important insight into turbines designed in such a way that they may consistently start from rest without requiring external inputs to the system. While this is less of a concern for water turbines (which experience a near-constant flow over short time intervals), most wind turbines cycle on and off in their operation depending on the incoming wind-speed. Simulation results verified the possibility that a

VAWT could start from rest, but only for those turbines that had articulating foils and a low resistance from a generator.

The generator loading was of vital importance to a smooth start-up. Establishing a dynamic generator load was what enabled several wind and water turbine models to both start easily from rest, and to operate efficiently in high TSR regions. A step function matching the generator load to the rotational speed doubled the power output of the machine in the model. One reason that having a dynamic generator load was so important was due to the nature of the start-up region that many models displayed.

While a dynamic generator may not be essential for a hydro-turbine, which sees a fairly consistent fluid velocity, it is vital for wind turbines. Wind turbines have very dynamic inputs; the continual changes in the wind's velocity make it difficult to maintain a certain TSR if the torsional resistance of the generator cannot be adjusted. The simulations indicated a clear advantage for VAWTs with dynamic generators. The models with dynamic generators were able to start more quickly and in lower wind speeds. These were the models that were able to best make use of the phenomena of the turbine's sudden increase from low rotational speeds to fast rotational speeds near start-up.

Hydroturbines

The model of the flip-wing turbine revealed the complexity of calculating efficiency in a restricted channel. The simulations demonstrated water level rises upstream of the turbine when there was blockage. This is one area where the model could be further developed and more work done on comparing various efficiencies and flow effects of different configurations and blockage ratios.

Future Work

Now that the model has been developed, it can be used to test new turbine designs and configurations. While some exploration was done on the effects of periodic and sinusoidal pitch articulation, there is much more that could be studied on the subject, specifically optimizing the angle of attack for maximum lift. The model itself could be further refined by accounting for friction in the bearings, and turbulence effects. More could also be done to better define the foil-to-foil interaction and the impact on wake for the foils during rotation. The model used data based on two-dimensional flow, and ignored span-wise flow or flow in the Z direction. To delve into this topic, one would need a new set of aerodynamic data. The data used in this study was organized according to the Reynold's number, which is based only on two-dimensional flow.

While some similarities were observed between empirical tests and the MATLAB simulations of the hydroturbines, it is clear that there were some major differences in behavior that could not be accounted for. While the research provided an exploratory model, further testing and refinement is needed before manufacturers can use the information from the simulations to their advantage.

Summary

Overall, the construction of the MATLAB model was able to inform the discussion on wind and water turbine design. The model verified the unique start-up behavior of certain VAWT designs. The high TSR regime and the high efficiencies at fast rotational speeds suggests that manufacturers explore designs that can tolerate fast rotations and have dynamic generator loads that allow the turbines to spin up in relatively low-velocity conditions. The model showed the advantages of having both a dynamic

generator and foil articulation, and could be used as a tool for those who wish to weigh the advantages of dynamic generators and articulating foils against the added costs of assembly associated with such features. Those seeking to optimize dynamic generator loading could use the model as a tool to find the ideal power curve. The model allowed the prediction of changes to the water level upstream of a turbine installed in a narrow channel. It also revealed the unique equations associated with calculating the potential energy of this type of system, showing that the Betz efficiency equation is not applicable for these conditions. It is hoped that this thesis and computer model offers insight into the unique behavior of VAWTs and turbines in restricted channels, and that such insight can be applied to future turbine designs.

REFERENCES

- [1] U.S. Department of Energy and the American Wind Energy Association, "Vertical Axis Wind Turbines: The History of the DOE Program," Sandia National Laboratories , Albuquerque.
- [2] World Wind Energy Association, "World Wind Energy Report 2010," World Wind Energy Association, Bonn, Germany, 2011.
- [3] National Renewable Energy Laboratory, "20% Wind Energy by 2030: Increasing Wind Energy's Contribution to the U.S. Electric Supply," Department of Energy, Oak Ridge, 2008.
- [4] Energy Information Administration, "Annual Energy Review 2011," U.S. Energy Information Administration, Washington DC, 2012.
- [5] H. Riegler, "HAWT versus VAWT: Small VAWTs Find a Clear Niche," *Refocus*, pp. 44-46, July/August 2003.
- [6] U.S. Green Building Council, "LEED Rating Systems," Leadership in Energy Efficient Design, 2012. [Online]. Available: <https://new.usgbc.org/leed/rating-systems>. [Accessed 23 July 2012].
- [7] G. Muller, M. Jentsch and E. Stoddart, "Vertical Axis Resistance-Type Wind

Turbines for Use in Buildings," *Renewable Energy*, vol. 34, pp. 1407-1412, 2009.

- [8] Hadjerioua, "An Assessment of Energy Potential at Non-Powered Dams in the United States," Oak Ridge National Laboratory, Oak Ridge, 2012.
- [9] M. Khan, G. Bhuya, M. Iqbal and J. Quaicoe, "Hydrokinetic Energy Conversion Systems and Assessment of Horizontal and Vertical Axis Turbines for River and Tidal Applications: A Technology Status Review," *Applied Energy*, vol. 86, no. 10, pp. 1823-1835, 2009.
- [10] T. Benson, "Shape Effects on Lift," National Aeronautics and Space Administration , 28 July 2010. [Online]. Available: <http://www.grc.nasa.gov/WWW/k-12/airplane/shape.html>. [Accessed 14 March 2013].
- [11] J. Scott, "Aerospaceweb.org," 19 September 2004. [Online]. Available: <http://www.aerospaceweb.org/question/aerodynamics/q0194.shtml>. [Accessed 15 February 2013].
- [12] Y. Cengel and J. Cimbala, *Fluid Mechanics: fundamentals and applications*, New York: McGraw-Hill, 2006.
- [13] R. Sheldahl and P. Klimas, "Aerodynamic Characteristics of Seven Symmetrical Airfoil Sections through 180-Degree Angle of Attack for Use in Aerodynamic Analysis of Vertical Axis Wind Turbines," Sandia National Laboratory, Albuquerque, 1981.

- [14] P. Klimas, "Tailored Airfoils for Vertical Axis Wind Turbines," Sandia National Laboratory, Albuquerque and Livermore, 1992.
- [15] Y. Staelens, F. Saeed and P. I., "A Straight-Bladed Variable-Pitch VAWT Concept for Improved Power Generation," in *ASME Wind Energy Symposium*, Reno, 2003.
- [16] J. Manwell, J. McGowan and A. Rogers, *Wind Energy Explained*, Amherst: University of Massachusetts, 2006.
- [17] K. Pope, I. Diner and G. Naterer, "Energy and Exergy Efficiency Comparison of Horizontal and Vertical Axis Wind Turbines," *Renewable Energy*, vol. 35, pp. 2102-2113, 2010.
- [18] Hi-VAWT Technology Corp., "Taiwan SWT Brief and Hi-VAWT Wind System," in *International Small and Medium Wind Conference*, Glasgow, 2009.
- [19] H. Hill, R. Dominy, G. Ingram and J. Dominy, "The Physics of Self-Starting," in *Institute of Mechanical Engineers, PartA: journal of power and energy*, 2009.
- [20] F. Ponta and G. Dutt, "An Improved Vertical-Axis Water Current Turbine Incorporating a Channeling Device," *Renewable Energy*, vol. 20, pp. 223-241, 2000.
- [21] M. Hansen, A. Hansen, L. Torben, S. Oye, P. Sorenson and P. Fugslang, "Control Design for a Pitch-Regulated, Variable Speed Wind Turbine," Riso National

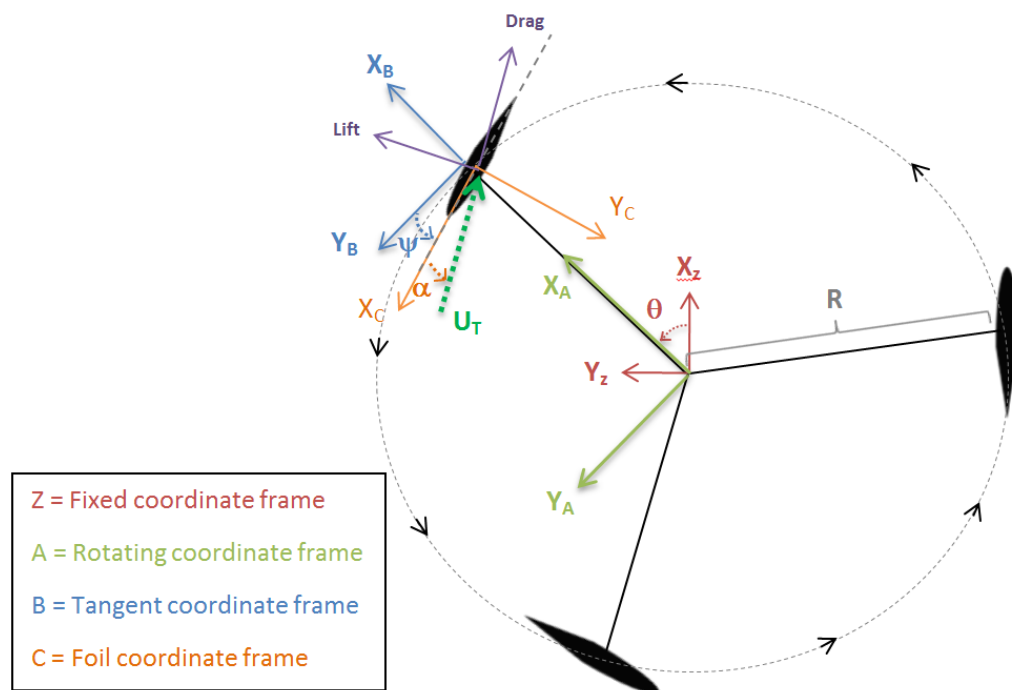
Laboratory, Roskilde, 2005.

- [22] B. Boatner, "Vertical Axis Wind Turbine With Articulating Rotor". United States of America Patent 7,677,862, 2 March 2010.
- [23] G. M. Angle II, F. A. Pertl, M.-A. Clarke and J. E. Smith, "Lift Augmentation for Vertical Axis Wind Turbines," *International Journal of Engineering*, vol. 4, no. 5, pp. 430-442, 2010.
- [24] M. El-Samanoudy, A. Ghorab and S. Youssef, "Effect of Some Design Parameters on the Performance of a Giromill Vertical Axis Wind Turbine," *Ain Shams Engineering Journal*, vol. 1, no. 1, pp. 85-95, 2010.
- [25] O. Guerri, A. Sakout and K. Bouhadeif, "Simulations of the Fluid Flow around a rotating Vertical Axis Wind Turbine," *Wind Engineering*, vol. 31, no. 3, pp. 149-163, 2007.
- [26] J. Whelan, J. Graham and J. Piero, "A Free-Surface and Blockage Correction for Tidal Turbines," *Journal of Fluid Mechanics*, vol. 624, pp. 281-291, 2009.
- [27] H. Beri and Y. Yao, "Double Multiple Stream Tube Model and Numerical Analysis of Vertical Axis Wind Turbine," *Energy and Power Engineering*, vol. 3, pp. 262-270, 2011.
- [28] S. Draper, G. Houlby, M. Oldfield and A. Borthwick, "Modelling Tidal Energy Extraction in a Depth-Averaged Coastal Domain," *IET Renewable Power Generation*, vol. 4, no. 6, pp. 545-554, 2010.

- [29] R. McAdam, G. Houlsby, M. Oldfield and M. McCulloch, "Experimental Testing of the Transverse Horizontal Axis Water Turbine," *IET Renewable Power Generation*, vol. 4, no. 6, pp. 510-518, 2010.
- [30] W. B. Hamner, "Hinged-Blade Cross-Axis Turbine for Hydroelectric Power Generation". United States of America Patent 2010/0237626, 23 3 2010.
- [31] N. Caplan and T. N. Gardner, "A fluid dynamic investigation of the Big Blade and Macon oar blade," *Journal of Sports Sciences*, vol. 6, no. 25, pp. 643-650, 2007.
- [32] Hydrovolts, "Hydrovolts Products," Hydrovolts, 2012. [Online]. Available: <http://hydrovolts.com/products/>. [Accessed 30 January 2012].

APPENDIX A

Geometric Transformation by Matrices



Frame Z: A fixed coordinate frame describing the rotation of the turbine about the Z-axis and transformed to **Frame A:** A rotating coordinate frame with X along theta. Transform from Z to A, $\mathbf{\Pi}_A =$

$$\begin{bmatrix} \cos(\theta) & -\sin(\theta) & 0 & 0 \\ \sin(\theta) & \cos(\theta) & 0 & 0 \\ 0 & 0 & 1 & 0 \\ 0 & 0 & 0 & 1 \end{bmatrix}$$

Frame B: A set of axes out at the edge of the rotor with X along theta and Y tangent to the circle of rotation. This can be transformed by the following matrix, which also inverts the Z axis transforming the geometric description to the edge of rotation (where the blades are) where R = turbine radius: $\mathbf{\Pi}_B =$

$$\begin{bmatrix} 1 & 0 & 0 & -R \\ 0 & 1 & 0 & 0 \\ 0 & 0 & 1 & 0 \\ 0 & 0 & 0 & 1 \end{bmatrix}$$

Frame C: The coordinate frame at the foil that includes the pitch ψ . This can be transformed from **Frame B** and shares the same Z-axis as **B**: $\mathbf{\Pi}_C =$

$$\begin{bmatrix} \cos(90 + \psi) & -\sin(90 + \psi) & 0 & 0 \\ \sin(90 + \psi) & \cos(90 + \psi) & 0 & 0 \\ 0 & 0 & 1 & 0 \\ 0 & 0 & 0 & 1 \end{bmatrix}$$

To transform coordinates and vectors from the fixed axes at the center of rotation to the

set of axes at the foil, one must follow: ${}^C\Pi_Z = {}^C\Pi_B \times {}^B\Pi_A \times {}^A\Pi_Z$

$$\begin{aligned} & \Pi_A \times \Pi_B \\ & \begin{bmatrix} \cos(\theta) & -\sin(\theta) & 0 & 0 \\ \sin(\theta) & \cos(\theta) & 0 & 0 \\ 0 & 0 & 1 & 0 \\ 0 & 0 & 0 & 1 \end{bmatrix} \times \begin{bmatrix} 1 & 0 & 0 & -R \\ 0 & 1 & 0 & 0 \\ 0 & 0 & 1 & 0 \\ 0 & 0 & 0 & 1 \end{bmatrix} \\ & = \begin{bmatrix} \cos(\theta) & -\sin(\theta) & 0 & -R*\cos(\theta) \\ \sin(\theta) & \cos(\theta) & 0 & R*\sin(\theta) \\ 0 & 0 & 1 & 0 \\ 0 & 0 & 0 & 1 \end{bmatrix} \end{aligned}$$

$$\begin{aligned} & \Pi_A \times \Pi_B \times \Pi_C \\ & \begin{bmatrix} \cos(\theta) & -\sin(\theta) & 0 & -R*\cos(\theta) \\ \sin(\theta) & \cos(\theta) & 0 & R*\sin(\theta) \\ 0 & 0 & 1 & 0 \\ 0 & 0 & 0 & 1 \end{bmatrix} \times \begin{bmatrix} \cos(90 + \psi) & -\sin(90 + \psi) & 0 & 0 \\ \sin(90 + \psi) & \cos(90 + \psi) & 0 & 0 \\ 0 & 0 & 1 & 0 \\ 0 & 0 & 0 & 1 \end{bmatrix} \\ & = \begin{bmatrix} \cos(\theta)*\cos(90 + \psi) - \sin(\theta)*\sin(90 + \psi) & -\cos(\theta)*\sin(90 + \psi) - \sin(\theta)*\cos(90 + \psi) & 0 & -R*\cos(\theta) \\ \sin(\theta)*\cos(90 + \psi) + \cos(\theta)*\sin(90 + \psi) & -\sin(\theta)*\sin(90 + \psi) - \cos(\theta)*\cos(90 + \psi) & 0 & R*\sin(\theta) \\ 0 & 0 & 1 & 0 \\ 0 & 0 & 0 & 1 \end{bmatrix} \end{aligned}$$

This can be simplified using trigonometric identities:

$${}^C\Pi_Z = \begin{bmatrix} \cos(\theta + 90 + \psi) & -\sin(\theta + 90 + \psi) & 0 & -R*\cos(\theta) \\ \sin(\theta + 90 + \psi) & \cos(\theta + 90 + \psi) & 0 & R*\sin(\theta) \\ 0 & 0 & 1 & 0 \\ 0 & 0 & 0 & 1 \end{bmatrix}$$

This transformation matrix can also be written using different trigonometric identities:

$${}^C \mathbf{\Pi}_Z = \begin{bmatrix} -\sin(\theta + \psi) & -\cos(\theta + \psi) & 0 & -R \cdot \cos(\theta) \\ \cos(\theta + \psi) & -\sin(\theta + \psi) & 0 & R \cdot \sin(\theta) \\ 0 & 0 & 1 & 0 \\ 0 & 0 & 0 & 1 \end{bmatrix}$$

The same process follows for calculating ${}^Z \mathbf{\Pi}_C$ (just in the reverse order of multiplication), which transforms from the fixed global axes to the axes at the foil:

Frame Z to Frame A to Frame B to Frame C

$${}^Z \mathbf{\Pi}_C = \begin{bmatrix} -\sin \theta + \psi & \cos \theta + \psi & 0 & R \sin \psi \\ -\cos \theta + \psi & -\sin \theta + \psi & 0 & R \cos \psi \\ 0 & 0 & 1 & 0 \\ 0 & 0 & 0 & 1 \end{bmatrix}$$

APPENDIX B

MATLAB Code and Simulink Figures

The function “comp_torq” was used to calculate the lift and drag forces on each foil, and the resulting torque on the rotor:

```
function torque = comp_torq(u)
%
% u(1) = ux in 0
% u(2) = uy in 0
% u(3) = uz in 0
% u(4) = theta
% u(5) = omega
%
global R C H rho mu Cd Cl Re alpha;

%
psi=th2psi(u(4));
Utotalin0=[u(1)+u(5)*R*sin(u(4)) u(2)-u(5)*R*cos(u(4)) u(3) 0];
UinC=z2c(Utotalin0,u(4),psi);
alpha1=atan2(-UinC(2),-UinC(1));
sa=sign(alpha1); % tells whether alpha is positive or negative
if alpha1<0
    alpha1=alpha1+2*pi;
end
alphad=alpha1*180/pi;
Utotal=(UinC(1)^2+UinC(2)^2+UinC(3)^2)^.5;
Reno=rho*Utotal*C/mu;
if Reno < 1E4
    Reno = 1E4; % this is due to the limitations in the data
available
end
Clift=interp2(Re,alpha,Cl,Reno,alphad);
Cdrag=interp2(Re,alpha,Cd,Reno,alphad);
%
L=sa/2*Clift*rho*Utotal^2*C*H;
D=1/2*Cdrag*rho*Utotal^2*C*H;
%
torque=R*L*sin(psi+alpha1)-R*D*cos(psi+alpha1);
end
```

The `comp_torq` function calls on two other scripts to operate. The first of these is `psi`, which describes the articulation function:

```
function psi=th2psi(theta)
%
psi=0*(pi/180)+9*(pi/180)*cos(theta);

end
```

The second piece of code is the `z2c` script, which acts as the transformational

matrix Π

```
function vinc=z2c(vinz,th,psi)
global R
a=th+psi;
zTc=[-sin(a) cos(a) 0 R*sin(psi);-cos(a) -sin(a) 0 R*cos(psi);0 0 1 0;
0 0 0 1];
vinc=zTc*vinz';
end
```

The function “delta_H” was used to calculate the change in height in the water level upstream of the turbine. The change in height was determined by solving the quartic equation from [25] regarding obstructions in channel flow:

```
function delta_H = delta_H(u)
%
% u(1) = height (hh)
% u(2) = Power
% u(3) = velocity at blades (V)
% u(4) = base width of stream or canal
%
%
global R C H g rho mu Ct Re alpha;
%
%
hh=u(1);
T=u(2)/u(3);
% Thrust = Power/velocity
V=u(3);
b=u(4);
%
dh=hh - (((V^4*hh^4)/g^2 - (2*b*rho*V^2*hh + b*g*rho*hh^2 -
2*T)^3/(27*b^3*g^3*rho^3))^(1/2) + (V^2*hh^2)/g)^(1/3)/2 -
(2*b*rho*V^2*hh + b*g*rho*hh^2 - 2*T)/(6*b*g*rho*((V^4*hh^4)/g^2 -
(2*b*rho*V^2*hh + b*g*rho*hh^2 - 2*T)^3/(27*b^3*g^3*rho^3))^(1/2) +
(V^2*hh^2)/g)^(1/3)) + (3^(1/2))*(((V^4*hh^4)/g^2 - (2*b*rho*V^2*hh +
b*g*rho*hh^2 - 2*T)^3/(27*b^3*g^3*rho^3))^(1/2) + (V^2*hh^2)/g)^(1/3) -
(2*b*rho*V^2*hh + b*g*rho*hh^2 - 2*T)/(3*b*g*rho*((V^4*hh^4)/g^2 -
(2*b*rho*V^2*hh + b*g*rho*hh^2 - 2*T)^3/(27*b^3*g^3*rho^3))^(1/2) +
(V^2*hh^2)/g)^(1/3))) * i) / 2;
%
%
delta_H=dh;
end
```

The function for determining the angle of attack for the Hydrovolts flip-wing turbine was given by the following function:

```
if 0<u(4)<pi
alpha1=u(4);
if pi<u(4)<2*pi
alpha1=0;
end
end
```

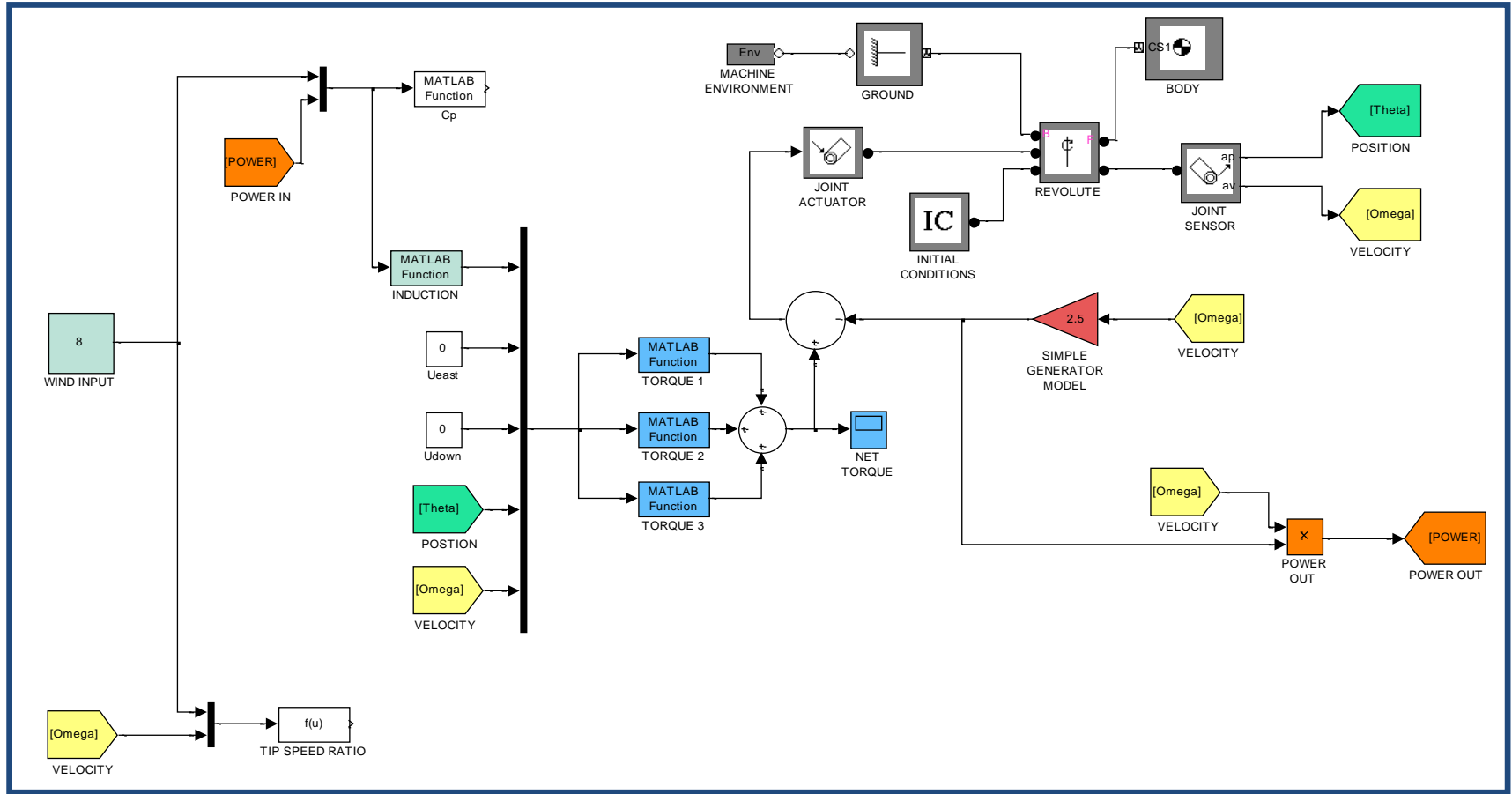


Figure 45: Schematic of full MATLAB model for wind turbines

APPENDIX C

Additional Tables and Figures



Figure 46: Close-up of a BlackHawk TR-10 VAWT developed by Bruce Boatner [21] showing tilt and articulation

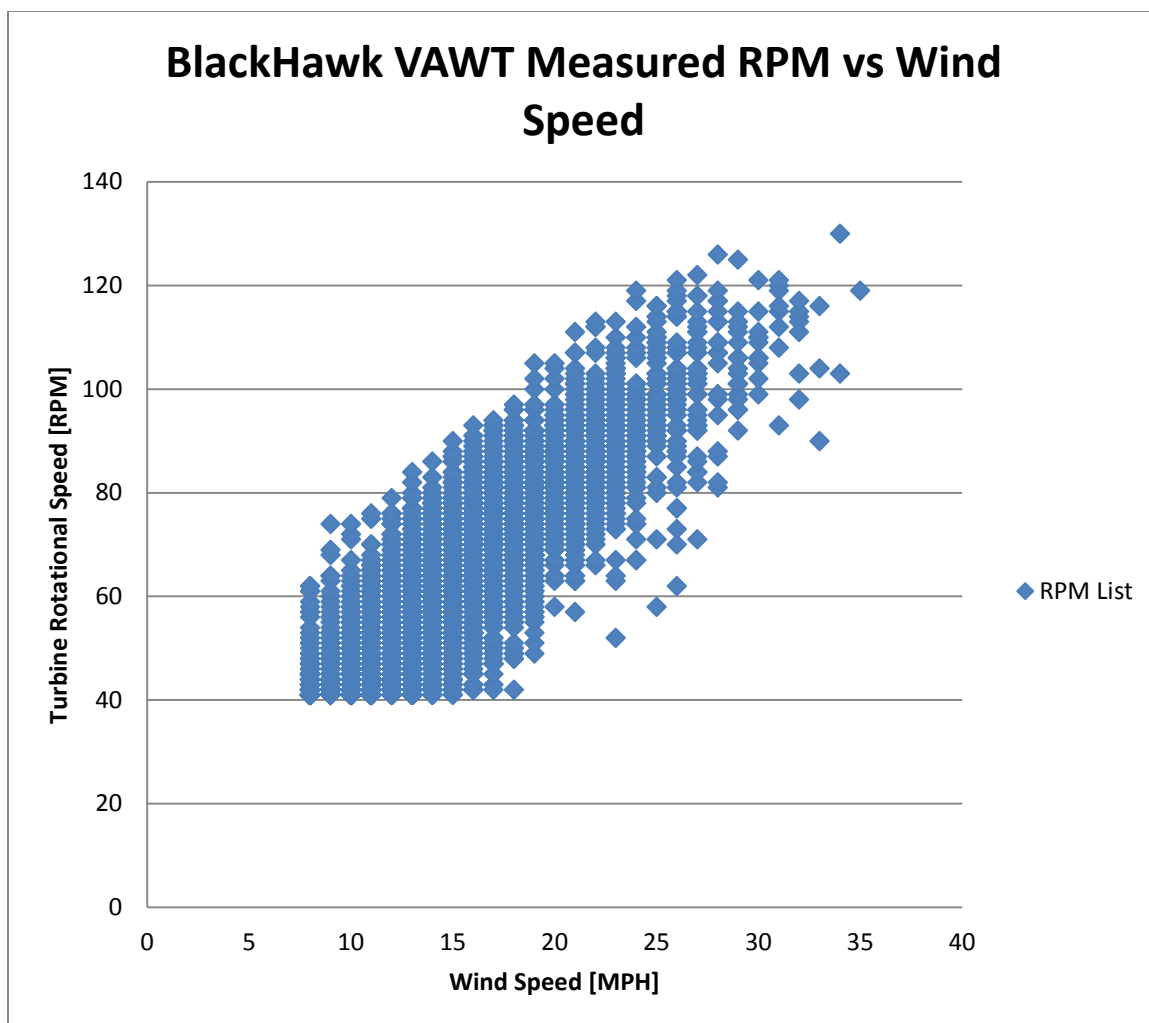


Figure 47: SCADA Data Provided by BlackHawk Showing Measurements of RPM vs Wind-Speed

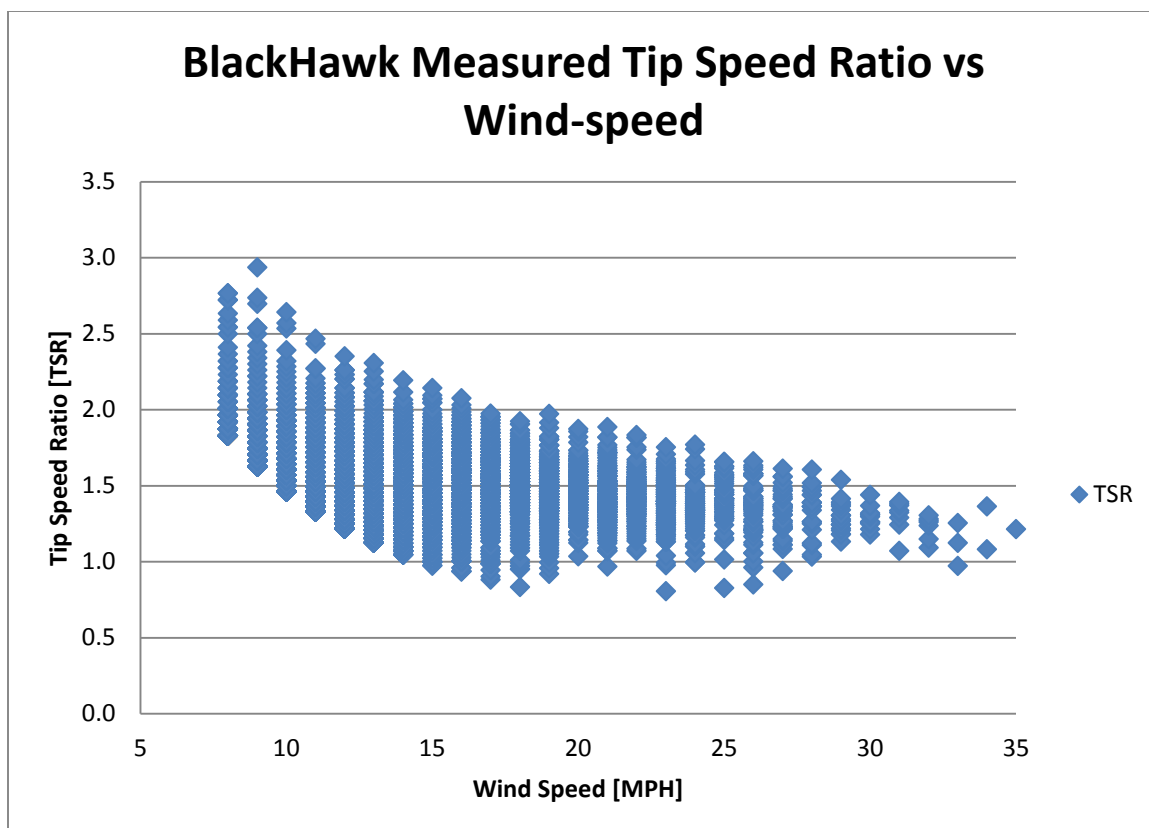


Figure 48: SCADA Data Provided by BlackHawk Showing Measurements of TSR versus Wind-Speed

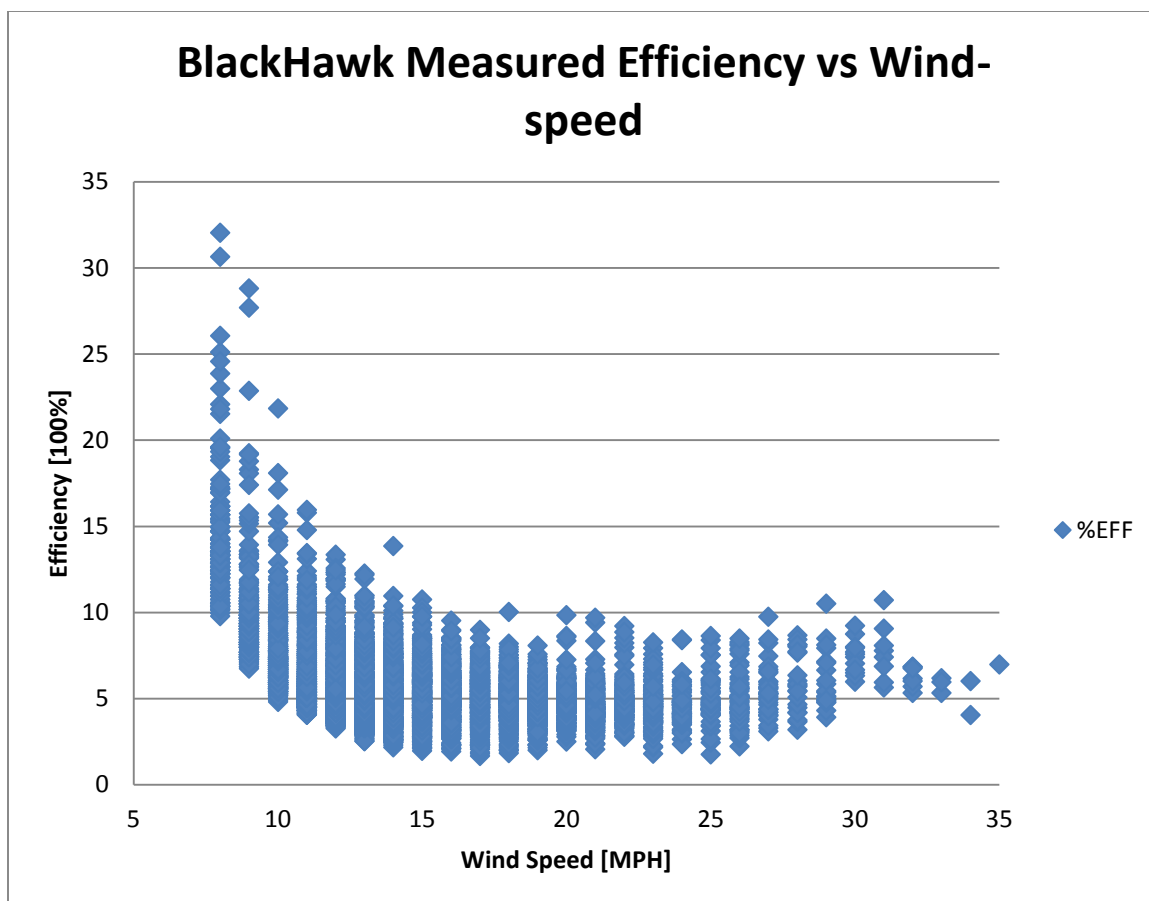


Figure 49: SCADA Data Provided by BlackHawk Showing Measurements of Efficiency vs Wind-speed

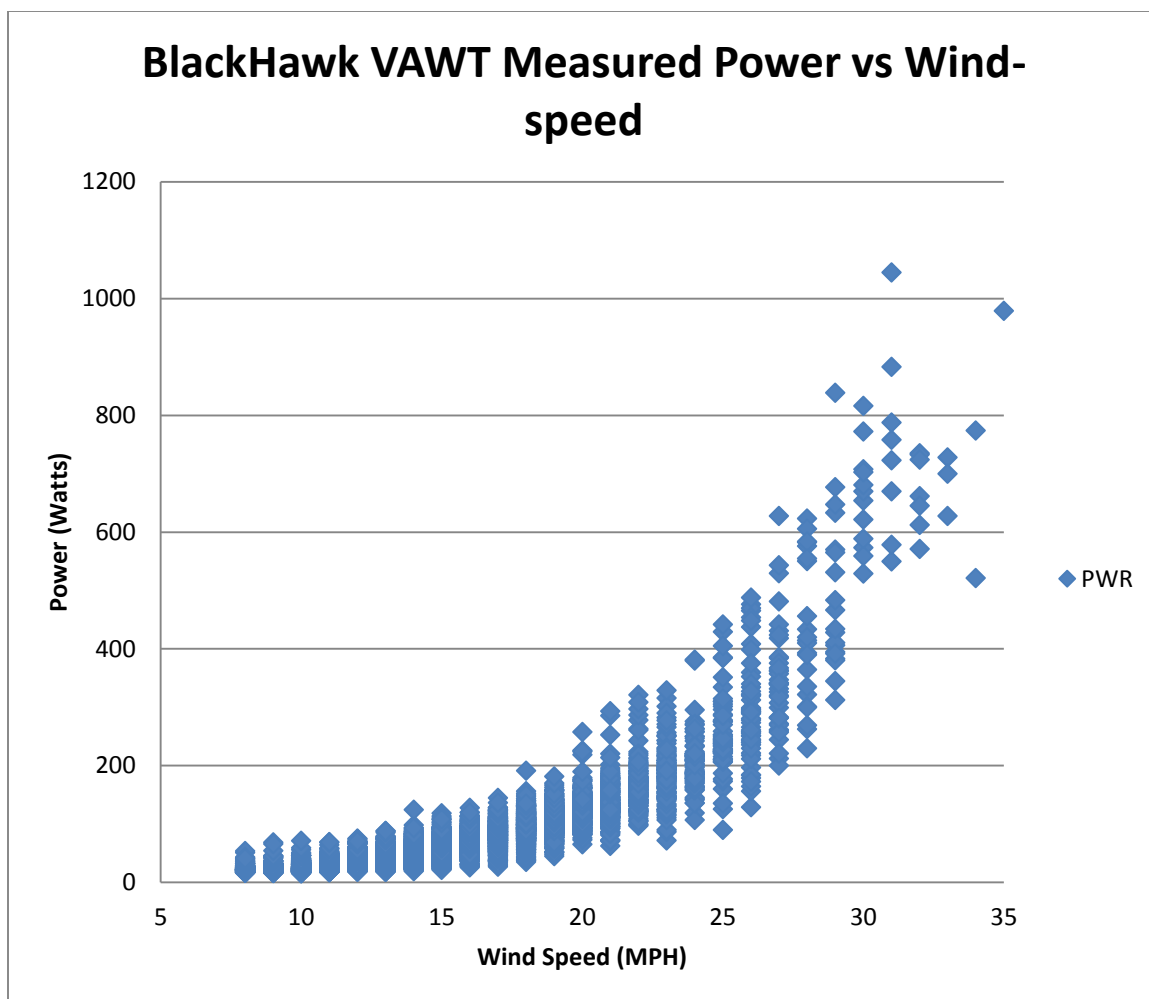


Figure 50: SCADA Data Provided by BlackHawk Showing Measurements of Power vs. Wind-speed

Table 1: Outputs of MATLAB model simulations for sinusoidal pitch articulation and low resistance

Model outputs based on Blackhawk TR10 dimensions with sinusoidal pitch articulation $\pm 9^\circ$ and high TSR (low resistance)						
Windspeed		TSR	RPM	Torque	Cp	Power
m/s	mph	-	RPM	N-m	-	Watts
1	2.2	0.8	4.8	0.1	0.01	0
2	4.5	5.3	66.8	1.7	0.16	5
3	6.7	4.7	88.8	5.0	0.35	34
4	8.9	4.2	106.0	6.5	0.42	99
5	11.2	4.0	124.1	20.2	0.45	205
6	13.4	3.8	141.3	31.0	0.47	375
7	15.7	3.7	164.2	27.0	0.49	619
8	17.9	3.5	176.7	62.3	0.49	927
9	20.1	3.5	195.8	67.0	0.52	1,360
10	22.4	3.3	205.3	87.0	0.50	1,900
11	24.6	3.3	224.4	96.8	0.53	2,560
12	26.8	3.2	236.8	135.0	0.51	3,340
14	31.3	3.1	274.1	185.0	0.54	5,350
16	35.8	3.0	298.9	250.0	0.52	8,050
18	40.3	2.9	326.6	330.0	0.53	11,500
20	44.7	2.8	353.3	420.0	0.52	15,800

Table 2: Outputs of MATLAB model simulations for sinusoidal pitch articulation and high resistance

Model outputs based on Blackhawk TR10 dimensions with sinusoidal pitch articulation $\pm 9^\circ$ and lower TSR (higher resistance)						
Windspeed		TSR	RPM	Torque	Cp	Power
m/s	mph	-	rpm	N-m	-	Watts
1	2.2	0.8	4.8	0.1	0.01	0
2	4.5	1.6	21.0	0.7	0.03	1
3	6.7	1.4	25.8	1.0	0.04	4
4	8.9	1.3	32.5	3.2	0.04	10
5	11.2	1.4	45.8	3.5	0.07	30
6	13.4	1.3	50.6	5.6	0.06	50
7	15.7	1.1	48.7	22.3	0.05	59
8	17.9	1.0	51.6	23.9	0.05	84
9	20.1	1.1	64.0	27.0	0.06	158
10	22.4	1.1	66.8	40.0	0.06	204
11	24.6	1.1	73.5	41.0	0.06	350
12	26.8	1.1	81.2	45.0	0.06	425
14	31.3	1.0	89.8	52.0	0.06	590
16	35.8	1.0	106.0	80.0	0.07	1,000
18	40.3	0.9	100.3	92.0	0.05	1,082
20	44.7	1.0	128.0	121.0	0.07	1,800

Table 3: Outputs of MATLAB model simulations for a fixed pitch turbine

Model outputs based on Blackhawk TR10 dimensions with fixed pitch of 0°						
Wind-speed		TSR	RPM	Torque	Cp	Power
m/s	mph	-	rpm	N-m	-	Watts
1	2.2	0.2	1.5	0.1	0.00	0
2	4.5	0.3	4.1	0.1	0.00	0
3	6.7	0.4	8.0	0.1	0.00	0
4	8.9	0.3	6.7	0.4	0.00	1
5	11.2	0.3	8.6	1.2	0.00	1
6	13.4	0.3	9.5	2.0	0.00	3
7	15.7	0.3	12.4	3.0	0.00	4
8	17.9	0.3	12.4	5.0	0.00	7
9	20.1	0.3	12.4	5.2	0.00	9
10	22.4	0.3	13.4	6.0	0.00	13
11	24.6	0.3	16.2	10.0	0.00	18
12	26.8	0.3	17.2	12.5	0.00	25
14	31.3	0.3	20.1	17.5	0.00	43
16	35.8	0.2	21.0	24.0	0.01	70
18	40.3	0.2	22.9	32.5	0.01	115
20	44.7	0.2	26.7	42.5	0.06	150

Table 4: Outputs of MATLAB model simulations for THAWT with fixed pitch

TSR	Cp	Power (W)	Fr	ΔH (cm)	Pitch °	Load	Time to ss (s)
16.22	0.13	12	0.24	0.002	0	0	3
8.26	0.51	48	0.24	0.97	0	0.025	3
7.25	0.53	49	0.24	0.99	0	0.05	3
6.55	0.546	50	0.24	1.02	0	0.075	3
6.01	0.552	51	0.24	1.03	0	0.1	3
5.59	0.554	51	0.24	1.04	0	1.25	3
5.23	0.552	51	0.24	1.03	0	1.5	3
4.92	0.546	50	0.24	1.02	0	1.75	3
4.66	0.529	49	0.24	0.99	0	0.2	3
4.23	0.51	47	0.24	0.95	0	0.25	3
3.89	0.477	44	0.24	0.89	0	0.3	3
3.36	0.691	64	0.24	1.3	0	0.4	3
3	0.677	62	0.24	1.27	0	0.5	3
2.671	0.654	60	0.24	1.23	0	0.6	3
2.38	0.606	56	0.24	1.14	0	0.7	3
0.103	0	0	0.24	0	0	0.8	3



Figure 51: Hydrovolts [29] Class II Turbine 1 - 10 kW capacity depending on flow. Photo courtesy of Hydrovolts Inc. [32]

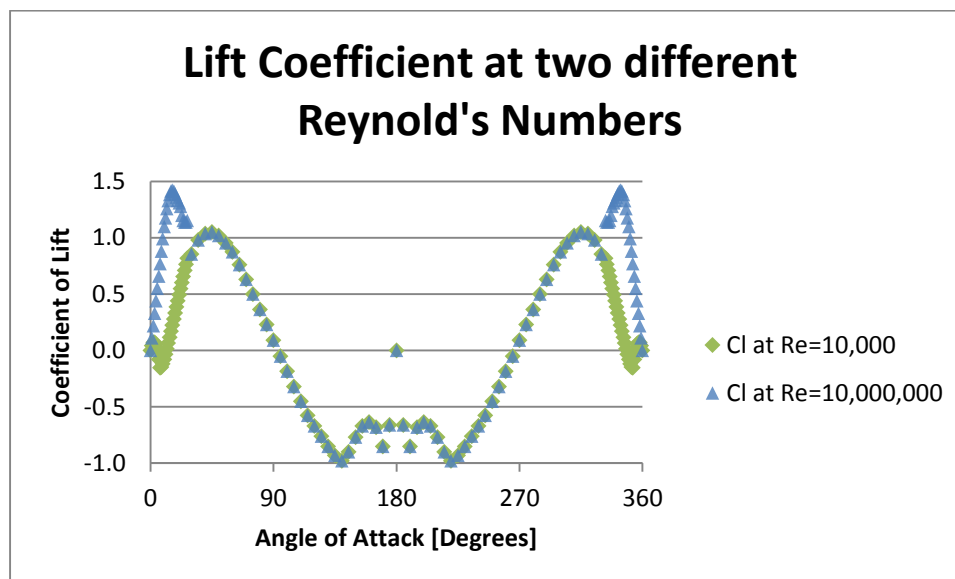


Figure 52: The Lift Coefficient of a NACA 0014 airfoil at Two Different Reynold's numbers from Sandia Wind-Tunnel tests [12]

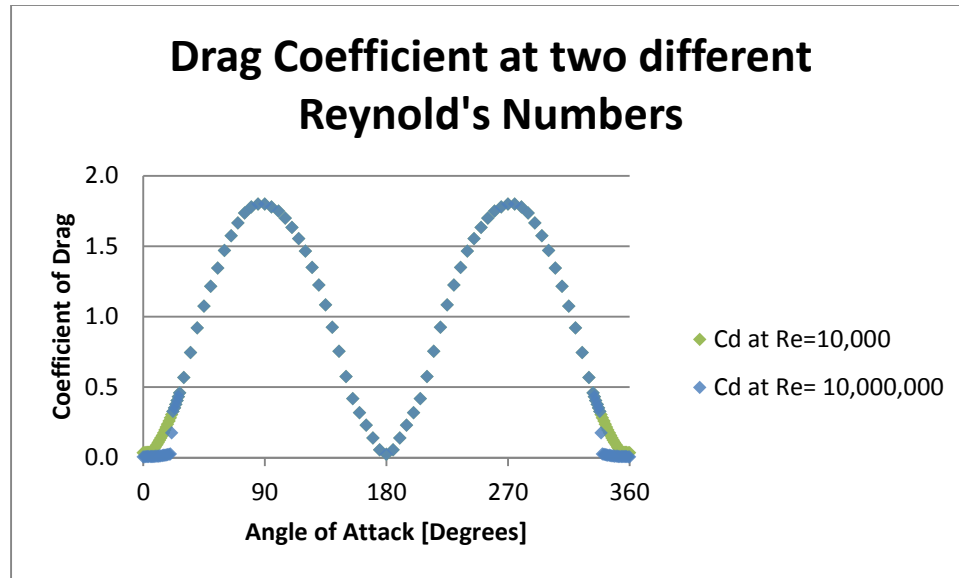


Figure 53: The Drag Coefficient of a NACA 0014 airfoil at Two Different Reynold's numbers from Sandia Wind-Tunnel tests